**WAVE PROPAGATION IN DENSITY STRATIFIED FLUIDS**
GEAR, JOHN ANTHONY
*ProQuest Dissertations and Theses;* 1984; ProQuest Dissertations & Theses Global

## INFORMATION TO USERS

This reproduction was made from a copy of a document sent to us for microfilming. While the most advanced technology has been used to photograph and reproduce this document, the quality of the reproduction is heavily dependent upon the quality of the material submitted.

The following explanation of techniques is provided to help clarify markings or notations which may appear on this reproduction.

1. The sign or "target" for pages apparently lacking from the document photographed is "Missing Page(s)". If it was possible to obtain the missing page(s) or section, they are spliced into the film along with adjacent pages. This may have necessitated cutting through an image and duplicating adjacent pages to assure complete continuity.

2. When an image on the film is obliterated with a round black mark, it is an indication of either blurred copy because of movement during exposure, duplicate copy, or copyrighted materials that should not have been filmed. For blurred pages, a good image of the page can be found in the adjacent frame. If copyrighted materials were deleted, a target note will appear listing the pages in the adjacent frame.

3. When a map, drawing or chart, etc., is part of the material being photographed, a definite method of "sectioning" the material has been followed. It is customary to begin filming at the upper left hand corner of a large sheet and to continue from left to right in equal sections with small overlaps. If necessary, sectioning is continued again—beginning below the first row and continuing on until complete.

4. For illustrations that cannot be satisfactorily reproduced by xerographic means, photographic prints can be purchased at additional cost and inserted into your xerographic copy. These prints are available upon request from the Dissertations Customer Services Department.

5. Some pages in any document may have indistinct print. In all cases the best available copy has been filmed.

University Microfilms International
300 N. Zeeb Road
Ann Arbor, MI 48106

Reproduced with permission of the copyright owner. Further reproduction prohibited without permission.

Reproduced with permission of the copyright owner. Further reproduction prohibited without permission.

8429717

**Gear, John Anthony**

WAVE PROPAGATION IN DENSITY STRATIFIED FLUIDS

*University of Melbourne (Australia)* PH.D. 1984

University
Microfilms
International 300 N. Zeeb Road, Ann Arbor, MI 48106

Reproduced with permission of the copyright owner. Further reproduction prohibited without permission.

Reproduced with permission of the copyright owner.  Further reproduction prohibited without permission.

PLEASE NOTE:

In all cases this material has been filmed in the best possible way from the available copy. Problems encountered with this document have been identified here with a check mark _✓_.

1. Glossy photographs or pages _____
2. Colored illustrations, paper or print _____
3. Photographs with dark background _✓_
4. Illustrations are poor copy _____
5. Pages with black marks, not original copy _____
6. Print shows through as there is text on both sides of page _____
7. Indistinct, broken or small print on several pages _✓_
8. Print exceeds margin requirements _____
9. Tightly bound copy with print lost in spine _____
10. Computer printout pages with indistinct print _____
11. Page(s) _____ lacking when material received, and not available from school or author.
12. Page(s) _____ seem to be missing in numbering only as text follows.
13. Two pages numbered _____. Text follows.
14. Curling and wrinkled pages _✓_
15. Other _____

University Microfilms International

Reproduced with permission of the copyright owner. Further reproduction prohibited without permission.

Reproduced with permission of the copyright owner. Further reproduction prohibited without permission.

# WAVE PROPAGATION IN DENSITY STRATIFIED FLUIDS.

BY

**JOHN ANTHONY GEAR**

(B.Sc. (HONS) (Monash))

**A THESIS SUBMITTED FOR THE DEGREE OF**

**DOCTOR OF PHILOSOPHY**

IN THE

DEPARTMENT OF MATHEMATICS

AT THE

UNIVERSITY OF MELBOURNE

JANUARY 1984.

Reproduced with permission of the copyright owner. Further reproduction prohibited without permission.

# ERRATUM.

PAGE I, PARA 2, LINE 7: the length scale are all determined.

P II, L 8: though, the coupled.....

P II, L(-2): Finally several numerical.....

P VIII, L 12: very useful result.....

P 2, L 1: forms an eigenvalue.....

P 4, L 6, L 9, L 12, L 15, L 17, L(-2); P 5, L 2, L(-2); P 6, L 4, L 6: Banks et al. .....

P 4, L 9: (cf. the definition.....

P 5, L 12: ..... , (1.1.9)

where this formula.....

P 7, L 13: inferred that: .....

P 8, L 1: $\kappa \to \infty$, .....

P 10, L 10; P 11, L 8; P 19, L 7, L 15; P 164, L 19: and Stegun ....

P 15, L(-3): evaluation at $z = 0$.

P 21, PARA 2, L 1: To integrate numerically.....

P 23, L (-3): foolproof only.....

P 23, L (-3): to its actual.....

P 38, L 7: If the flow is assumed to be steady.....

P 41, L 3: to at least three.....

P 41, L 12: Note here .....

P 47, L(-1): the length scale.....

P 79, L(-6): be compared with the.....

P 99, L(-4): in hydrostatic equilibrium.....

P 143, L(-8): $\Delta s/\Delta\xi^3$ ....

P 165, L 5: Deutsche .....

P 165, L(-9), L(-12): "Théorie .....

P 170, L 4: Ter-Krikorov A.M., 1963: "Théorie ....

Reproduced with permission of the copyright owner. Further reproduction prohibited without permission.

## ABSTRACT

This thesis falls into three distinct sections. In chapter one the fundamental properties of internal gravity waves are investigated, with respect to the effect that the basic physical quantities of fluid velocity, and buoyancy frequency, have upon the propagation of these waves. Among others things, it is shown that when the wavenumber tends to infinity the wave phase speeds are then found to depend only upon the local behavior of the mean flow near an overall maximum or minimum of the velocity profile. Also, the phase speed and group velocity are plotted against wavenumber, when the fluid velocity has a hyperbolic tangent and a hyperbolic secant profile. Several interesting phenomena are observed in these plots.

In shallow stratified fluids internal solitary waves are described, to first order in wave amplitude, by the Korteweg-de Vries equation; the solution for a single solitary wave has the familiar "$\text{sech}^2$"-profile and a phase speed which varies linearly with wave amplitude. In chapter two this theory is extended to second order in wave amplitude. The second order correction to the wave profile and the phase speed and the first order correction to the wavelength are all determined. Four special cases are considered in detail. It is shown that in certain special circumstances the first order theory may fail due to the vanishing of the nonlinear coefficient in the Korteweg-de Vries equation. When this occurs it is shown that a different theory is required which leads to an equation with both quadratic and cubic nonlinearities.

In chapter three the strong interaction between weakly nonlinear long internal gravity wave modes is studied. Strong interactions occur when the wave phase speeds are nearly equal although the waves belong to different modes. In shallow stratified fluids it is shown that this




Reproduced with permission of the copyright owner. Further reproduction prohibited without permission.

situation is described by two coupled Korteweg-de Vries equations, which possess both dispersive and nonlinear coupling terms. It is shown that these coupled equations possess three conserved quantities as well as an exact analytical solution involving the characteristic "$sech^2$"-profile of the Korteweg-de Vries equation. Also it is shown that when the coefficients satisfy some special conditions, the coupled equations possess an n-soliton solution in terms of the Korteweg-de Vries n-soliton solution. In general though the coupled equations are found not to be amenable to solution by inverse scattering technique, and thus a numerical method has been employed in order to solve the equations. This numerical method is described in detail in Appendix A. Finally severall numerical solutions of the coupled equations are presented.



Reproduced with permission of the copyright owner. Further reproduction prohibited without permission.

ACKNOWLEDGEMENTS

It is a pleasure to acknowledge the guidance and advice of my supervisor, Dr. R. Grimshaw. His encouragement and interest, over the past four years, has been invaluable.

It is also a pleasure to thank the many people who have had a beneficial effect upon my work. I thank Dr. W.W. Woods, Dr. G. Morris, Mr. K. Toohey, Mr. J. Rogers, Mr. G. Nassios and Dr. L. Trudzik. I also wish to thank the Australian Government for their support through a Commonwealth Postgraduate Research Award.

I am deeply indebted to my wife Debra for being persuaded to type this thesis. As well as her superb typing, she is responsible for keeping me sane and well fed throughout the past four years.

Finally, I wish to thank Debra, Bernice, Laurie, Rhonda, Bruce, Malcolm, Ann, Troy, Mark and Amber for their constant interest and encouragement.

Despite the help of many people involved in the preparation of this thesis I accept full responsibility for the errors which no doubt remain.



Reproduced with permission of the copyright owner. Further reproduction prohibited without permission.

Attestation.

I hereby attest that this thesis contains no material which has been accepted for the award of any other degree or diploma in any university and that, to the best of my knowledge and belief, the thesis contains no material previously published or written by another person, except where due reference is made in the text of the thesis.

.....



Reproduced with permission of the copyright owner. Further reproduction prohibited without permission.

Table of Contents.


| | | |
|---|---|---|
| Abstract | | I |
| Acknowledgements | | III |
| Attestation | | IV |
| Table of contents | | V |
| Introduction and Background | | VII |
| Chapter 1: | The properties of internal gravity waves in a parallel flow. | 1 |
| | 1.1 Introduction. | 1 |
| | 1.2 The effect of large wavenumber upon internal gravity wave modes. | 9 |
| | 1.3 Numerical results. | 21 |
| Chapter 2: | A second order theory for solitary waves in shallow fluids. | 34 |
| | 2.1 Introduction. | 34 |
| | 2.2 Analysis. | 41 |
| | 2.3 Discussion. | 50 |
| | 2.3(I) Shear layer. | 50 |
| | 2.3(II) Uniform stratification. | 62 |
| | 2.3(III) Inversion layer. | 72 |
| | 2.3(IV) Two-layer fluid. | 76 |
| | 2.4 Regularization when $\mu \to 0$. | 83 |




Reproduced with permission of the copyright owner. Further reproduction prohibited without permission.

Chapter 3: Strong interactions between internal solitary waves. 95

3.1 Introduction. 95

3.2 Formulation. 99

3.3 Some properties of the evolution equations. 105

3.4 Inverse scattering and the Painlevé criterion. 110

3.5 Numerical solutions. 117

Appendix A: Numerical method of chapter three. 141

Appendix B: Three layer fluid. 145

Appendix C: "A second order theory for solitary waves in shallow fluids", Phys. Fluids, 26, 14-29, 1983. 148

Bibliography 164



Reproduced with permission of the copyright owner. Further reproduction prohibited without permission.

## Introduction and Background

Internal gravity waves are an important feature of the atmosphere and ocean, they are usually found propagating along the boundary between two fluids of different density (the pycnocline), usually they are dispersive and can be nonlinear even for modest amplitudes. In this thesis both the linear and nonlinear aspects of internal gravity waves will be investigated. In Chapter one internal gravity waves will be investigated, with respect to the effect that the fluid velocity, and buoyancy frequency have upon the propagation of these waves. In the absence of a basic flow, internal gravity waves have been studied extensively (see the books of Turner (1973) and Yih (1980)), and are recognized as important in many applications. Yet in the phenomena to which the theory of internal gravity waves is applied there is frequently substantial shear in the mean flow. Analytical studies of internal gravity waves in parallel shear flows, may be dated from the closely related works of Taylor (1931) and Goldstein (1931). These two papers, dealing primarily with specific flow configurations, were followed closely by Synge's (1933) study of the general boundary-value problem.

Taylor (1931) considered a semi-infinite flow above a horizontal wall with constant shear and constant Brunt-Väisälä frequency. Taylor concluded that only neutral modes (modes for which the phase speed is real) could exist when the Richardson number (Ri) was greater than $\frac{1}{4}$ and no waves could exist for $0 < Ri < \frac{1}{4}$. These results were clarified and extended by Eliassen, Hoilland and Riis (1953), who considered flow between two parallel walls with $U'$ and $N^2$ constant (here U is the horizontal fluid velocity and $N^2$ is the Brunt-Väisälä frequency). Goldstein (1931) considered an imbedded shear layer of thickness 2h, with both $U'$ and $N^2$ constant in $|z| < h$ and vanishing in $|z| > h$ (here z is the vertical



Reproduced with permission of the copyright owner. Further reproduction prohibited without permission.

co-ordinate). He concluded that harmonic perturbations would be stable for $Ri > \frac{1}{4}$ and unstable for all wavelengths where $0 < Ri < \frac{1}{4}$. Drazin (1958), Menkes (1959, 1961) and Holmboe (1960) considered more realistic profiles for U and $N^2$. They also concluded that harmonic perturbations would be stable for $Ri > \frac{1}{4}$, but predicted instability only for a finite range of wavelengths when $0 < Ri < \frac{1}{4}$. For internal gravity waves the most significant results in linear stability theory are due to Miles (1961) and Howard (1961). Miles (1961) considered the stability of parallel flow when the velocity and density distributions are assumed to be analytic. Several theorems were presented, some of which were improvements on known results due to Synge (1933) and some were entirely new. These theorems culminated in the very usefully result that the flow is stable if the velocity is monotonic and if the Richardson number is everywhere greater than $\frac{1}{4}$. Howard (1961) extended this theorem to apply when the velocity and density are not assumed to be analytic and the velocity is not assumed to be monotonic. He has also shown that the complex phase speed c for any unstable mode must lie inside the semi-circle in the upper half-plane which has the range of U for the diameter (the semi-circle theorem). In addition, an upper bound for the growth rate is given, and the connection with Rayleigh's theorem is discussed. For more information on the linear stability theory of plane parallel flows see the surveys of Drazin and Howard (1966) and Howard and Maslowe (1973).

So far the papers discussed have basically considered only the linear stability of plane parallel flow, none have considered the overall pattern, of the normal modes. Recently though, the works of Bell (1974), Banks et al (1976) and Leibovich (1979) have investigated the behavior of the dispersion relation for internal gravity waves with shear. Using Sturmian methods, Bell (1974) has shown that (a) if $Ri > \frac{1}{4}$ for all z of interest, a denumerably infinite set of normal modes exist for each



Reproduced with permission of the copyright owner. Further reproduction prohibited without permission.

fixed value of the wavenumber $\kappa$ and that the phase speed c of these modes has a finite maximum (minimum) and converges to $U_{max}$ ($U_{min}$) as n increases indefinitely, and (b) for fixed mode number n, $|c|$ is a decreasing function of the wavenumber which tends to $U_{max} + N_{max}/\kappa$ ($|U_{min}| + N_{max}/\kappa$) as $\kappa$ increases. In the work of Banks et al (1976), the general analytic treatment concentrates on bounded flows with constant Brunt-Väisälä frequency, and applies spectral theory to deduce the mode pattern as the Richardson number varies. Asymptotic results for large Richardson number are derived and variable Brunt-Väisälä frequency is also considered in this section. The case of small Richardson number is examined analytically by the method of matched asymptotic expansions. These asymptotic results are confirmed and complimented by direct integration of the Taylor-Goldstein equation for the case of a sinusoidal basic velocity profile and for the Bickley jet. Leibovich (1979) has proven that: if the maximum speed $U_{max}$ or minimum speed $U_{min}$ occurs at an interior point of the fluid, then the phase speed of any mode takes all values from $U_{max}$ (or $U_{min}$) to $+\infty$ ($-\infty$) as the overall Richardson number varies from 0 to $\infty$. (Note the overall Richardson number is defined in Chapter one.) If $U_{max}$ ($U_{min}$) is attained at a boundary point with finite rate of strain, there is a positive nonzero critical Richardson number below which one or both branches of the dispersion relation terminate. The bounds on the group velocity of propagating neutral modes have also been established by Leibovich (1979). For some numerically calculated dispersion relations see Thorpe (1978) and Liu and Benney (1981). Also Bell (1974) has a comprehensive list of references where dispersion relations have been calculated for both shear flows and flows where U' is zero.

Solitary internal gravity waves are defined as waves of single elevation which propagate at uniform velocity without change of form. The existence of these stationary waves may be viewed as being the



Reproduced with permission of the copyright owner. Further reproduction prohibited without permission.

consequence of equilibrium between the competing effects of nonlinearity and dispersion. The study of solitary waves began with the observations of Russell (1838, 1845). Whilst observing the movement of a canal barge, Russell noticed a novel type of water wave on the surface of the canal, he observed that this wave moved forward with great velocity, assuming the form of a large solitary elevation, which continued its course along the channel apparently without change of form or diminution of speed. Following this observation Russell carried out extensive experiments where he produced solitary waves in a laboratory channel by either releasing an impounded elevation of water or dropping a weight at one end of the channel. There was subsequently a gap of more than sixty years between Russell's observations of the shallow water solitary wave and any theoretical treatment of the phenomenon. Initial theoretical confirmation of Russell's work had to wait until Korteweg and de Vries (1895), derived their now famous equation for the propagation of waves in one direction on the surface of a canal. Their equation had permanent wave solutions, including solitary waves. Boussinesq (1871, 1872), also derived a nonlinear evolution equation governing such long waves. Both Boussinesq (1871, 1872) and Rayleigh (1876) obtained solitary wave solutions.

Current interest in solitary waves stem from the discovery by Zabusky and Kruskal (1965), that solitary wave solutions of the Korteweg-de Vries equation with different amplitudes, and hence different speeds, pass through one another without any permanent loss of identity and suffer only phase shifts, even though nonlinear distortion is quite significant during the interaction. They termed these solutions solitons. Subsequently, Gardner, Greene, Kruskal and Miura (1967, 1974), Zakharov and Shabat (1972) and Ablowitz, Kaup, Newell and Segur (1973, 1974) developed a method of solution for the Korteweg-de Vries equation and other nonlinear evolution equations, by making use of the ideas of direct and inverse



Reproduced with permission of the copyright owner. Further reproduction prohibited without permission.

scattering. This procedure has been termed the inverse scattering transform.

In shallow stratified fluids small amplitude internal solitary waves are described, to first order in wave amplitude, by the Korteweg-de Vries equation; the solution for a single solitary wave has the familiar "$\text{sech}^2$"-profile and a phase speed which varies linearly with wave amplitude. Solitary waves in shallow stratified two layer fluids have been considered by Keulegan (1953), Long (1956) and Kakutani and Yamasaki (1978). For continuously stratified shallow fluids they have been considered by Long (1965), Peters and Stoker (1960), Benjamin (1966), Benney (1966), Leonov and Miropol'skiy (1975), Weidman (1978) and Miles (1979). Benjamin (1966), Benney (1966), Long (1956) and Miles (1979) also allow for shear. Observations of internal solitary waves show that moderate or large amplitudes are quite common. In contrast, theories for finite amplitude solitary waves are very sparse being confined mainly to cases involving two-layer fluids or weakly stratified fluids. Hence, in chapter two, finite amplitude internal solitary waves are investigated by constructing an amplitude expansion which leads to an integrated Korteweg-de Vries equation at first order, and then continuing this expansion to second order in wave amplitude. In some situations it is found that the first order theory may fail due to the vanishing of the nonlinear coefficients in the Korteweg-de Vries equation. In this situation it is shown that a different theory is required which leads to, at first order, an equation containing both quadratic and cubic nonlinearities. Note that Long (1956), Kakutani and Yamasaki (1978) and Miles (1979) also consider the case where cubic nonlinearity is comparable with quadratic nonlinearity. Also note that the work in chapter two was performed in collaboration with Dr. R. Grimshaw.

In chapter three strong interactions between nonlinear long



Reproduced with permission of the copyright owner. Further reproduction prohibited without permission.

internal gravity wave modes are studied. Strong interactions occur when the wave phase speeds are nearly equal although the waves belong to different modes. This terminology is adapted from Miles (1977a,b) who considered the oblique interaction of surface solitary waves. Weak interactions between different modes occur when the phase speeds of these modes differ by an order one quantity with respect to the small parameter which measures dispersion (see §3.1). Weak interactions between surface solitary waves have been considered by Oikawa and Yajima (1973) and Su and Mirie (1980), while the weak interaction between internal solitary waves have been considered by Gear and Grimshaw (1984). It is shown in these papers that weak interactions allow linear superposition of the individual solutions of the Korteweg-de Vries equation at leading order. However, there is a phase shift and Su and Mirie (1980) show that secondary waves are also shed during these interactions. Strong interactions between internal solitary waves have been considered by Liu et al (1980, 1982) and Gear and Grimshaw (1984). Liu et al (1980, 1982) consider the interaction between internal solitary waves in neighboring pycnoclines, when the pycnoclines are widely separated they found that the interactions were governed by a pair of coupled nonlinear equations, each equation having the form of the intermediate depth equation (Joseph (1977) or Kubota, Ko and Dobbs (1978)) and a dispersive coupling term. Also Weidman and Johnson (1982) have experimentally investigated the strong interaction between internal solitary waves on widely separated pycnoclines. Their experimental results agree quantitatively with the results of Liu et al (1980, 1982). Finally it should be noted that the strong interaction case discussed in chapter three differs from the direct resonance recently discussed by Akylas and Benney (1980, 1982). Direct resonance requires both the wave phase speeds and the modal functions, which describe the vertical extent of the waves, to be nearly equal. In chapter three this



Reproduced with permission of the copyright owner. Further reproduction prohibited without permission.

latter condition cannot occur, due to the orthogonality of the modal functions. For more information on the interaction of internal and surface solitary waves see the review by Miles (1980).



Reproduced with permission of the copyright owner. Further reproduction prohibited without permission.

## Chapter 1: The properties of internal gravity waves in a parallel flow.

### §1.1 Introduction

Consider waves propagating horizontally in an inviscid, incompressible fluid, with the x-axis in the direction of propagation. The horizontal waveguide is characterized by a basic density profile $\rho_0(z)$ and a basic velocity profile U(z), bounded above and below by rigid boundaries at z = 0 and z = h, with z increasing upwards. In the theory of internal wave propagation, the vertical particle displacement at any point in the fluid is given by

$$\eta(x, z; t) = \phi(z) \exp[i\kappa(x - ct)] , \qquad (1.1.1)$$

where $\phi(z)$ is the vertical modal function, defined by (see Miles (1961))

$$\frac{d}{dz}\left(\rho_0(c - U)^2 \frac{d\phi}{dz}\right) + \rho_0\left(N^2 - \kappa^2(c - U)^2\right)\phi = 0 \quad \text{for } 0 < z < h , \qquad (1.1.2a)$$

$$\phi = 0 \quad \text{at} \quad z = 0 , \qquad (1.1.2b)$$

$$\phi = 0 \quad \text{at} \quad z = h . \qquad (1.1.2c)$$

Here $\kappa$ is the wavenumber, c is the wave phase speed, and $N^2(z)$ is the Brunt-Väisälä frequency, defined by

$$N^2(z) = -\frac{g}{\rho_0}\frac{d\rho_0}{dz} , \qquad (1.1.3)$$

where g is the acceleration of gravity. Equation (1.1.2a) is a second order, self adjoint, Sturmian equation, which together with (1.1.2b and c)



Reproduced with permission of the copyright owner. Further reproduction prohibited without permission.

forms and eigenvalue problem for $\phi$ where c is the eigenvalue and $\kappa$ is regarded as a fixed parameter. It is well known from the theory of stratified shear flow stability (Miles (1961, 1963), Howard (1961)) that a sufficient condition that c be real for real $\kappa$ is that the Richardson number Ri(z), where

$$Ri(z) = \frac{N^2(z)}{(U'(z))^2} \qquad (1.1.4)$$

is greater than one quarter for $0 \leq z \leq h$. That is if the local Richardson number is greater than one quarter throughout the flow, only real valued phase speeds need be considered. It has been shown by Bell (1974) that this condition on the Richardson number is also sufficient to insure the existence of a denumerably infinite set of internal gravity wave modes in the solution of the governing system (1.1.2a,b,c). Here an internal wave of mode number n is defined as a solution of (1.1.2a,b and c) which has exactly (n - 1) nodes or zeros in the open interval (0, h). Using Kneser's oscillation theorem (see Swanson (1968) §2.1) Bell has shown that if the local Richardson number is greater than one quarter thoughout the flow, then solutions of equations (1.1.2a,b,c) may be made to oscillate infinitely rapidly by choosing the phase speed c to be within the range of U (i.e. $U_{min} \leq c \leq U_{max}$ where $U_{max}$ ($U_{min}$) represents the maximum (minimum) of the velocity U in the interval (0, h)). In particular, if the local Richardson number is greater than one quarter, then as c approaches $U_{max}$ from above or $U_{min}$ from below, the solutions of (1.1.2a,b,c) may be made to oscillate arbitrarily rapidly in z. This conclusion remains valid if $U_{max}$ or $U_{min}$ occurs on a point interior to (0, h), at which point U' vanishes and Ri(z) is infinite. Thus there exists an infinite number of modes propagating in the +x (-x) direction and as the mode number n tends to infinity the phase speed for these modes tends to $U_{max}$ ($U_{min}$).



Reproduced with permission of the copyright owner. Further reproduction prohibited without permission.

It has also been shown by Bell (1974) that a sufficient condition such that throughout the interval (0, h) the solutions of (1.1.2a) are non-oscillatory or oscillatory can be obtained by invoking the Sturm-Picone comparison theorem (see Ince (1956) §10.32). Using this theorem it is readily shown that if $c > c_0$, where

$$c_0 = U_{max} + \frac{(\rho_0 N^2)_{max}}{\rho_{0min}[\kappa^2 + \pi^2/h^2]^{1/2}}, \qquad (1.1.5)$$

then no solution of (1.1.2a) can satisfy both boundary conditions (1.1.2b,c). Thus $c_0$ represents a finite upper bound on the eigenvalues c for any given $\kappa$. In fact using the Sturm-Picone comparison theorem it is possible to show that a finite upper bound on the $n^{th}$ mode is given by

$$c_{0n} = U_{max} + \frac{(\rho_0 N^2)_{max}}{\rho_{0min}[\kappa^2 + n^2\pi^2/h^2]^{1/2}}, \qquad (1.1.6)$$

That is if $c > c_{0n}$, then no solution of (1.1.2a) that has n - 1 nodes in $0 < z < h$, can satisfy both boundary conditions (1.1.2b,c). Note that here $(\rho_0 N^2)_{max}$ ($\rho_{0min}$) represents the maximum (minimum) of $\rho_0 N^2$ ($\rho_0$) in the interval $0 \leq z \leq h$. Note also that a completely analogous result may be obtained for waves travelling in the - x direction by replacing $U_{max}$ with the magnitude of $U_{min}$ and considering the magnitude of c. It should also be noted that equation (1.1.6) implies that $|c|$ is a decreasing function of the wavenumber $\kappa$. Using the Sturm-Picone comparison theorem it was also shown by Bell (1974) that, if for some ($\kappa_s$, $c_s$) the system (1.1.2a,b and c) has a non-trivial solution, then a small increase in $\kappa$ will cause the solution of (1.1.2a), with $\phi(0) = 0$, to oscillate less rapidly, and the zero at z = h will move out of the range $0 < z \leq h$. However a subsequent



Reproduced with permission of the copyright owner. Further reproduction prohibited without permission.

decrease in c will retrieve the zero at z = h, so that for any mode number n, c is a decreasing function of $\kappa$ which tends to $U_{max} + (\rho_0 N^2)_{max}/\rho_{0min}\kappa$ as $\kappa$ increases. Similarly for waves travelling in the -x direction c is an increasing function of $\kappa$ which tends to $U_{min} - (\rho_0 N^2)_{max}/\rho_{0min}\kappa$ as $\kappa$ increases.

The effects of varying the Richardson number, upon the solutions of (1.1.2a,b and c) have been investigated by Banks et al (1976) and Leibovich (1979). An overall Richardson number which is characteristic of Ri(z) over the interval [0, h] can be defined by (c.f. the definition of Leibovich (1979) and Banks et al (1976))

$$J = \frac{N^2(z)}{\hat{N}^2(z)} \qquad (1.1.7)$$

where $\hat{N}^2(z)$ is a normalized function describing the shape of $N^2(z)$. Banks et al (1976) have investigated the solutions of (1.1.2a,b,c) as $J \to \infty$, they showed that the phase speed c and the eigenfunction $\phi$ have a power series expansion in powers of $J^{-1/2}$, for sufficiently large J. Both Leibovich (1979) and Banks et al (1976) have shown that $|c| \propto J^{1/2}$ as $J \to \infty$. The effects upon the solutions of (1.1.2a,b and c), as $J \to 0$ have been investigated by both Leibovich (1979) and Banks et at (1976). Leibovich has shown that c decreases with decreasing J for all $c > U_{max}$ and c increases with decreasing J for all $c < U_{min}$. In fact if the fluid velocity has an extreme value at a point interior to the flow, say $U(z_0)$ is an extreme value of U(z), where $U'(z_0) = 0$ and $z_0 \in (0, h)$, then it has been shown that as $J \to 0$, the phase speed $c \to U_{extreme}$. Using matched asymptotic expansions for the case where $U'(z_0) = 0$, $z_0 \in (0, h)$, Banks et al have shown that the phase speed has the expansion

$$c_n = U(z_0) - \frac{2J\hat{N}^2(z_0)}{U''(z_0)n(n+2)} + O(J^2) \quad \text{as} \quad J \to 0 \ . \qquad (1.1.8)$$



Reproduced with permission of the copyright owner. Further reproduction prohibited without permission.

Note here that $c_n$ is the phase speed of the $n^{th}$ mode. It should also be stated that in deriving (1.1.8), Banks et al have only assumed that $c - U(z_0)$ is small, thus the expansion (1.1.8) is valid provided the term $2J\hat{N}^2(z)/[U''(z_0)n(n+2)]$ is small. Then (1.1.8) is a valid expansion for the phase speed c as the overall Richardson number $J \to 0$, or as the mode number $n \to \infty$, or as $U''(z_0) \to \infty$. An example of the last case could be $U(z) = \mu(z - \frac{h}{2})^2$, then $U''(\frac{h}{2})$ tends to infinity as $\mu \to \infty$. It should also be noted that if $U'(z_0) = 0$ and $z_0$ is a boundary point of the flow (i.e. $z_0$ is either 0 or h), then using matched asymptotic expansions it can be shown that the required asymptotic formula for the phase speed of the $n^{th}$ mode, is

$$c_n \simeq U(z_0) - \frac{J\hat{N}^2(z_0)}{2U''(z_0)n(n+1)} . \qquad (1.1.9)$$

Where this formula is a valid approximation provided that either $J \to 0$, $n \to \infty$ or $U''(z_0) \to \infty$.

The above ideas are applicable only at extreme values of the velocity where $U'(z) = 0$. Consider the case where an extreme value of the velocity occurs at a boundary point with $U' \neq 0$ there. Note, that at this extreme point of the velocity the local Richardson number may be less than 1/4, unlike the previously discussed case where $Ri(z_0)$ was infinite. In this case it has been shown by Leibovich (1979) that as $c \to U_{extreme}$ the overall Richardson number J does not necessarily tend to zero. In other words as $c \to U_{extreme}$, J approaches some positive constant other than zero. It has been shown by Banks et al (1976) that for all but p modes (where p is some positive integer possibly zero), the phase speed $c \to U(z_c)$ (if $U(z_0)$ is the extreme point where $U'(z_0) \neq 0$), provided that $J \downarrow \frac{1}{4} U'^2(z_0)/\hat{N}^2(z_0)$ (or $Ri(z_0) \downarrow \frac{1}{4}$). In fact Banks et al have shown using matched asymptotic expansions that in this case the phase speed of the $n^{th}$



Reproduced with permission of the copyright owner. Further reproduction prohibited without permission.

mode is given by the following approximation.

$$c_n \simeq U(z_0) - U'(z_0)\, D\, e^{-j\pi/\omega} \quad \text{as} \quad \omega \to 0\,, \quad \text{for} \quad j = 1, 2, \text{---}\,, \tag{1.1.10a}$$

where

$$\omega = \left(\frac{J\hat{N}^2(z_0)}{U'^2(z_0)} - \frac{1}{4}\right)^{1/2}\,. \tag{1.1.10b}$$

Here the constant D is determined by the outer expansion (see Banks et al (1976)) and $j = n - p$ where n the mode number is greater than p. For the final p modes it was shown by Banks et al that for $J < \frac{1}{4}U'^2(z_0)/\hat{N}^2(z_0)$ as $c \to U(z_0)$ the overall Richardson number J, approaches a positive constant other than zero. In summary then, if $J_m$ is a positive constant which may be less than or greater than $\frac{1}{4}U'^2(z_0)/\hat{N}^2(z_0)$, as $J \to J_m$ the phase speed of the $m^{th}$ mode $c_m \to U(z_0)$. In deriving (1.1.10a) Banks et al have only assumed that $c - U(z_0)$ is small, thus the expansion (1.1.10a) is a valid approximation, provided $U'(z_0)e^{-n\pi/\omega}$ is small. Then (1.1.10a) is a valid approximation for the phase speed c as $\omega \to 0$, or as $n \to \infty$.

It should be noted that none of the approximations (1.1.8), (1.1.9) or (1.1.10a) consider the effect of infinite wavenumber, upon the phase speed c, and the modal functions $\phi$. In §1.2 this situation will be discussed in some detail and asymptotic expansions for the phase speed c when $\kappa$ is large, will be determined for the case where the velocity has a simple extremum at an interior point of the fluid or at a boundary point of the flow; and where the velocity has an extreme value at a boundary of the flow and U' there, is non zero. In §1.3 the eigenvalue problem (1.1.2a,b and c) will be solved for two specific flows by using a numerical technique. The phase speed c and the group velocity are then plotted versus the wavenumber $\kappa$ for in one case thirteen modes and in the other case ten modes. The numerical method used to determine the phase speed is



Reproduced with permission of the copyright owner. Further reproduction prohibited without permission.

described in detail in §1.3.

It finally remains to discuss the group velocity. Now, for any internal gravity wave mode the group velocity is defined to be

$$c_g(\kappa) = \frac{d}{d\kappa}(\kappa c) = c + \kappa \frac{dc}{d\kappa} . \qquad (1.1.11)$$

To determine how the group velocity corresponding to a given branch of the dispersion relation (i.e. $c > U_{max}$ or $c < U_{min}$) is related to the phase speed on that branch Leibovich (1979) differentiated (1.1.2a) with respect to $\kappa$ and after some manipulations involving variational techniques has shown that

$$\kappa \frac{dc}{d\kappa} = \frac{-\kappa^2 \int_0^h \rho_0 (c - U)^2 \phi^2 dz}{\int_0^h \rho_0 (c - U)(\phi'^2 + \kappa^2 \phi^2) dz} . \qquad (1.1.12)$$

Now by hypothesis, for all admissible values of c, U - c is either strictly positive or strictly negative, depending upon which branch is selected for $c(\kappa)$. From (1.1.12) it therefore may be inferred that; $\kappa dc/d\kappa$ has the same sign as (U - c), thus for $c > U_{max}$, $c_g < c$, and for $c < U_{min}$, $c_g > c$. Also $\kappa dc/d\kappa \to 0$ as $\kappa \to 0$, hence $c_g \uparrow c$ if $c > U_{max}$ and $c_g \downarrow c$ if $c < U_{min}$ in the limit $\kappa \to 0$.

Another important property of the group velocity was derived by Leibovich (1979) after he noticed that $\kappa^2\phi^2 < \kappa^2\phi^2 + \phi'^2$, then (1.1.12) can be manipulated to give

$$\int_0^h \rho_0 (c - U)(c_g - U)(\phi'^2 + \kappa^2 \phi^2) dz > 0 . \qquad (1.1.13)$$

From (1.1.13) it can be seen that if $c > U_{max}$ then $c_g > U_{min}$ and if $c < U_{min}$ then $c_g < U_{max}$. Also from (1.1.5) and (1.1.6) it is seen that as



Reproduced with permission of the copyright owner. Further reproduction prohibited without permission.

$\kappa \to \infty$ $c-U_{extreme}$ is proportional to $\kappa^{-1}$. Thus, as $\kappa \to \infty$ $\kappa dc/d\kappa$ is proportional to $\kappa^{-1}$, and then $c_g \to c \to U_{extreme}$. In summary, for the upper branch ($c > U_{max}$), $U_{min} < c_g < c$, $c_g(0) = c(0)$ and $c_g \to c \to U_{max}$ as $\kappa \to \infty$; while for the lower branch ($c < U_{min}$), $c < c_g < U_{max}$, $c_g(0) = c(0)$ and $c_g \to c \to U_{min}$ as $\kappa \to \infty$.



Reproduced with permission of the copyright owner. Further reproduction prohibited without permission.

## §1.2 THE EFFECT OF LARGE WAVENUMBER UPON INTERNAL GRAVITY WAVE MODES

It has been shown by Bell (1974) and stated in §1.1 that the modulus of the phase speed is a decreasing function of the wavenumber $\kappa$, and that as the wavenumber tends to infinity the nodes of the eigenfunctions congregate at an extreme value of the velocity (i.e. as c tends to $U_{max}$ or $U_{min}$ the solutions of (1.1.2a,b and c) oscillate arbitrarily rapidly in the neighborhood of the extreme point). To investigate the effect of large wavenumber upon internal gravity waves, transform equations (1.1.2a,b and c) into canonical form. Thus (1.1.2a,b,c) become

$$\frac{d^2\psi}{dz^2} + q^2(z)\,\psi = 0 , \tag{1.2.1a}$$

$$\psi(0) = \psi(h) = 0 , \tag{1.2.1b}$$

where

$$q^2(z) = -\kappa^2 + \frac{N^2}{(c - U)^2} + \frac{U''}{(c - U)} + \frac{\rho_0'U'}{\rho_0(c - U)} - \frac{1}{2}\left(\frac{\rho_0'}{\rho_0}\right)' - \frac{1}{4}\left(\frac{\rho_0'}{\rho_0}\right)^2 \tag{1.2.1c}$$

and

$$\psi(z) = -i\kappa(c - U)\sqrt{\rho_0}\,\phi(z) . \tag{1.2.1d}$$

Here $\psi(z)$ represents the structure of the vertical velocity multiplied by the square root of the density. Also note that when the Boussinesq approximation is taken (i.e. $\rho_0$ = const.) then (1.2.1a) reduces to the Taylor-Goldstein equation (Bell (1974), Thorpe (1969)).

An approximate method of solving (1.2.1a and b) is the W.K.B. method (Olver (1974)). If an extreme value of the velocity, U(z), occurs



Reproduced with permission of the copyright owner. Further reproduction prohibited without permission.

at $z = z_0$, where $z_0 \in [0, h]$, then as the wavenumber $\kappa$ tends to infinity, the phase speed c must approach $U(z_0)$. Suppose that as $\kappa \to \infty$, $q^2(z_0 - \delta_1) = q^2(z_0 + \delta_2) = 0$, where $1 \gg \delta_1, \delta_2 > 0$. Then in the interval $(z_0 - \delta_1, z_0 + \delta_2)$, $q^2(z)$ will be positive and the solutions of (1.2.1a,b) will be oscillatory, whereas in the intervals $[0, z_0 - \delta_1)$, $(z_0 + \delta_2, h]$, $q^2(z)$ will be negative and the solutions of (1.2.1a and b) will be exponential. The points $z = z_0 - \delta_1, z_0 + \delta_2$ are called transition points, and at such points the W.K.B. approximation is invalid. Near these transition points the solutions of (1.2.1a and b) are given in terms of Airy functions (Abramowitz and Stegan (1965)). The Airy functions possess the property that when their argument is positive, they are exponential, and when their argument is negative, they are oscillatory.

Consider the transition point at $z = z_0 - \delta_1$, if $\hat{z}_1$ is any interior point of $(z_0 - \delta_1, z_0 + \delta_2)$, and suppose that $z_1^*$ is an element of $(0, z_0 - \delta_1)$. Then in the interval $(z_1^*, \hat{z}_1)$ equation (1.2.1a) has an approximate solution of the form (Olver (1974) ch. 11),

$$\phi_1(z) = (-q^2/\zeta_1)^{-1/4}\{a_1 Ai(\zeta_1) + b_1 Bi(\zeta_1)\} , \qquad (1.2.2a)$$

where

$$\zeta_1 = \mp\left|\frac{3}{2}\int_{z_0-\delta_1}^{z} q(t)dt\right|^{2/3} , \quad z \gtrless z_0 - \delta_1 . \qquad (1.2.2b)$$

Here $Ai(\zeta_1)$ and $Bi(\zeta_1)$ are Airy functions of the first and second kind respectively. In order to satisfy the boundary condition at $z = 0$, it is necessary to choose $b_1$ equal to zero, this is because $Bi(\zeta_1)$ grows exponentially large as $z \to 0$. Similarly, if $\hat{z}_2$ is an interior point of $(z_0 - \delta_1, z_0 + \delta_2)$, and $z_2^* \in (z_0 + \delta_2, h)$, then in the interval $(\hat{z}_2, z_2^*)$ a solution of (1.2.1a) which is recessive at $z = h$ is given by

$$\phi_2(z) = a_2 (-q^2/\zeta_2)^{-1/4} Ai(\zeta_2) , \qquad (1.2.3a)$$



Reproduced with permission of the copyright owner. Further reproduction prohibited without permission.

where $$\zeta_2 = \pm\left|\frac{3}{2}\int_{z_0+\delta_2}^{z} q(t)dt\right|^{2/3}, \quad z \gtrless z_0 + \delta_2 . \qquad (1.2.3b)$$

If $\hat{z}_2$ is less than $\hat{z}_1$, then the two solutions, $\phi_1(z)$ and $\phi_2(z)$ must not be independent in the interval $(\hat{z}_2, \hat{z}_1)$. Thus the Wronskian of $\phi_1$ and $\phi_2$ must vanish in the open interval $(\hat{z}_2, \hat{z}_1)$. Before evaluating the Wronskian of $\phi_1$ and $\phi_2$, suppose that $z = Z$ is an interior point of $(\hat{z}_2, \hat{z}_1)$, and also suppose that at $z = Z$, both $\zeta_1$ and $\zeta_2$ are large and negative, then the Airy function Ai in (1.2.2a) and (1.2.3a) may be replaced by its asymptotic expansion for large negative argument (see Abramowitz and Stegan (1965)). At $z = Z$, $\phi_1$, $\phi_2$ and their derivatives are approximated by

$$\phi_1(Z) = a_1\pi^{-1/2}q(Z)^{-1/2}\{\sin(\theta + \tfrac{\pi}{4}) + O(\kappa^{-1/2})\}, \qquad (1.2.4a)$$

$$\phi_1'(Z) = a_1\pi^{-1/2}q(Z)^{1/2}\{\cos(\theta + \tfrac{\pi}{4}) + O(\kappa^{-1/2})\}, \qquad (1.2.4b)$$

where $$\theta = \int_{z_0-\delta_1}^{Z} q(t)dt \qquad (1.2.4c)$$

and $$\phi_2(Z) = (-1)^{n-1}a_2\pi^{-1/2}q(Z)^{-1/2}\{\sin(n\pi + \hat{\theta} + \tfrac{\pi}{4}) + O(\kappa^{-1/2})\}, \qquad (1.2.4d)$$

$$\phi_2'(Z) = (-1)^{n-1}a_2\pi^{-1/2}q(Z)^{1/2}\{\cos(n\pi + \hat{\theta} + \tfrac{\pi}{4}) + O(\kappa^{-1/2})\}, \qquad (1.2.4e)$$

where $$\hat{\theta} = \int_{z_0+\delta_2}^{Z} q(t)dt . \qquad (1.2.4f)$$

Note that here it has been assumed that the phase of the solution $\phi_2$ at $z = h$, is $n\pi$, or, the solutions $\phi_1$, $\phi_2$ correspond to the $n^{th}$ mode. Now the condition that the Wronskian of $\phi_1$ and $\phi_2$ vanishes at $z = Z$ gives



Reproduced with permission of the copyright owner. Further reproduction prohibited without permission.

$$0 = (-1)^n a_1 a_2 \pi^{-1} \{\sin(\theta - \hat{\theta} - n\pi) + O(\kappa^{-1/2})\} \qquad (1.2.5a)$$

and accordingly

$$I = \theta - \hat{\theta} = \int_{z_0 - \delta_1}^{z_0 + \delta_2} q(t)dt = n\pi + O(\kappa^{-1/2}) \ . \qquad (1.2.5b)$$

Now from (1.2.1c), put

$$q^2(z) = -\kappa^2 + \frac{M^2(z)}{(c - U(z))^2} \ , \qquad (1.2.6a)$$

where
$$M^2(z) = N^2(z) + (c - U)\left(U'' + U' \frac{\rho_0'}{\rho_0}\right)$$

$$- (c - U)^2 \left(\frac{1}{2}\left\{\frac{\rho_0'}{\rho_0}\right\}' + \frac{1}{4}\left\{\frac{\rho_0'}{\rho_0}\right\}^2\right) \ , \qquad (1.2.6b)$$

and also let

$$g(z) = \kappa \ \mathrm{sign}(U_0'') \ \frac{(U(z) - c)}{M(z)} \ . \qquad (1.2.6c)$$

where $U_0''$ signifies $U''(z_0)$. It has already been stated that in the interval $(z_0 - \delta_1, z_0 + \delta_2)$, $q^2(z)$ is positive, while outside this interval $q^2(z)$ is negative, thus, there must be a point in $(z_0 - \delta_1, z_0 + \delta_2)$, say $z = \bar{z}$, where $q^{2\prime}(\bar{z})$ is zero. It is then easily verified, using (1.2.6c) that $g'(\bar{z}) = 0$. Let $\gamma = g(\bar{z})$ and noting that $U'(z_0) = 0$, then by expanding $U(\bar{z})$ and $M(\bar{z})$ in Taylor series about $z_0$, $\gamma$ can be written as

$$\gamma = \kappa \ \mathrm{sign}(U_0'') \ \frac{(U_0 - c)}{N_0} \ (1 + O(\kappa^{-1})) \ . \qquad (1.2.7)$$



Reproduced with permission of the copyright owner. Further reproduction prohibited without permission.

Here $U_0$ ($N_0$) represents $U(z_0)$ ($N(z_0)$) and it has been assumed that if $z \varepsilon (z_0 - \delta_1, z_0 + \delta_2)$ then $c - U(z)$ is $O(\kappa^{-1})$, this obviously must be correct otherwise $q^2(z)$ cannot be positive in $(z_0 - \delta_1, z_0 + \delta_2)$. Now in order to evaluate (1.2.5b), it is convenient to define a new variable v, such that

$$v^2 = g(z) - g(\bar{z}) = g(z) - \gamma. \tag{1.2.8}$$

If g(z) is expanded in a Taylor series about the point $z = \bar{z}$ then (1.2.8) can be written as

$$\begin{aligned} v^2 &= \frac{1}{2} g''(\bar{z}) (z - \bar{z})^2 + O\big((z - \bar{z})^3\big) \\ &= \frac{(z - \bar{z})^2 |U_0''| \kappa}{2N_0} \{1 + O(z - \bar{z}) + O(\kappa^{-1})\} \end{aligned} \tag{1.2.9}$$

and thus v is a regular function of z. Now substituting (1.2.6c) and (1.2.8) into (1.2.6a) gives

$$q^2 = \kappa^2 \Big(\frac{1}{(\gamma + v^2)^2} - 1\Big) . \tag{1.2.10}$$

Then substituting (1.2.10) into (1.2.5b) and using (1.2.9) to change the differential, (1.2.5b) becomes

$$\begin{aligned} I &= \Big\{\frac{8N_0\kappa}{|U_0''|}\Big\}^{1/2} y(\gamma) \{1 + O(\kappa^{-1/2})\} \\ &= n\pi \{1 + O(\kappa^{-1/2})\} \end{aligned} \tag{1.2.11a}$$

where $$y(\gamma) = \int_0^{(1-\gamma)^{1/2}} \Big(\frac{1}{(\gamma + v^2)^2} - 1\Big)^{1/2} dv . \tag{1.2.11b}$$

It should be noted that by substituting (1.2.10) into (1.2.2b) and (1.2.3b), and then using (1.2.9) to change the differential, it is possible



Reproduced with permission of the copyright owner. Further reproduction prohibited without permission.

to show that $\zeta_1$ and $\zeta_2$, are $O(\kappa^{1/3})$ and hence it was legitimate to use the large argument expansion of the Airy function. As c cannot lie within the range of U(z), then from (1.2.7) it is obvious that $\gamma$ is greater than zero, while, from (1.2.11b) it is seen that $\gamma$ must be less than one otherwise $y(\gamma)$ will be complex and meaningless. It should be noted that as $\gamma$ varies from zero to one, $y(\gamma)$ takes all values between infinity and zero. Thus, given the mode number n, $y(\gamma)$ can be found from (1.2.11a) and hence a value of $\gamma$ in the range (0, 1] can be found from (1.2.11b). Then the phase speed c can be determined from (1.2.7). From (1.2.7) and (1.2.11a and b) it can be seen that as the wavenumber tends to infinity the wave phase speed, depends only upon the local behavior of the mean flow near the extreme point $z = z_0$. As a further indication of this point consider (1.2.11b) when $\gamma$ is approximately one, this would be expected when the mode number is small or the overall Richardson number is large, then (1.2.11b) can be expanded in powers of $(1 - \gamma)$ to give

$$y(\gamma) = \frac{\pi\sqrt{2}}{4}(1-\gamma)\left\{1 + \frac{9}{16}(1-\gamma) + O[(1-\gamma)^2]\right\} . \qquad (1.2.12)$$

If (1.2.12) is truncated at the first power of $(1 - \gamma)$, then the phase speed c is given by

$$c = U_0 - \frac{N_0 \operatorname{sign}(U_0'')}{\kappa} + \frac{n \operatorname{sign}(U_0'')(|U_0''|N_0)^{1/2}}{\kappa^{3/2}} + O(\kappa^{-2}) . \qquad (1.2.13)$$

Equation (1.2.13) is valid provided $n(|U_0''|/N_0\kappa)^{1/2}$ is small and $\kappa$ is large. As another comparison consider the case when say the mode number is large or the overall Richardson number is small, then it would be expected that $\gamma$ is approximately zero, expanding (1.2.11b) for $\gamma \simeq 0$ gives

$$y(\gamma) = \frac{\pi}{2\sqrt{\gamma}} - 1 - \sum_{k=0}^{\infty} \frac{(2k)!}{2^{2k+1}\, k!\,(k+1)!\,(4k+3)} + O(\gamma)$$



Reproduced with permission of the copyright owner. Further reproduction prohibited without permission.

$$= \frac{\pi}{2\sqrt{\gamma}} - 1.19814 + O(\gamma) \ . \qquad (1.2.14)$$

Putting $\gamma \simeq \pi^2/4y^2$, the phase speed c is given by

$$c = U_0 - \frac{2N_0^2}{U_0'' n^2} + O(\kappa^{-1/2}) \ . \qquad (1.2.15)$$

If $\kappa$ is large and either the mode number $n \to \infty$ or the overall Richardson number $J \to 0$ or $U_0'' \to \infty$, then (1.2.15) is a valid approximation. Note that (1.2.15) agrees with (1.1.8) in the limit of infinite mode number.

Suppose now that the extreme value of the velocity, U(z), occurs at z = 0, with U'(0) = 0 and suppose that the transition point is at $z = \delta$, where $1 \gg \delta > 0$. Then in the interval $[0, \delta)$, $q^2(z)$ will be positive and the solutions of (1.2.1a,b) will be oscillatory, while in the interval $(\delta, h]$, $q^2(z)$ will be negative and the solutions of (1.2.1a,b) will be exponential. A solution of (1.2.1a) which is recessive at z = h is then given by (1.2.3a and b) with $z_0 = 0$ and $\delta_2 = \delta$. If z = Z is an interior point of $[0, \delta)$ and suppose that at z = Z, $\zeta_2$ in (1.2.3a,b) is large and negative, then as before the Airy function Ai in (1.2.3a) can be replaced by its asymptotic expansion for large negative argument, this gives (1.2.4d) for $\psi_2$ where $\hat{\theta}$ is given by (1.2.4f) with $z_0 = 0$ and $\delta_2$ replaced by $\delta$. Applying the boundary condition at z = 0 then gives

$$\int_0^{\delta} q(t)\, dt = (n - \tfrac{1}{4})\pi \{1 + O(\kappa^{-1/2})\} \qquad (1.2.16)$$

As above define $q^2(z)$ by (1.2.6a) and g(z) by (1.2.6c) where the zero subscript now denotes evaluation of z = 0. Now because c - U(z) is $O(\kappa^{-1})$ in the interval $[0, \delta)$ then there must exist a point $z = \tilde{z}$ (near z = 0) where $q^{2\prime}(\tilde{z}) = 0$ and hence $g'(\tilde{z}) = 0$. Note that if $q^{2\prime}(\tilde{z}) = 0$ then



Reproduced with permission of the copyright owner. Further reproduction prohibited without permission.

$U'(\hat{z})M(\hat{z}) + M'(\hat{z})(c - U(\hat{z})) = 0$, or $U'(\hat{z}) = O(\kappa^{-1})$, thus $z = \hat{z}$ must be a point close to $z = 0$ but not necessarily in the interval $[0, \delta)$. Now let $\gamma = g(\hat{z})$ and by expanding $U(\hat{z})$, $M(\hat{z})$ in Taylor series about $z = 0$, $\gamma$ again has the form (1.2.7). Defining v by (1.2.8), $q^2$ can then be written in the form (1.2.10), then substituting (1.2.10) into (1.2.16) and using (1.2.9) to change the differential, (1.2.16) becomes

$$y(\gamma) = \left\{\frac{|U_0''|}{2N_0\kappa}\right\}^{1/2} (n - \tfrac{1}{4})\pi \left\{1 + O(\kappa^{-1/2})\right\} , \qquad (1.2.17)$$

where $y(\gamma)$ is given by (1.2.11b). As before $\gamma$ lies between zero and one and $y(\gamma)$ takes all values between infinity and zero. Given a mode number n, $y(\gamma)$ can be determined from (1.2.17), then $\gamma$ can be found from (1.2.11b) and the phase speed c is determined from (1.2.7). If it is assumed that $\gamma$ is approximately one (i.e. this would occur when the mode number is small or the overall Richardson number is large), then replacing $y(\gamma)$ by its asymptotic expansion in powers of $(1 - \gamma)$ (1.2.12), the phase speed c then has the approximate form (c.f. (1.2.13))

$$c = U_0 - \frac{N_0 \operatorname{sign}(U_0'')}{\kappa} + \frac{2(n - \frac{1}{4})\operatorname{sign}(U_0'')(|U_0''|N_0)^{1/2}}{\kappa^{3/2}} + O(\kappa^{-2}) . \qquad (1.2.18)$$

Note that (1.2.18) is valid provided $(n - \frac{1}{4})(|U_0''|/N_0\kappa)^{1/2}$ is small and $\kappa$ is large. If it is assumed that $\gamma$ is approximately zero (i.e. the mode number is large or the overall Richardson number is small) then $y(\gamma)$ has the asymptotic expansion (1.2.14) and the phase speed c has the approximate form (c.f. (1.2.15))

$$c = U_0 - \frac{N_0^2}{2U_0''(n - \frac{1}{4})^2} + O(\kappa^{-1/2}) . \qquad (1.2.19)$$

Note that (1.2.19) is a valid approximation if $N_0^2/U_0''n^2$ is small and $\kappa$ is



Reproduced with permission of the copyright owner. Further reproduction prohibited without permission.

large, also the reader should note the similarity between (1.2.19) and (1.1.9).

This section has so far only considered extreme values of the velocity where $U'(z) = 0$. Now suppose that the velocity has a maximum or minimum at a point where $U'(z) \neq 0$. For obvious reasons this extreme point must either be at $z = 0$ or $h$. For simplicity assume that $U(0)$ is an extreme value of the velocity where $U'(0) \neq 0$. As $\kappa \to \infty$, $q^2(z)$ will then have a transition point at $z = \delta$, where $0 < \delta << 1$. Previously the solution of (1.2.1a) near a transition point was represented in terms of Airy functions, but when $U'(0) \neq 0$, the Airy function solutions are only valid if $Ri(0)$ is large. Note that in the previous case the local Richardson number at the extreme point was infinite. To obtain a uniformly valid solution of (1.2.1a), for all $Ri(0) > 1/4$, as $\kappa \to \infty$, it is proposed to use the method of matched asymptotic expansions. Now as the wavenumber $\kappa$, tends to infinity, the phase speed c tends to $U_0$ ($U_0 = U(0)$), so to derive an outer equation formally put $c = U_0$ in (1.2.1a), and assuming that $\kappa^2$ is much greater than $m^2(z)/(U_0 - U)^2$, where z is not near to zero and m is given by (1.2.6b), then the required outer equations are

$$\frac{d^2\psi_o}{dz^2} - \kappa^2\psi_o = 0 , \qquad (1.2.20a)$$

and

$$\psi_o(h) = 0 . \qquad (1.2.20b)$$

Note that the subscript "o" denotes the outer expansion. The solution of (1.2.20a and b) is

$$\psi_o(z) = D \sinh \kappa(z - h) \qquad (1.2.21)$$

where D is an arbitrary constant of normalization.

Examination of the balance of terms in (1.2.1a) near the extreme point $z = 0$ suggests that the inner variable is



Reproduced with permission of the copyright owner. Further reproduction prohibited without permission.

$$\xi = \frac{zU_0'}{(U_0 - c)} \tag{1.2.22}$$

Then expanding $U(z)$, $\rho_0(z)$ and $N^2(z)$ in Taylor series near the point $z = 0$, the inner equation is found to be

$$\frac{d^2\psi_i}{d\xi^2} + \sqrt{Ri(0)}\left(\frac{1}{(1+\xi)^2} - \mu^2\right)\left\{1 + O(\kappa^{-1})\right\}\psi_i(\xi) = 0 , \tag{1.2.23a}$$

where $$\psi_i(0) = 0 \tag{1.2.23b}$$

and $$\mu = \frac{\kappa \,\mathrm{sign}(U_0')(U_0 - c)}{N_0} . \tag{1.2.23c}$$

Here the subscript "i" denotes the inner expansion. A solution of (1.2.23a) which is recessive for large $\xi$ is

$$\psi_i(\xi) = A\,(1+\xi)^{1/2}\, K_{i\omega}\left(\mu\sqrt{Ri(0)}\,(1+\xi)\right) , \tag{1.2.24}$$

where $\omega$ is defined by (1.1.10b) and $K_\nu(z)$ is the modified Bessel function of the second kind. To match $\psi_o$ and $\psi_i$, first let $\xi$ tend to infinity then (1.2.24) becomes

$$\psi_i(\xi) = A\left\{\frac{\pi U_0'}{2\kappa(U_0 - c)}\right\}^{1/2} e^{-\kappa z} . \tag{1.2.25}$$

Matching (1.2.25) with the inner limit as $z \to 0$ of the outer solution (1.2.21) it is found that

$$D = -A\left\{\frac{\pi U_0'}{2\kappa(U_0 - c)}\right\}^{1/2} e^{-\kappa h} . \tag{1.2.26}$$

Equation (1.2.26) gives D in terms of the constant A once the phase speed c



Reproduced with permission of the copyright owner. Further reproduction prohibited without permission.

is determined. To evaluate the phase speed c it is necessary to apply the boundary condition (1.2.23b) to the inner solution (1.2.24), it is then found that

$$K_{i\omega}\left(\mu\sqrt{Ri(0)}\right) = 0 , \qquad (1.2.27)$$

and thus the zeros of $K_{i\omega}$ determine the phase speed c. Note that if $Ri(0) \leq \frac{1}{4}$ then $\omega$ is either complex or zero, and (1.2.27) has no real solutions for $\mu$ (see Abramowitz and Stegan (1965)). In Figure 1.1, $\mu$ is plotted against $\sqrt{Ri(0)}$ for the first five zeros of (1.2.27). It can be seen that as $\sqrt{Ri(0)} \downarrow \frac{1}{2}$, the eigenvalues $\mu$ decrease until they eventually coalesce with the horizontal axis at some $\sqrt{Ri(0)} > \frac{1}{2}$. The work of Banks et al (1976) showed that in this case (i.e. $U_0' \neq 0$) it was possible for the local Richardson number to be less than $\frac{1}{4}$ as $c \to U_0$, but for large $\kappa$ this obviously no longer applies.

If Ri(0) is large, then using a large order expansion of $K_\nu(z)$ (Abramowitz and Stegan (1965)) it is possible to show that (1.2.27) reduces to

$$\frac{\mu \exp\{(1-\mu^2)^{1/2}\}}{1+(1-\mu^2)^{1/2}} \simeq \exp\{-(n-\tfrac{1}{4})\tfrac{\pi}{\omega}\} . \qquad (1.2.28)$$

In Figure 1.1 the solutions of (1.2.28) for $\mu$, are plotted against $\sqrt{Ri(0)}$ for the first three modes. The approximate solution (1.2.28) shows good agreement with the solutions of (1.2.27) even for relatively small values of Ri(0). If it is assumed that $\mu$ is small then the left hand side of (1.2.28) can be expanded in powers of $\mu$ to give

$$\frac{\mu e^1}{2}\left(1 - \frac{\mu^2}{4} + O(\mu^6)\right) = \exp\{-(n-\tfrac{1}{4})\tfrac{\pi}{\omega}\} . \qquad (1.2.29)$$

Truncating (1.2.29) at the first power in $\mu$ and substituting into (1.2.23c)



Reproduced with permission of the copyright owner. Further reproduction prohibited without permission.

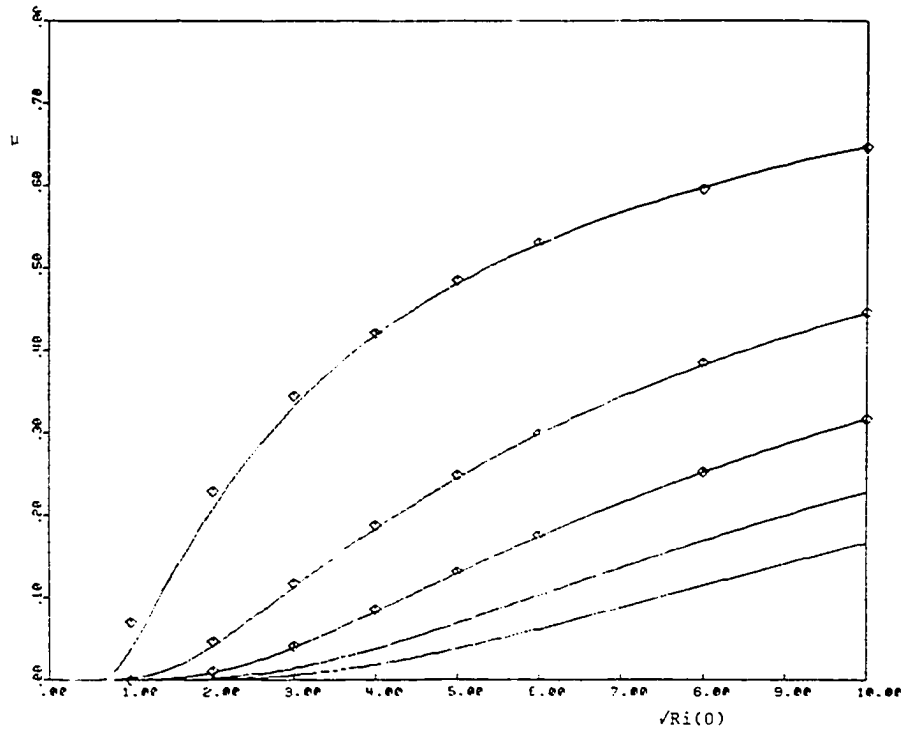


Figure 1.1: A plot of $\mu$ against $\sqrt{Ri(0)}$ for the first five modes. The large order expansion of (1.2.27) for the first three modes is represented by diamonds.

gives

$$c \simeq U_0 - \frac{2N_0 \operatorname{sign}(U_0')}{\kappa e^1} \exp\{-(n - \tfrac{1}{4})\tfrac{\pi}{\omega}\} . \qquad (1.2.30)$$

Thus from (1.2.30) it is seen that the phase speed c is dependent only upon the local behavior near $z = 0$ as $\kappa \to \infty$. Also if equation (1.2.30) is compared with (1.1.10a) it is seen that in each case $c - U_0$ is proportional to $e^{-n\pi/\omega}$.



Reproduced with permission of the copyright owner. Further reproduction prohibited without permission.

## §1.3 Numerical Results

In general, for an arbitrary velocity and density profile it is impossible to solve (1.1.2a,b and c) analytically. In this section the dispersion relation and group velocity as a function of wavenumber, are discussed for two specific flows. In each case analytic solutions do not exist so (1.1.2a,b and c) have been numerically integrated using a technique known as the shooting method.

To numerically integrate the second order, ordinary differential equation (1.1.2a) it is necessary to transform it into a system of two first order differential equations. If then

$$Y_1 = \phi \tag{1.3.1a}$$

and

$$Y_2 = \frac{d\phi}{dz} , \tag{1.3.1b}$$

then the two first order equations to be integrated are

$$\frac{d}{dz} Y_1 = Y_2 \tag{1.3.2a}$$

and

$$\frac{d}{dz} Y_2 = Y_2 \frac{d}{dz} \ln\left(\rho_0 (c - U)^2\right) + \left(\kappa^2 - \frac{N^2}{(c - U)^2}\right) Y_1 . \tag{1.3.2b}$$

With suitable initial conditions (1.3.2a and b) can then be integrated from $z = 0$ to h, using a fourth order Runge-Kutta method (see Kuo (1972)). The initial conditions here, are

$$Y_1 = 0 \quad \text{at} \quad z = 0 \tag{1.3.3a}$$

$$Y_2 = \text{const.} \neq 0 \quad \text{at} \quad z = 0 . \tag{1.3.3b}$$



Reproduced with permission of the copyright owner. Further reproduction prohibited without permission.

Where (1.3.3a) is just (1.1.2b). Note that if it is likely that $Y_1$ will grow exponentially large as z increases then it is expedient to choose the constant in (1.3.3b) to be small. A good rule in this case is to let $Y_2 = e^{-\kappa}$ at $z = 0$, then as $\kappa$ increases the initial condition decreases. If for a given $\kappa$ the eigenvalue $c(\kappa)$ is known then integrating (1.3.2a and b) with (1.3.3a and b) from $z = 0$ to h, the boundary condition (1.1.2c) should be satisfied (i.e. $Y_1(h) = 0$). In general the eigenvalue $c(\kappa)$ will not be known and thus the boundary condition at $z = h$ will not be satisfied. A useful technique in this situation is to assume that if $Y_1(h,c) \neq 0$ then $Y_1(h,c + dc) = 0$. Then if $Y_1$ is a function of c expanding $Y_1(h,c + dc)$ to first order in a Taylor series, the change in c, dc, can be evaluated i.e.

$$0 = Y_1(h,c) + dc \frac{\partial Y_1(h,c)}{\partial c} . \qquad (1.3.4)$$

At $z = h$, $Y_1$ is known but the partial derivative of $Y_1$ with respect to c, at the moment is unknown, to find $\partial Y_1/\partial c$, it is necessary to define two new functions,

$$Y_3 = \frac{\partial Y_1}{\partial c} \qquad (1.3.5a)$$

and

$$Y_4 = \frac{\partial Y_2}{\partial c} , \qquad (1.3.5b)$$

where $Y_3$ and $Y_4$ satisfy the following two first order differential equations

$$\frac{d}{dz} Y_3 = Y_4 \qquad (1.3.6a)$$



Reproduced with permission of the copyright owner. Further reproduction prohibited without permission.

and $$\frac{d}{dz} Y_4 = Y_4 \frac{d}{dz} \ln(\rho_0(c - U)^2) + Y_2 \frac{d}{dz} 2\rho_0(c - U)$$

$$+ \left(\kappa^2 - \frac{N^2}{(c - U)^2}\right) Y_3 - \frac{2U'N^2}{(c - U)^3} Y_1 \, . \qquad (1.3.6b)$$

As the initial conditions (1.3.3a and b) are not functions of c, then using (1.3.5a and b) the initial conditions for $Y_3$ and $Y_4$ are

$$Y_3 = 0 \quad \text{at} \quad z = 0 \qquad (1.3.7a)$$

and $$Y_4 = 0 \quad \text{at} \quad z = 0 \, . \qquad (1.3.7b)$$

Now given an initial guess for the eigenvalue c it is possible to integrate (1.3.2a,b) and (1.3.6a,b) from z = 0 to h, using the initial conditions (1.3.3a,b) and (1.3.7a,b). If $Y_1(h) \neq 0$, then a better guess for the eigenvalue c can be found by calculating the change in c as

$$dc = -\frac{Y_1}{Y_3} \quad \text{at} \quad z = h \, . \qquad (1.3.8)$$

In the numerical integrations presented here this method was repeated until the absolute value of dc/c was less than $10^{-6}$. To build up a total dispersion relation for c as a function of $\kappa$, the wavenumber $\kappa$ was then given a slight increase and the above procedure was repeated using the old value of c as an initial guess. At each value of $\kappa$ the group velocity $c_g$ was calculated using (1.1.11) and (1.1.12), the integrals in (1.1.12) were calculated using Simpsons rule (see Kuo (1972)).

The method described above for finding the eigenvalue c is fool proof only when the initial guess for c is close to it's actual value. To find this guess for c (when $\kappa = 0$) it is necessary to bracket the correct value of c (i.e. find values above and below the actual value). If



Reproduced with permission of the copyright owner. Further reproduction prohibited without permission.

$c > U_{max}$ then (1.1.5) was used as an upper bound on c, (1.3.2a and b) were then integrated from $z = 0$ to h and the sign of $Y_1(h)$ noted. The eigenvalue c was then decreased by units of $(c_0 - U_{max})/50$ (see (1.1.5)) until the sign of $Y_1(h)$ changes. This then brackets the actual value of c. To get closer to the correct value of c, the half interval search method (see Kuo (1972)) was used on the values of c above and below the actual value. That is, let $\hat{c} = (c_a + c_b)/2$, where $c_a$ and $c_b$ represent the values of above and below the correct value. Then integrate (1.3.2a and b) from $z = 0$ to h, and if the sign of $Y_1(h)$ for $c = \hat{c}$ is equal (opposite) to the sign of $Y_1(h)$ for $c = c_a$, choose $c_a = \hat{c}$ ($c_b = \hat{c}$). This procedure was repeated twenty times and thus guaranteed that the initial guess for c used above, was very close to the actual value. To bracket the next eigenvalue (at $\kappa = 0$) the value of c from the previous mode was used as an upper bound and the interval between this upper bound and $U_{max}$ was then searched in the same manner as described above. To find initial guesses for the modes when $c < U_{min}$ the same procedure is used but in this case the analogue of (1.1.5) is used to find a lower bound on c for the first mode.

Consider a fluid of constant Brunt-Väisälä frequency where the fluid velocity has the jet like structure,

$$U = 0.1 \operatorname{sech}^2\left(20\left(\frac{z}{h} - \frac{1}{2}\right)\right) \quad \text{for} \quad 0 \leq z \leq h , \tag{1.3.9a}$$

and

$$N^2 = 1 \quad \text{for} \quad 0 \leq z \leq h . \tag{1.3.9b}$$

For simplicity the Boussinesq approximation shall be taken so that $\rho_0$ in (1.1.2a) and subsequent equations is regarded as a constant. The fluid velocity U has a maximum at $z = \frac{h}{2}$ where $U'(\frac{h}{2}) = 0$ and $U''(\frac{h}{2}) = -80$. The velocity is symmetrical about the point $z = \frac{h}{2}$ and the velocity minimum occurs at the two boundary points $z = 0$ and $z = h$, and at these points $U' \neq 0$. The local Richardson number varies from infinity at $z = \frac{h}{2}$ to $\frac{27}{64}$ at



Reproduced with permission of the copyright owner. Further reproduction prohibited without permission.

(1.2a)

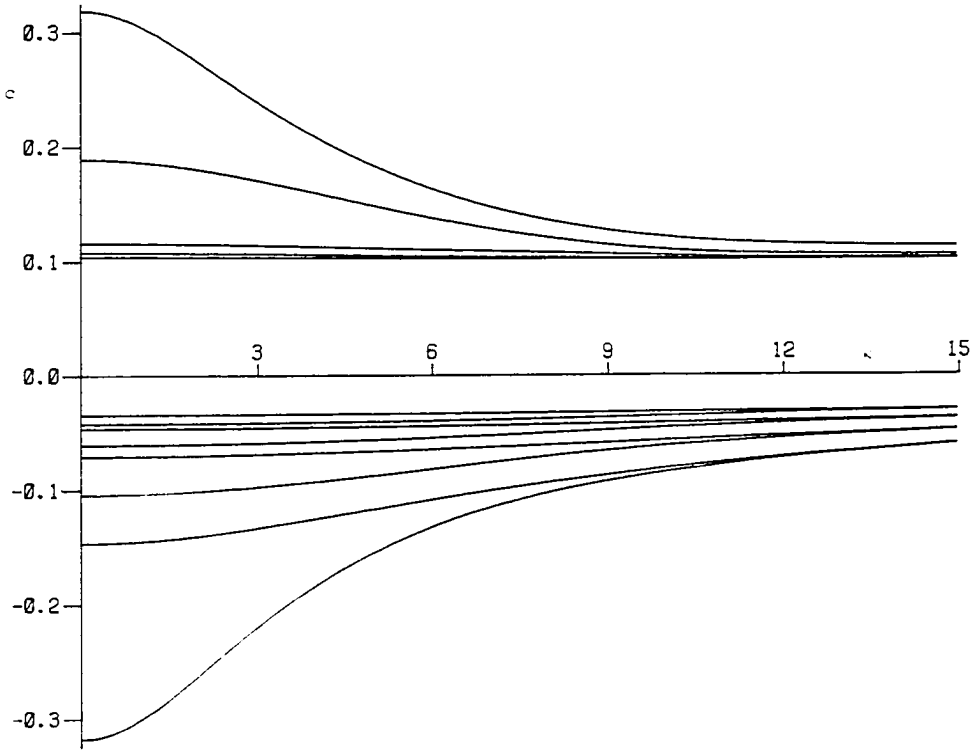


Figure 1.2: A plot of (a)the phase speed and (b)the group velocity as a function of wavenumber for the first five positive modes ($c > U_{max}$) and the first eight negative modes ($c < U_{min}$), when the fluid velocity and Brunt-Väisälä frequency are given by (1.3.9a and b).

$\frac{z}{h}$ = 0.5 ± 0.033 and to 9.2 x $10^{14}$ at z = 0 and h.

To find the phase speed and group velocity as a function of wavenumber for the flow (1.3.9a and b), (1.1.2a,b and c) were integrated numerically by the method previously described in this section. Figures 1.2a and b show respectively the phase speed c and the group velocity $c_g$, as a function of wavenumber κ, for the first five positive modes ($c > U_{max}$) and the first eight negative modes ($c < U_{min}$), as κ varies from 0 to 15. In Figure 1.2a an important feature that is readily noticed is that as κ



Reproduced with permission of the copyright owner. Further reproduction prohibited without permission.

(1.2b)

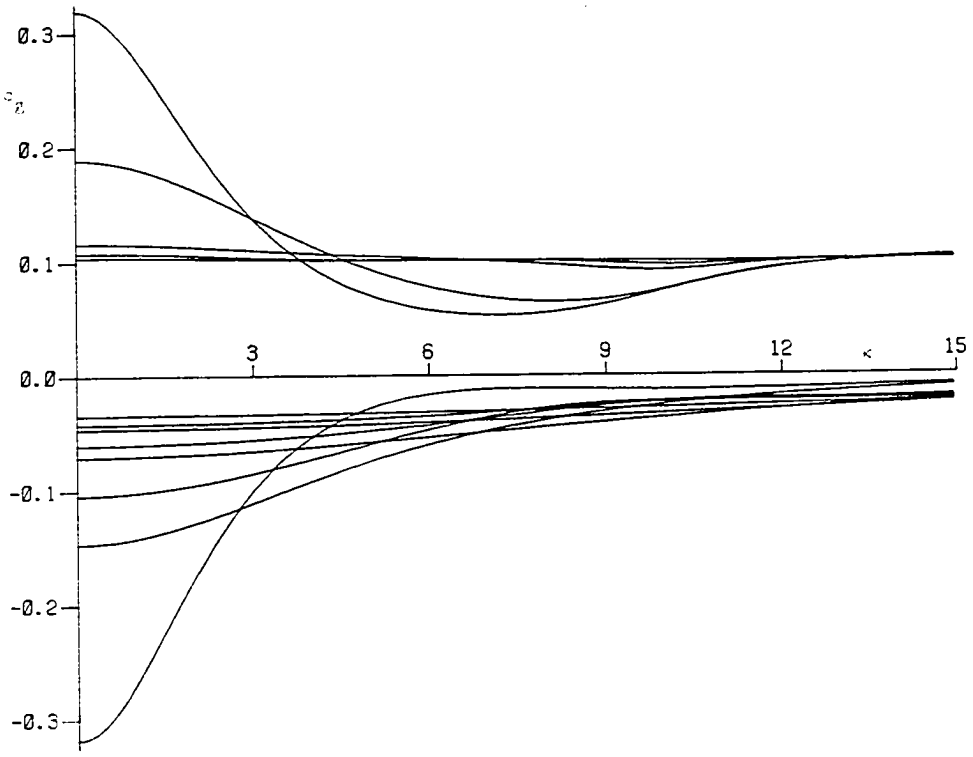


tends to infinity, consecutive modes (for $c < U_{min}$) tend to the same limit. That is $c_{2m-1}$ and $c_{2m}$ (m = 1,2,3,---), tend to the same limit. This phenomenon is due to the fact that the minimum of the fluid velocity occurs at two distinct points in the fluid (i.e. z = 0 and h). In this case as $c \uparrow U_{min}$ the fluid sees two boundary layers instead of one. Due to the symmetry of (1.3.9a and b) about $z = \frac{h}{2}$ the eigenmodes of (1.1.2a) must be symmetrical (asymmetrical) about $z = \frac{h}{2}$, when the mode number is odd (even), that is $\phi(z) = (-1)^{n-1} \phi(h-z)$, where n is the mode number The domain of the problem can be reduced to the half interval $0 \leq z \leq \frac{h}{2}$, by imposing a symmetry condition at $z = \frac{h}{2}$. Thus when n is odd, it is required that

$$\frac{d\phi}{dz} = 0 \qquad \text{at} \quad z = \frac{h}{2} \tag{1.3.10a}$$

and when n is even, it is required that



Reproduced with permission of the copyright owner. Further reproduction prohibited without permission.

$$\phi = 0 \qquad \text{at} \qquad z = \frac{h}{2} . \tag{1.3.10b}$$

In this new domain as $c \uparrow U_{min}$ the fluid now only sees one boundary layer at $z = 0$. As $\kappa$ tends to infinity it has been shown in §1.2 that the phase speed c depends only upon the local behavior of the fluid at the extreme point $z = 0$. Due to the symmetry in this case, as $\kappa \to \infty$ the number of nodes inside the boundary layer at $z = 0$, will be the same for consecutive modes $c_{2m-1}$ and $c_{2m}$ ($m = 1,2,3,---$). Then as the phase speed does not depend upon the symmetry conditions (1.1.10a and b) at $z = \frac{h}{2}$, the phase speeds $c_{2m-1}$ and $c_{2m}$ must tend to the same limit as $\kappa \to \infty$. In a similar problem where the flow is symmetrical about a mid point in the fluid, Banks et al (1976), used matched asymptotic expansions to show that as the overall Richardson number J tends to zero the phase speeds of two consecutive modes tend to the same limit. Similarly, it can be shown that as the mode number tends to infinity the phase speeds of consecutive modes tend to the same limit. It can be conjectured then that any flow that has the same extreme value of velocity at more than one point in the fluid domain, but the flow is not necessarily symmetrical, will have consecutive eigenmodes that have the same limiting phase speed as $n \to \infty$, $\kappa \to \infty$ or as $J \to 0$ (i.e. in these limits the phase speed is only dependent upon the local behavior of fluid in the neighborhood of the extreme points).

Next in Figure 1.2a compare the proximity of the phase speeds to their associated extreme points of the velocity. It is seen that the positive modes ($c > U_{max}$) are much more compressed onto $U_{max}$ than the negative modes are onto $U_{min}$, this is due to a number of factors. At $z = \frac{h}{2}$, where $U' = 0$, $U'' = -80$ so that, $2N^2/U''n(n+2)$ and $2N^2/U''n^2$ in equations (1.1.8) and (1.2.15) will become small at moderately small values of the mode number n and thus the phase speed will be approximately equal to $U_{max}$. On the other hand at $z = 0$ and h, $U' \neq 0$, but the local



Reproduced with permission of the copyright owner. Further reproduction prohibited without permission.

Richardson number there, is extremely large (= $9.2 \times 10^{14}$) so the formula (1.1.10a) and (1.2.30) should not be applicable unless the mode number is very large.

In Figure 1.2b it is seen that the group velocity $c_g$ of each mode equals the phase speed c at $\kappa = 0$ (as predicted in §1.1). As $\kappa$ increases $c_g$ is always less than c, for the positive modes and greater than c for the negative modes. As distinct from the phase speeds, the group velocity of two different modes may be the same at some values of $\kappa$ (i.e. the group velocity curves can be seen to cross each other). At these points where the group velocity of two different modes is the same, it would be possible for energy to transfer from one mode to the other. In this way energy could be transferred from low mode number eigenmodes to high mode number eigenmodes until eventually the scale of the motion becomes so small that molecular forces become important. That is energy in one mode could be transferred to other modes and eventually dissipated by molecular effects. It can also be seen in Figure 1.2b that the group velocity of the first three positive modes ($c > U_{max}$), lies within the range of U (i.e. $U_{min} < c_g < U_{max}$). This phenomenon was shown to be possible by Leibovich (1979). Note also that Thorpe (1978) and Liu and Benney (1981) give some numerical examples where $c_g$ lies within the range of U. The implications of this are that energy should readily pass from the fluid to the waves where $c_g$ equals U and thus the waves can draw energy from the mean flow.

As a second example, consider a fluid of constant Brunt-Väisälä frequency where the fluid velocity has the boundary layer structure,

$$U = 0.04 \tanh\left(20 \frac{z}{h}\right) \quad \text{for} \quad 0 \leq z \leq h , \qquad (1.3.11a)$$

and

$$N^2 = 1 \quad \text{for} \quad 0 \leq z \leq h . \qquad (1.3.11b)$$



Reproduced with permission of the copyright owner. Further reproduction prohibited without permission.

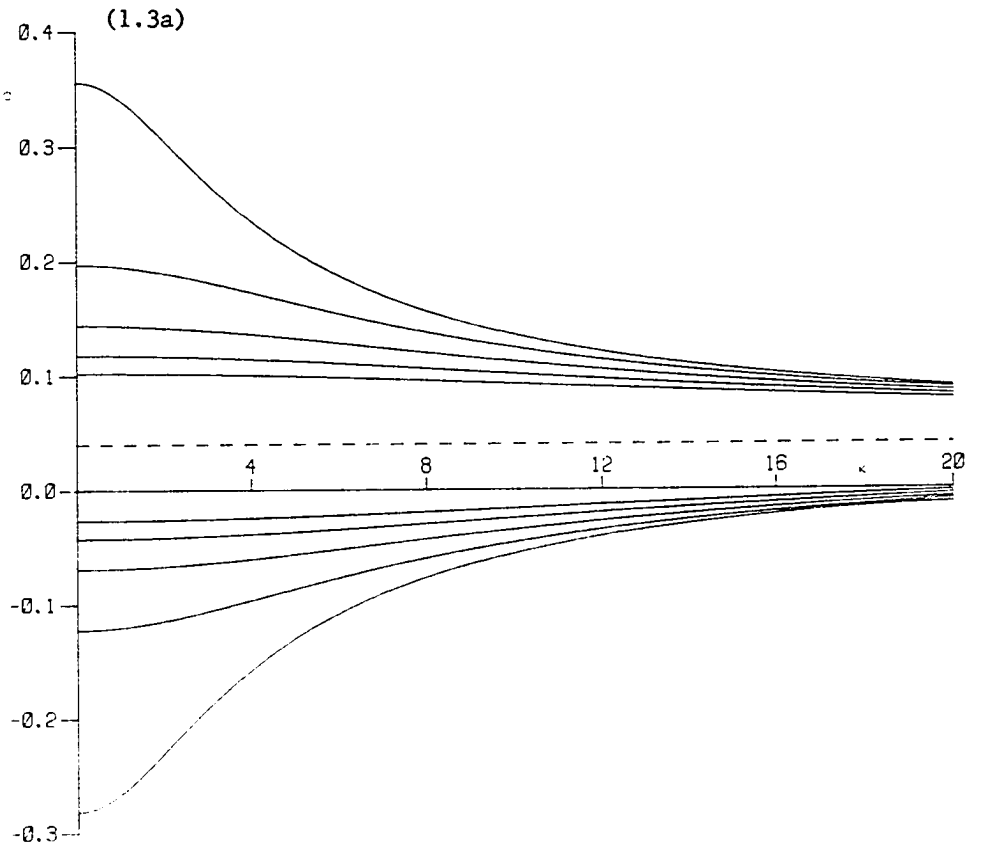


Figure 1.3: A plot of (a)the phase speed and (b)the group velocity as a function of wavenumber for the first five positive modes ($c > U_{max}$) and the first five negative modes ($c < U_{min}$), when the fluid velocity and Brunt-Väisälä frequency are given by (1.3.11a and b).

Again the Boussinesq approximation shall be taken so that $\rho_0$ is regarded as constant in (1.1.2a) and subsequent equations. The fluid velocity now has a minimum at $z = 0$, where $U = 0$ and $Ri(0) = \frac{25}{16}$, the velocity maximum now occurs at $z = h$, where $U \simeq 0.04$ and the local Richardson number $Ri(h) = 5.4 \times 10^{33}$. The eigenvalue problem has been solved numerically when the velocity U and the Brunt-Väisälä frequency are given by (1.3.11a and b) respectively, and the phase speed c and group velocity $c_g$ have been plotted against the wavenumber $\kappa$ for the first five positive modes ($c > U_{max}$) and



Reproduced with permission of the copyright owner. Further reproduction prohibited without permission.

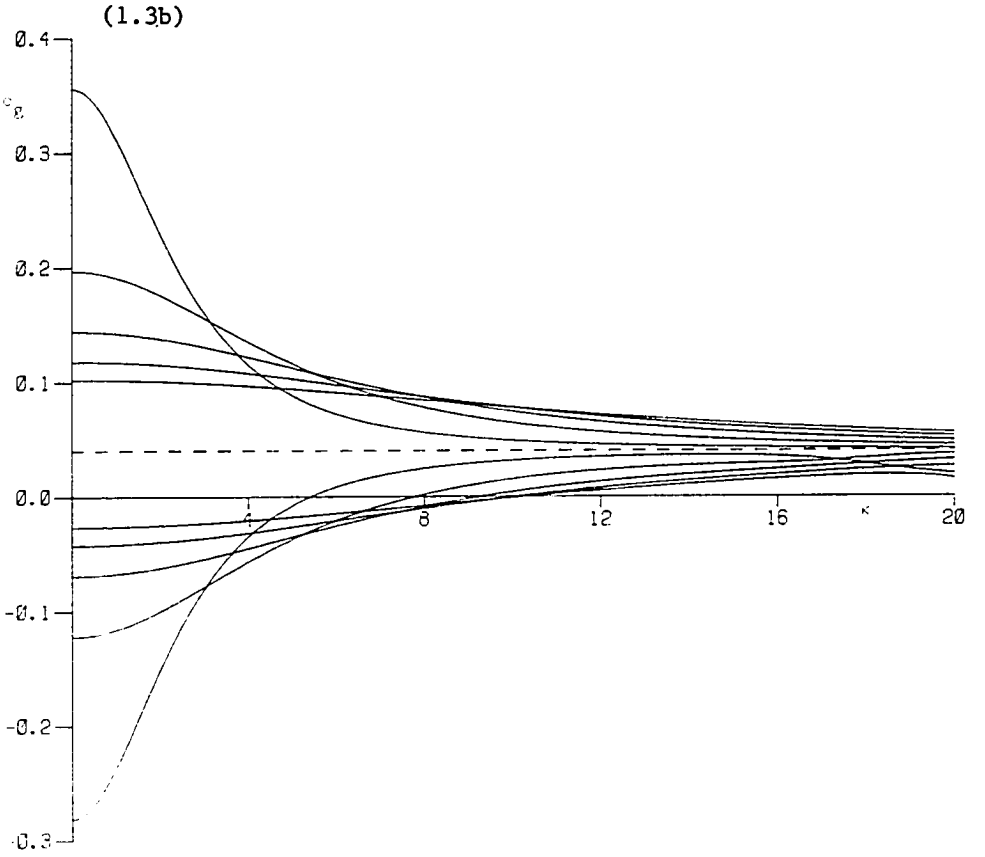


the first five negative modes ($c < U_{min}$). Figures 1.3a and b show respectively the phase speed c and the group velocity $c_g$ as a function of wavenumber $\kappa$, for $\kappa \in [0,20]$.

In Figure 1.3a it can be seen that the first five negative modes ($c < U_{min}$) are much closer to $U_{min}$ than the first five positive modes are to $U_{max}$. This is due to the fact that Ri(0) is much less than Ri(h). At $z = h$ $\omega$ (1.1.10b) is $7.35 \times 10^{16}$ and so (1.1.10a) does not apply to the positive modes unless the mode number is very large, or for a similar reason (1.2.30) will not apply unless the wavenumber is very large. On the other hand at $z = 0$ $\omega$ is $\sqrt{21}/4$, and so (1.1.10a) will apply for moderately small values of the mode number, and (1.2.30) will be applicable at smaller values of the wavenumber than it will be for the positive modes.

In Figure 1.3b, it can be seen, as in the previous case, that the group velocity $c_g$ of each mode equals the phase speed c at $\kappa = 0$. Then



Reproduced with permission of the copyright owner. Further reproduction prohibited without permission.

| MODE NUMBER | NUMERICAL | ASYMPTOTIC |
|---|---|---|
| 1 | 0.111822 | 0.111189 |
| 2 | 0.104313 | 0.104073 |
| 3 | 0.102170 | 0.102073 |
| 4 | 0.101297 | 0.101251 |
| 5 | 0.100860 | 0.100836 |

Table 1.1: A comparison between the numerical results and the asymptotic formula for the first five positive phase speeds c, when $\kappa = 15$ and U and $N^2$ are given by (1.3.9a and b).

as $\kappa$ increases $c_g$ is always less than c, for the modes where $c > U_{max}$ and $c_g$ is always greater than c when $c < U_{min}$. Again it can be seen that the group velocity curves cross each other frequently and that for the negative modes ($c < U_{min}$) it is possible for the group velocity to lie within the range of U. Thus it seems plausible that the modes that propagate against the fluid velocity ($c < U_{min}$) will be able to draw substantial energy from the basic flow. This energy could then be passed from one mode to another and so on, until it is finally dissipated by frictional effects.

Finally it remains to compare the asymptotic formulae of §1.2 with the numerical results of §1.3. Table 1.1 compares the first five (positive) numerically predicted phase speeds with their corresponding asymptotic values when U and $N^2$ are given by (1.3.9a and b) and the wavenumber $\kappa$ is 15. The asymptotic results were derived from equations (1.2.7) and (1.2.11a and b). That is (1.2.11a) gives $y(\gamma)$ as a function of mode number n, (1.2.11b) is then used to determine $\gamma$ from $y(\gamma)$ and then (1.2.7) gives the phase speed c. Comparing the values in Table 1.1 it is



Reproduced with permission of the copyright owner. Further reproduction prohibited without permission.

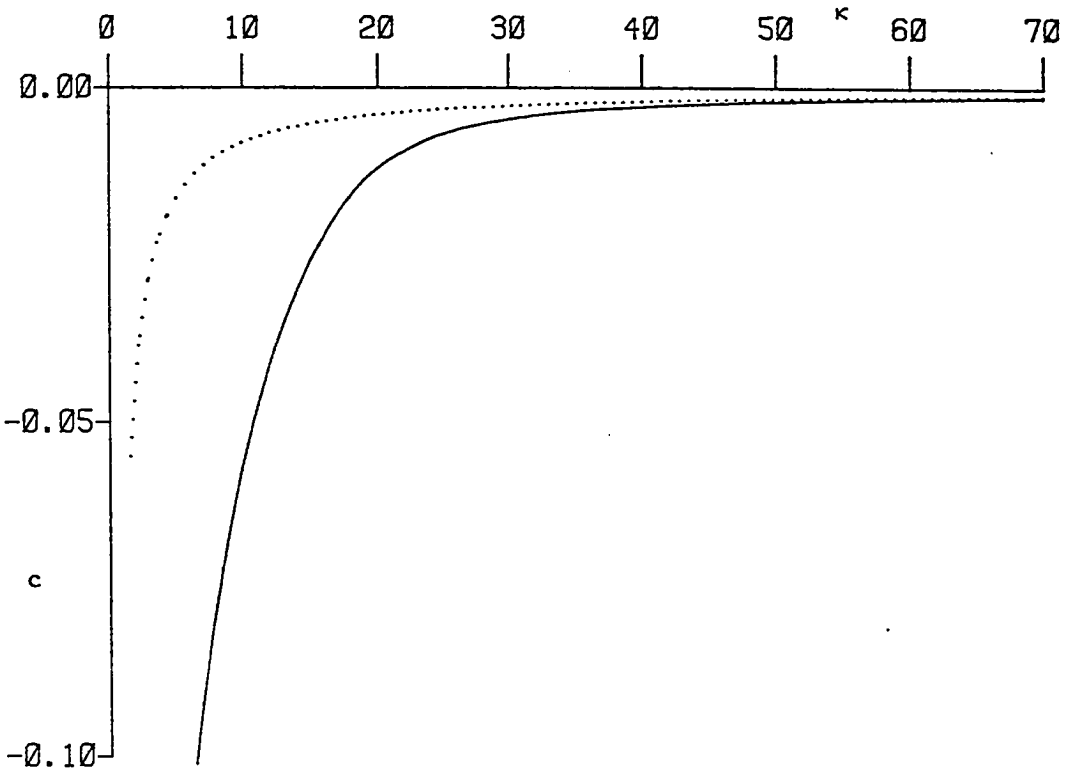


Figure 1.4: A plot of the phase speed as a function of wavenumber for the first negative mode, when U and N2 are given by (1.3.11a and b); ———, numerical result; ·····, asymptotic theory.

seen that the asymptotic results slightly underpredict the phase speeds but are very accurate even for small mode numbers. The error between the asymptotic and numerical results ranges from 0.55% for the first mode to 0.023% for the fifth mode. As a second comparison consider Figure 1.4, which is a plot of the numerically and asymptotically predicted phase speed for the first negative mode when U and $N^2$ are given by (1.3.11a and b) and $\kappa$ varies from 0 to 70. In this case the asymptotic solution was determined from (1.2.23c) and (1.2.27), that is, given $\omega$ (1.1.10b) and Ri(0), the first value of $\mu$ which solves (1.2.27) was found numerically and substituted into (1.2.23c) to give the phase speed c as a function of wavenumber. Examining Figure 1.4 it is seen that the asymptotic formula is



Reproduced with permission of the copyright owner. Further reproduction prohibited without permission.

a very good approximation to the numerically predicted phase speed when $\kappa > 45$. The results of both Figure 1.4 and Table 1.1 suggest that the asymptotic formulae of §1.2 are extremely accurate when used under the correct limits i.e. $\kappa \to \infty$ and $c \simeq U_{extreme}$.



Reproduced with permission of the copyright owner. Further reproduction prohibited without permission.

# Chapter 2: A SECOND ORDER THEORY FOR SOLITARY WAVES IN SHALLOW FLUIDS.

## §2.1 INTRODUCTION

Small amplitude solitary waves in density stratified fluids of shallow depth have a characteristic "sech$^2$"-profile, phase speeds that vary linearly with the wave amplitude and wavelengths that vary inversely as the square root of the wave amplitude (see Benney (1966) or the recent review by Miles (1980)). However, observations of internal solitary waves show that moderate or large amplitudes are quite common. In contrast, theories for finite amplitude solitary waves are very sparse being confined mainly to special cases involving either two-layer fluids or fluids with weak stratification. Hence, in this chapter it is proposed to discuss finite amplitude solitary waves by constructing an amplitude expansion which leads to the "sech$^2$"-profile at first order, and then continuing the expansion to second order in wave amplitude.

Consider an inviscid, incompressible fluid for which there is a basic density profile $\rho_0(z)$ and a basic velocity profile $u_0(z)$, bounded below by the rigid boundary $z = 0$, and above either by a free surface whose equilibrium position is at $z = h$, or by a rigid boundary at $z = h$. Here, $z$ is a vertical co-ordinate, and $x$ will be a horizontal co-ordinate in a frame which moves with the wave phase speed $c$. Weakly nonlinear long waves in shallow fluids are characterized by the equality of two small parameters $\varepsilon^2$ and $\alpha$; here $\varepsilon = H/L$ where $H$ is a vertical scale (typical for the fluid depth and the vertical structure of the waves) and $L$ is the horizontal scale of the waves, while $\alpha$ is a measure of the amplitude of the vertical displacement $\eta$ due to the solitary wave (Figure 2.1). Thus, let $\eta = \alpha A(X)\phi(z)$ where $X = \varepsilon x$, and $\phi(z)$ is the modal function which satisfies the following eigenvalue problem:



Reproduced with permission of the copyright owner. Further reproduction prohibited without permission.

$$[\rho_0(c_0 - u_0)^2\phi_z]_z + \rho_0 N^2\phi = 0 , \quad \text{for} \quad 0 < z < h , \qquad (2.1.1a)$$

$$\phi = 0 , \quad \text{for} \quad z = 0 , \qquad (2.1.1b)$$

$$\phi = p\sigma(c_0 - u_0)^2\phi_z , \quad \text{for} \quad z = h , \qquad (2.1.1c)$$

where $N^2 = -(\sigma\rho_0)^{-1}\rho_{0z}$ is the Brunt-Väisälä frequency, and the z subscripts denote derivatives. These equations are expressed in non-dimensional co-ordinates based on a length scale H and a velocity scale $N_1H$ where $N_1$ is a typical value of the Brunt-Väisälä frequency; $\sigma$ is then the parameter $N_1^2Hg^{-1}$ and is small in the Boussinesq approximation. The number p in (2.2.1c) takes the value 0 or 1 according as the upper boundary is rigid or free. The eigenvalue is $c_0$, the linear long wave phase speed. For simplicity it will be assumed that there are no critical layers and so $c_0$ is not equal to $u_0(z)$ for any value of z; a sufficient condition for this when the critical layers are viscosity dominated is that the local Richardson number is everywhere greater than 1/4, although there is no such restriction when the critical layer is nonlinearly dominated. The solitary wave is (Benney (1966))

$$A(X) = a \operatorname{sech}^2 (X/\lambda) \qquad (2.1.2)$$

and its phase speed $c \simeq c_0 + \varepsilon^2 c_1$, where

$$c_1 = \frac{1}{3}\mu a , \quad \lambda^2 a = \frac{12\delta}{\mu} . \qquad (2.1.3)$$

The coefficients $\mu$ and $\delta$ are known in terms of the modal function $\phi(z)$ and are given by (Benney(1966), or Grimshaw(1981b))



Reproduced with permission of the copyright owner. Further reproduction prohibited without permission.

$$\mu = \frac{3\int_0^h \rho_0(c_0 - u_0)^2\phi_z{}^3 dz}{2\int_0^h \rho_0(c_0 - u_0)\phi_z{}^2 dz} , \qquad (2.1.4a)$$

$$\delta = \frac{\int_0^h \rho_0(c_0 - u_0)^2\phi^2 dz}{2\int_0^h \rho_0(c_0 - u_0)\phi_z{}^2 dz} , \qquad (2.1.4b)$$

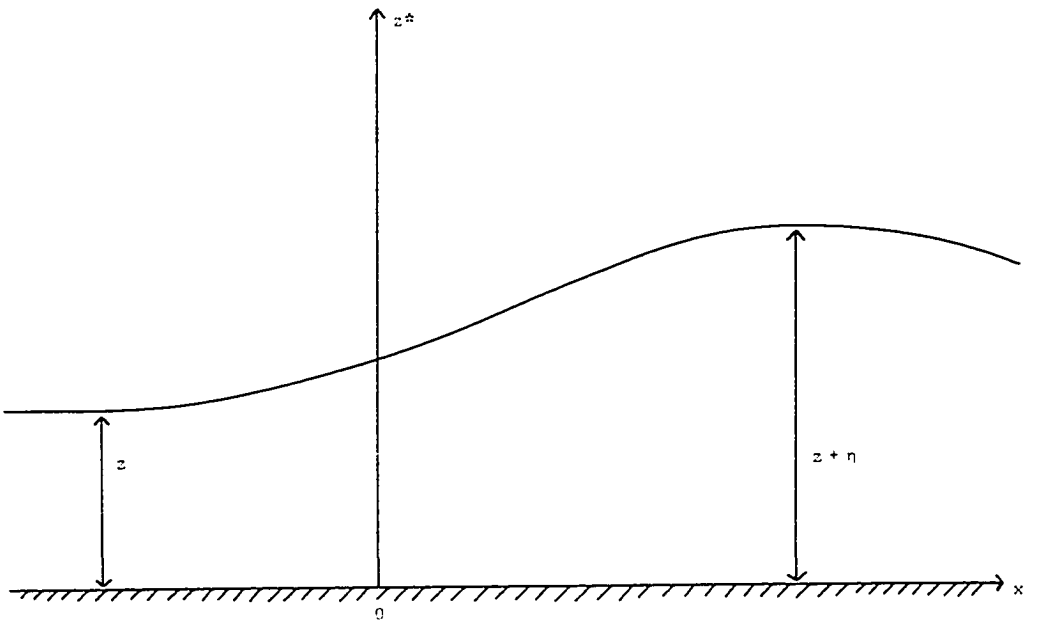


Figure 2.1: The co-ordinate system.

It is readily shown from (2.1.3) and (2.1.4b) that $c_1$ is positive for waves travelling to the right ($c_0 >$ max $u_0$), and negative for waves travelling to the left ($c_0 <$ min $u_0$); in both cases the solitary wave travels faster than the corresponding linear long wave. The derivation of these results from an amplitude expansion is described in §2.2. Benjamin (1966)



Reproduced with permission of the copyright owner. Further reproduction prohibited without permission.

has shown that the same result can be obtained from a variational approach.

The theory described in the previous paragraph is restricted to the first order in $\alpha$ (note $\alpha = \varepsilon^2$). In §2.2 the analysis which leads to the determination of the second order correction $\varepsilon^4\eta_2(X, z)$ to $\varepsilon^2 A(X)\phi(z)$, the second order correction $\varepsilon^4 c_2$ to the phase speed c (i.e. $\simeq c_0 + \varepsilon^2 c_1 + \varepsilon^4 c_2$) and the first order correction to the wavelength shall be described. This analysis is analogous to that described by Grimshaw (1981a) for second order solitary waves in deep fluids. This chapter is only concerned with the construction of the second order terms in the amplitude expansion, and does not consider questions of convergence although it shall be noted that some aspects of this problem have been considered by Ter-Krikorov (1963) and Tung, Chan and Kubota (1982). In §2.3 four special cases shall be discussed: (I) the basic shear flow is linear, and the Brunt-Väisälä frequency is constant; (II) there is no basic shear flow and the Brunt-Väisälä frequency is constant; (III) there is no basic shear flow and the Brunt-Väisälä frequency is piece-wise constant, forming a simple model of an inversion layer; (IV) there is no basic shear flow and the density stratification is that for a two-layer fluid. In (I) and (III) the Boussinesq approximation in also made so that the upper boundary is rigid; in (II) and (IV) the upper boundary can be either rigid or free. Note that the Boussinesq approximation is valid provided only that its use does not reduce the coefficient $\mu$ (2.1.4a) to zero, as then the first order solitary wave does not exist; in case (II) for instance the Boussinesq approximation cannot be made, but it is valid in all the other cases. Although analytical expressions have been obtained for each special case, they are generally very complicated and so it has been necessary to display the results in a graphical form. In many situations it is found that the nonlinear coefficient $\mu$ (2.1.4a) is quite small indicating that a re-scaling is necessary. This aspect is discussed



Reproduced with permission of the copyright owner. Further reproduction prohibited without permission.

in §2.4 where it is shown that the re-scaling leads to an equation for A in which both quadratic and cubic nonlinearities appear; the solitary wave solution then differs from (2.1.2) by a factor $(1 - b \tanh^2 (X/\lambda))^{-1}$ where b is a constant (< 1) related to the wave amplitude a.

The remainder of this section shall be concerned with the formulation of the equations which govern finite amplitude waves in inviscid incompressible fluids. Assuming that the flow is steady in a frame moving with the phase speed of the wave, the equations may be formulated in terms of the stream function $\psi$. Then the density is $\rho(\psi)$, the pressure is determined from the Bernoulli relation along a streamline, and $\psi$ itself is given by Long's equation (Long (1953))

$$\psi_{z^*z^*} + \psi_{xx} + \frac{1}{\sigma\rho}\frac{d\rho}{d\psi}\left(\frac{1}{2}\sigma(\psi_{z^*}^2 + \psi_x^2) + z^*\right) = \frac{1}{\rho}\frac{dH}{d\psi}, \qquad (2.1.5)$$

where $z^*$ is the Eulerian vertical co-ordinate and $H(\psi)$ is the Bernoulli constant and is to be determined by the conditions far upstream. If z is the upstream height of a streamline $\psi$ = const., then as $x \to -\infty$, $z^* \to z$ and

$$\rho \to \rho_0(z) = p_1 \exp(-\sigma \int_0^z N^2(z')dz'), \qquad (2.1.6a)$$

$$\psi \to -cz + \int_0^z u_0(z')dz', \qquad (2.1.6b)$$

then the Bernoulli constant H is given by

$$H = \frac{1}{2}\rho_0(c - u_0)^2 + \frac{\rho_0}{\sigma} z - \int_0^z \frac{\rho_0(z')}{\sigma} dz'. \qquad (2.1.6c)$$

Rather than work with Long's equation (2.1.5) it is more convenient to



Reproduced with permission of the copyright owner. Further reproduction prohibited without permission.

transform it into an equation for $\eta$, the vertical displacement of a streamline relative to its upstream height z. Thus put

$$z^* = z + \eta(x,z) \tag{2.1.7a}$$

then, if $(c - u_0)$ does not vanish anywhere, the relation

$$\frac{d}{d\psi} = \frac{-1}{(c - u_0)} \frac{d}{dz} , \tag{2.1.7b}$$

together with (2.1.7a), leads to (Benjamin (1967), Miles (1979))

$$Q \left(\frac{\eta_x}{1 + \eta_z}\right)_x + \left\{Q \frac{(\eta_z + \frac{1}{2}[\eta_z^2 - \eta_x^2])}{(1 + \eta_z)^2}\right\}_z + \rho_0 N^2 \eta = 0 , \tag{2.1.8a}$$

where $$Q(z) = \rho_0 (c - u_0)^2 . \tag{2.1.8b}$$

Note that here z is a Lagrangian co-ordinate, and that x and z form a quasi-Lagrangian co-ordinate system. On the rigid lower boundary $z = z^* = 0$, then from (2.1.7a) the appropriate boundary condition is

$$\eta = 0 , \quad \text{on} \quad z = 0 , \tag{2.1.9}$$

In a Lagrangian formulation the position of the free surface is a constant and is given by $z = 0$. If the pressure at the free surface is chosen to be zero, then using Bernoulli's equation the appropriate boundary condition at the surface is



Reproduced with permission of the copyright owner. Further reproduction prohibited without permission.

$$\rho_0 \eta = p\sigma Q \frac{(\eta_z + \frac{1}{2}[\eta_z^2 - \eta_x^2])}{(1 + \eta_z)^2} \quad \text{on} \quad z = h \,. \tag{2.1.10}$$

Here recall that p = 0, or 1, according as the upper boundary is rigid, or free. It shall be assumed that $\eta \to 0$ as $|x| \to \infty$ which is the appropriate condition for a solitary wave. The velocity components are

$$u = -\frac{(c - u_0)}{(1 + \eta_z)}, \quad w = -\frac{(c - u_0)\eta_x}{1 + \eta_z} \,. \tag{2.1.11}$$



Reproduced with permission of the copyright owner. Further reproduction prohibited without permission.

## §2.2 ANALYSIS

To obtain a second order approximation to finite stationary waves, the vertical displacement $\eta$ must be expanded to atleast three stages in an expansion in powers of the small parameter $\varepsilon^2$. At the same time x-derivatives in the equations must be arranged in order of magnitude by specifying a suitable stretched horizontal scale. Accordingly it shall be assumed that $\eta$ has the asymptotic expansion

$$\eta = \varepsilon^2\eta_1(X, z) + \varepsilon^4\eta_2(X, z) + \varepsilon^6\eta_3(X, z) + \dots , \qquad (2.2.1a)$$

and guided by §2.1 put

$$\eta_1 = A(X)\phi(z) , \qquad (2.2.1b)$$

and

$$X = \varepsilon\kappa x . \qquad (2.2.1c)$$

Note, here that it is assumed that the waves are so long that derivatives with respect to X are of the same order of magnitude as the small parameter $\varepsilon$. Also, to eliminate secular terms entering the expansion the wave phase speed c and the constant $\kappa$ are given the asymptotic expansions

$$c = c_0 + \varepsilon^2 c_1 + \varepsilon^4 c_2 + \dots , \qquad (2.2.2a)$$

$$\kappa = 1 + \varepsilon^2\kappa_1 + \dots . \qquad (2.2.2b)$$

The principal aim of the analysis is to proceed to higher order in $\varepsilon$, and so determine $\eta_2(X, z)$ and the constants $c_2$ and $\kappa_1$; $c_2$ is the second order term in the phase speed, while



Reproduced with permission of the copyright owner. Further reproduction prohibited without permission.

$$\lambda(\kappa\varepsilon)^{-1} = \lambda\varepsilon^{-1}(1 - \varepsilon^2\kappa_1 + \dots) \qquad (2.2.3)$$

is the horizontal length scale of the solitary wave.

Substituting (2.2.1a,b,c) and (2.2.2a,b) into (2.1.8a), (2.1.9) and (2.1.10), it is found that, at the lowest order in $\varepsilon$, equations (2.1.1a,b,c) are satisfied. At the next two orders in, $\varepsilon$, it is found that

$$\{Q_0\eta_{iz}\}_z + \rho_0 N^2\eta_i + f_i = 0 , \qquad (2.2.4a)$$

$$\eta_i = 0 \quad \text{on} \quad z = 0 , \qquad (2.2.4b)$$

$$\rho_0\eta_i - p\sigma Q_0\eta_{iz} + p\sigma\rho_0 g_i = 0 \quad \text{on} \quad z = h , \qquad (2.2.4c)$$

where i = 2, 3 and the inhomogeneous terms $f_2$, $g_2$, $f_3$ and $g_3$ are given by

$$f_2 = Q_0\eta_{1XX} + \{Q_1\eta_{1z}\}_z - \{\tfrac{3}{2}Q_0\eta_{1z}^2\}_z , \qquad (2.2.5a)$$

$$\rho_0 g_2 = - Q_1\eta_{1z} + \tfrac{3}{2}Q_0\eta_{1z}^2 \quad \text{on} \quad z = h , \qquad (2.2.5b)$$

$$f_3 = \{2\kappa_1 Q_0 + Q_1\}\eta_{1XX} + Q_0\eta_{2XX} - Q_0(\eta_{1X}\eta_{1z})_X$$

$$+ \{Q_2\eta_{1z} + Q_1(\eta_{2z} - \tfrac{3}{2}\eta_{1z}^2) + Q_0(-\tfrac{1}{2}\eta_{1X}^2 + 2\eta_{1z}^3 - 3\eta_{1z}\eta_{2z})\}_z , \qquad (2.2.5c)$$

and $\rho_0 g_3 = - Q_2\eta_{1z} - Q_1(\eta_{2z} - \tfrac{3}{2}\eta_{1z}^2) - Q_0(-\tfrac{1}{2}\eta_{1X}^2 + 2\eta_{1z}^3 - 3\eta_{1z}\eta_{2z})$
on $z = h$ , (2.2.5d)

where $$Q_0(z) = \rho_0(c_0 - u_0)^2 , \qquad (2.2.6a)$$

$$Q_1(z) = 2c_1\rho_0(c_0 - u_0) , \qquad (2.2.6b)$$

and $$Q_2(z) = 2\rho_0 c_2(c_0 - u_0) + \rho_0 c_1^2 . \qquad (2.2.6c)$$



Reproduced with permission of the copyright owner. Further reproduction prohibited without permission.

The solution of (2.2.4a,b) can be found by the method of variation of parameters,

$$\eta_i = A_i(X)\phi(z) + \eta_i^{(p)} , \tag{2.2.7a}$$

where

$$\eta_i^{(p)} = \phi\int_0^z \psi f_i dz - \psi\int_0^z \phi f_i dz . \tag{2.2.7b}$$

Here $\psi(z)$ is a solution of (2.1.1a) independent of $\phi(z)$, and is chosen to satisfy the conditions

$$\psi_z = 0 \quad \text{at} \quad z = 0 , \tag{2.2.8a}$$

$$Q_0(\phi\psi_z - \psi\phi_z) = 1 . \tag{2.2.8b}$$

The expression on the left-hand side of (2.2.8b) is the Wronskian of the solutions $\phi$ and $\psi$, and hence is a constant.

Now in order that $\eta_i$, given by (2.2.7a), should satisfy the remaining boundary condition (2.2.4c), it is necessary and sufficient that

$$\int_0^h \phi f_i dz + \{p\sigma Q_0 \phi_z g_i\}_{z=h} = 0 . \tag{2.2.9}$$

It will now be shown that if i = 2 the compatibility condition (2.2.9) will determine the amplitude A(X) and the constant $c_1$, while if i = 3 the compatibility condition (2.2.9) will determine $A_2(X)$ and the constants $c_2$ and $\kappa_1$. Consider first (2.2.9) when i = 2, then using (2.2.5a,b) it is found that



Reproduced with permission of the copyright owner. Further reproduction prohibited without permission.

$$-c_1 A + \frac{1}{2}\mu A^2 + \delta A_{XX} = 0 \qquad (2.2.10)$$

where $\mu$ and $\delta$ are defined by (2.1.4a,b) respectively. It can now be verified that (2.2.10), which is an integrated form of the Korteweg-de Vries equation, has the solitary wave solution (2.1.2) with $c_1$ and $\lambda$ given by (2.1.3). Before proceeding to consider (2.2.9) when i = 3 it is useful to note that from (2.2.5a) and (2.2.10)

$$f_2 = c_1 A\alpha_1(z) + A^2\alpha_2(z) , \qquad (2.2.11a)$$

where $$\alpha_1(z) = \frac{Q_0\phi}{\delta} + \{2\rho_0(c_0 - u_0)\phi_z\}_z , \qquad (2.2.11b)$$

and $$\alpha_2(z) = \frac{\mu}{2\delta} Q_0\phi - \{\frac{3}{2} Q_0\phi_z^2\}_z . \qquad (2.2.11c)$$

Hence, when i = 2 (2.2.7b) becomes

$$\eta_2^{(p)} = c_1 A\beta_1(z) + A^2\beta_2(z) , \qquad (2.2.12a)$$

where $$\beta_1(z) = \phi\int_0^z \psi\alpha_1 dz - \psi\int_0^z \phi\alpha_1 dz , \qquad (2.2.12b)$$

and $$\beta_2(z) = \phi\int_0^z \psi\alpha_2 dz - \psi\int_0^z \phi\alpha_2 dz , \qquad (2.2.12c)$$

Next, from (2.2.5c,d), (2.2.7a) and (2.2.12), the compatibility condition (2.2.9) with i = 3 becomes

$$- c_1 A_2 + \mu A A_2 + \delta A_{2XX} = F , \qquad (2.2.13a)$$



Reproduced with permission of the copyright owner. Further reproduction prohibited without permission.

where $$F = \sigma_1 A + \sigma_2 A^2 + \sigma_3 A^3 + c_2 A - \kappa_1 \delta A_{XX} \, . \qquad (2.2.13b)$$

The left-hand side of (2.2.13a) can be recognised as the linearised form of the left-hand side of (2.2.10). The right-hand side of (2.2.13a) is a known function of A, and hence of X; the coefficients $\sigma_1$, $\sigma_2$, and $\sigma_3$ are given by

$$\frac{I\sigma_1}{c_1^2} = \int_0^h \rho_0 \{\phi_z^2 + (c_0 - u_0)[2\phi_z \beta_{1z} - \frac{2}{\delta}\phi^2] - (c_0 - u_0)^2 \frac{1}{\delta} \beta_1 \phi\} \, dz \, , \qquad (2.2.14a)$$

$$\frac{I\sigma_2}{c_1} = \int_0^h \rho_0 \{(c_0 - u_0)[\frac{\mu}{\delta}\phi^2 - 3\phi_z^3 + 2\phi_z \beta_{2z}] + (c_0 - u_0)^2 [\frac{3}{2\delta} \phi_z \phi^2 - \frac{4}{\delta}\phi\beta_2 - 3\phi_z^2 \beta_{1z} + \frac{\mu}{2\delta} \phi\beta_1]\} \, dz \, , \qquad (2.2.14b)$$

$$I\sigma_3 = \int_0^h \rho_0 (c_0 - u_0)^2 \{2\phi_z^4 - \frac{2\mu}{3\delta} \phi^2 \phi_z - 3\phi_z^2 \beta_{2z} + \frac{5\mu}{3\delta} \phi\beta_2\} \, dz \, , \qquad (2.2.14c)$$

where $$I = 2\int_0^h \rho_0 (c_0 - u_0) \phi_z^2 \, dz \, . \qquad (2.2.14d)$$

It must now be shown that there is a solution of (2.2.13a) for $A_2$, which is symmetric in X and decays to zero as $|X| \to \infty$. In order for the latter condition to be satisfied, the term in F which is proportional to A must be eliminated. Hence using (2.2.10),

$$\sigma_1 + c_2 - 2\kappa_1 c_1 = 0 \, . \qquad (2.2.15)$$



Reproduced with permission of the copyright owner. Further reproduction prohibited without permission.

It may then be shown that the required solution of (2.2.13a) is

$$A_2 = \left(\frac{2\sigma_2}{\mu} + \frac{9c_1\sigma_3}{\mu^2} + 2\kappa_1\right)A - \frac{3\sigma_3}{2\mu}A^2 \ . \qquad (2.2.16)$$

At this stage there is still one disposable constant, either $c_2$ or $\kappa_1$. This is determined by selecting an appropriate measure of wave amplitude. It is convenient to choose this to be the coefficient of $\phi(z)$ in (2.2.1a) evaluated at $X = 0$, and to require that this is precisely $\varepsilon^2 a$; this is tantamount to a choice of the expansion parameter $\varepsilon$. It follows that $A_2(0) = 0$, or from (2.2.15) and (2.2.16),

$$c_2 = -\sigma_1 - \frac{2}{3}a\sigma_2 - \frac{1}{2}a^2\sigma_3 \ , \qquad (2.2.17a)$$

and

$$\mu\kappa_1 = -\sigma_2 - \frac{3}{4}a\sigma_3 \ . \qquad (2.2.17b)$$

Finally, from (2.1.2) and (2.2.16),

$$A_2 = \frac{3\sigma_3 a^2}{2\mu}\,\mathrm{sech}^2\left(\frac{X}{\lambda}\right)\tanh^2\left(\frac{X}{\lambda}\right) \qquad (2.2.18)$$

The complete solution for $\eta$ (2.2.1a) can now be constructed from (2.2.7a) and (2.2.12a).

$$\eta = (\varepsilon^2 A + \varepsilon^4 A_2)\phi(z) + \varepsilon^4(c_1 A\beta_1(z) + A^2\beta_2(z)) + O(\varepsilon^6) \qquad (2.2.19)$$

The phase speed of the wave is given by (2.2.2a), where $c_1$ is given by (2.1.3) and $c_2$ is given by (2.2.17a). The wavelength is given by (2.2.3)



Reproduced with permission of the copyright owner. Further reproduction prohibited without permission.

where $\lambda$ is given by (2.1.3) and $\kappa_1$ by (2.2.17b). To make further progress the coefficients $\sigma_1$, $\sigma_2$ and $\sigma_3$ must be calculated, and this can be done once the modal function $\phi(z)$ is known. However, examination of (2.2.14a,b,c) shows that it would be difficult to draw any general conclusions concerning these coefficients, and so in the next section a number of special cases shall be examined. Before considering these special cases it is useful to replace the small parameter $\varepsilon$ with another small parameter $\hat{\varepsilon}$, the latter being defined as a direct measure of the maximum wave amplitude. Thus, suppose that at the wave crest $X = 0$, the maximum wave amplitude is $|\eta_m|$ attained at $z = z_m$. Then, put

$$\eta_m = \hat{\varepsilon}^2 a\phi(z_m) \ . \tag{2.2.20}$$

From (2.2.19) it follows that

$$\hat{\varepsilon}^2 = \varepsilon^2 + \frac{\varepsilon^4 a}{\phi(z_m)}\{\tfrac{1}{3}\mu\beta_1(z_m) + \beta_2(z_m)\} + O(\varepsilon^6) \ . \tag{2.2.21}$$

Note that $z_m$ differs from the value of $z$ for which $|\phi(z)|$ attains its maximum by an $O(\varepsilon^2)$ quantity, and in the relationship (2.2.21) $z_m$ may be replaced by the latter value of $z$. In terms of $\hat{\varepsilon}$ the phase speed is given by

$$c = c_0 + \hat{\varepsilon}^2 c_1 + \hat{\varepsilon}^4 \hat{c}_2 + O(\hat{\varepsilon}^6) \tag{2.2.22a}$$

where

$$\hat{c}_2 = c_2 - \frac{\mu a^2}{3\phi(z_m)}\{\tfrac{1}{3}\mu\beta_1(z_m) + \beta_2(z_m)\} \ , \tag{2.2.22b}$$

while the wavelength is given by



Reproduced with permission of the copyright owner. Further reproduction prohibited without permission.

$$\lambda(\kappa\varepsilon)^{-1} = \hat{\lambda}\hat{\varepsilon}^{-1}(1 - \hat{\varepsilon}^2\hat{\kappa}_1 + \ldots) , \qquad (2.2.23a)$$

where $$\hat{\kappa}_1 = \kappa_1 - \frac{a}{2\phi(z_m)}\left\{\frac{1}{3}\mu\beta_1(z_m) + \beta_2(z_m)\right\} . \qquad (2.2.23b)$$

Finally $\eta$ is given by

$$\eta = (\hat{\varepsilon}^2 A + \hat{\varepsilon}^4\hat{A}_2)\phi(z) + \hat{\varepsilon}^4\left(c_1 A\beta_1(z) + A^2\beta_2(z)\right) , \qquad (2.2.24a)$$

where $$\hat{A}_2 = A_2 - \frac{a}{\phi(z_m)}\left\{\frac{1}{3}\mu\beta_1(z_m) + \beta_2(z_m)\right\}A . \qquad (2.2.24b)$$

Along the streamline $z = z_m$ on which the maximum wave amplitude is achieved, the wave shape is given by

$$\eta(z = z_m) = \hat{\varepsilon}^2 a\phi(z_m)\operatorname{sech}^2\left(\frac{X}{\lambda}\right)\left\{1 + \hat{\varepsilon}^2 a\gamma \tanh^2\left(\frac{X}{\lambda}\right)\right\} + O(\hat{\varepsilon}^6) \qquad (2.2.25a)$$

where $$\gamma = \frac{3\sigma_3}{2\mu} - \frac{\beta_2(z_m)}{\phi(z_m)} . \qquad (2.2.25b)$$

In the discussion in §2.3 the principal aim is to determine the coefficients $\hat{c}_2$, $\hat{\kappa}_1$ and $\gamma$; in particular the signs of these quantities are of considerable significance for the properties of second order solitary internal waves. Thus if $\hat{c}_2$ is positive (negative) the phase speed is increased (decreased) over that predicted by the first order theory; if $\hat{\kappa}_1$ is positive (negative) the wavelength is decreased (increased); and if $(a\gamma)$ is positive (negative) the wave shape is altered by a broadening (narrowing). Note the distinction between the interpretation $\kappa_1$ and $(a\gamma)$; the former measures the second order effect on the wavelength (see



Reproduced with permission of the copyright owner. Further reproduction prohibited without permission.

(2.2.23a)) which can be regarded as a measure of the rate of decay of the wave as $|x| \to \infty$; the latter measures the second order effect on the wave shape relative to this wavelength scale.



Reproduced with permission of the copyright owner. Further reproduction prohibited without permission.

## §2.3 DISCUSSION

(I) Shear layer: $u_0 = -kz$, $N^2 = N_0^2$.

Here k and $N_0$ are constants, and the basic state is that of a linear shear flow in a uniformly stratified fluid. The Richardson number is $N_0^2/k^2$ and it shall be assumed that this is greater than 1/4 so that the basic state is stable. It shall also be assumed that there are no critical layers. Then, using the Boussinesq approximation $\sigma \to 0$, so that $\rho_0$ in (2.1.1a) and similar subsequent equations is regarded as a constant, it follows readily from (2.1.1a,b and c) that

$$\phi(z) = M\left(1 + \frac{kz}{c_0}\right)^{-1/2} \sin\left\{r \log\left(1 + \frac{kz}{c_0}\right)\right\}, \qquad (2.3.1a)$$

$$c_0 = kh\left\{\exp\left(\frac{s\pi}{r}\right) - 1\right\}^{-1}, \quad s = \pm 1, \pm 2, \pm 3, \ldots, \qquad (2.3.1b)$$

where

$$r = \left(\frac{N_0^2}{k^2} - \frac{1}{4}\right)^{1/2}. \qquad (2.3.1c)$$

For a positive mode number s, $c_0/kh > 0$ and the wave is propagating in the opposite sense to the basic flow; for a negative mode number s, $c_0/kh < -1$ and the wave is propagating in the same sense as the basic flow. M is a constant, chosen so that the maximum value of $|\phi(z)|$ is 1. To leading order in $\varepsilon^2$, this value is attained at $z_m$, and it may be shown that

$$1 + \frac{kz_m}{c_0} = \exp\left\{\frac{1}{r} \tan^{-1} 2r + \frac{(s - |s|)\pi}{2r}\right\} \qquad (2.3.2a)$$



Reproduced with permission of the copyright owner. Further reproduction prohibited without permission.

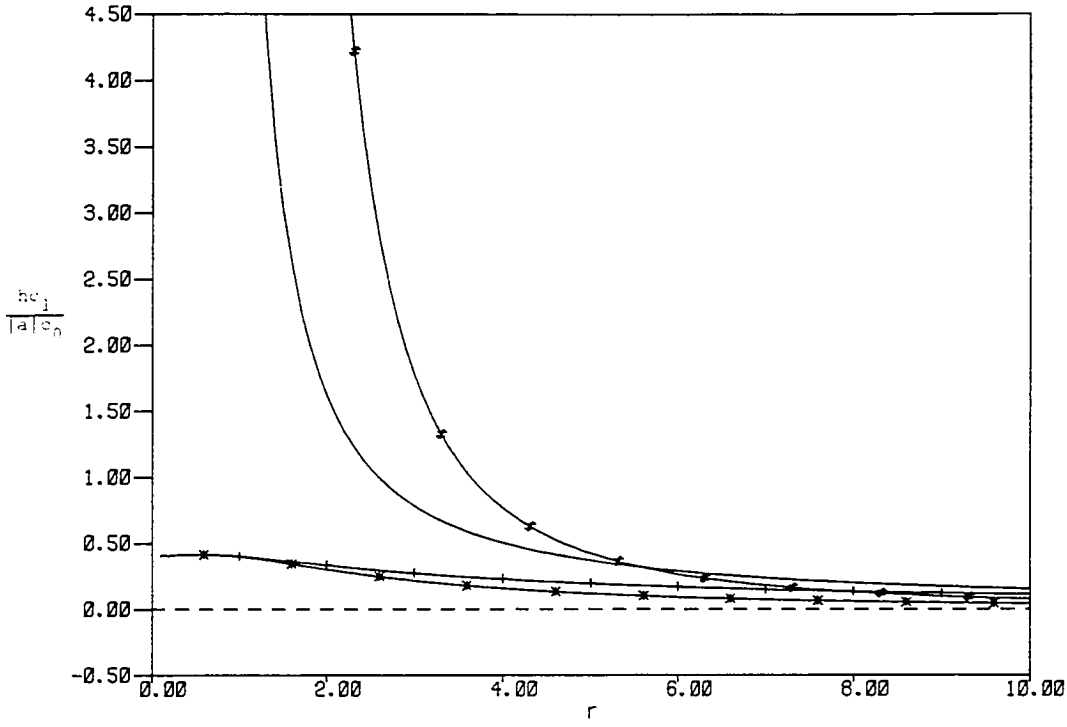


Figure 2.2: A plot of $c_1 h/|a|c_0$ as a function of r, in case (I), for modes s = 1 ———; s = -1 —+—+—; s = 2 —#—; and s = -2 —*—.

and
$$M = \left(1 + \frac{kz_m}{c_0}\right)^{1/2} \left(1 + \frac{1}{4r^2}\right)^{1/2} (-1)^{\frac{(s-|s|)}{2}} . \qquad (12.3.2b)$$

Note that for positive (negative) mode numbers, the maximum is attained close to $z = O(h)$, and that $\phi(z_m) = 1$. For large Richardson numbers, $r \to \infty$, and it is found that

$$c_0 = (\text{sign } k)\, \frac{hN_0}{s\pi} \left\{1 - \frac{s\pi}{2r} + O\left(\frac{s^2}{r^2}\right)\right\} . \qquad (2.3.3)$$

Thus the effect of the basic shear flow is, for s positive, to decrease the



Reproduced with permission of the copyright owner. Further reproduction prohibited without permission.

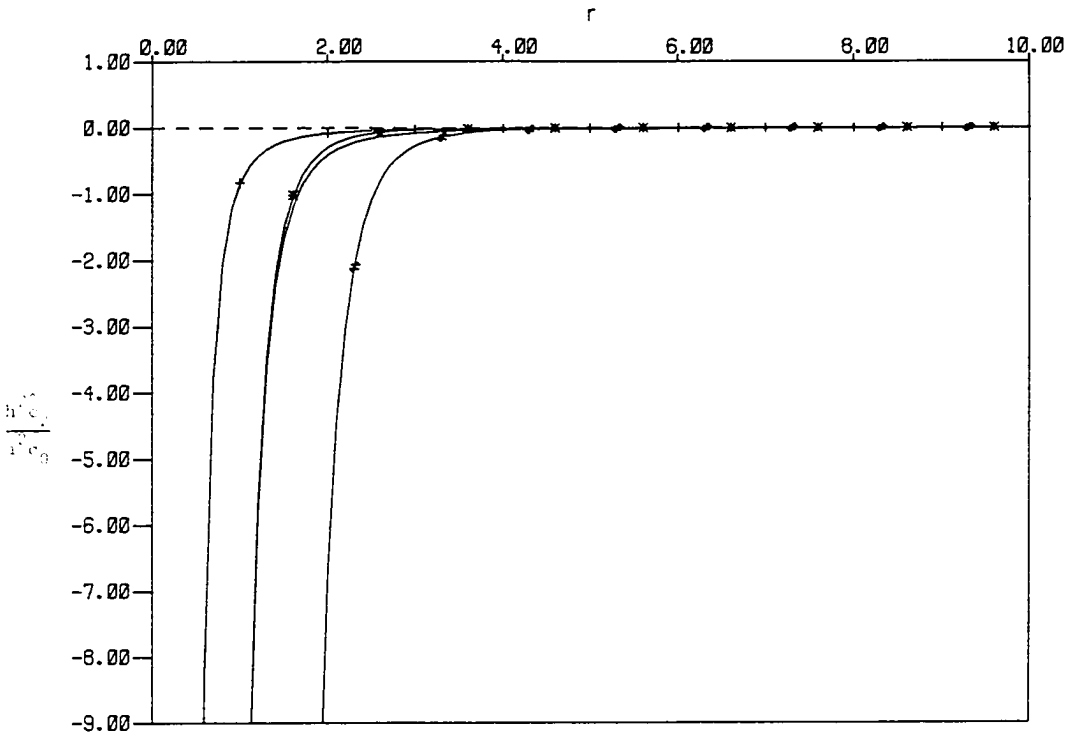


Figure 2.3: A plot of $\hat{c}_2 h^2/a^2 c_0$ as a function of r, in case (I), for modes s = 1 ——; s = -1 -+-+-; s = 2 —#—; and s = -2 —*—.

absolute value of $c_0$, and for s negative, to increase the absolute value.

Next, from (2.3.1a,b and c) it is possible to evaluate $\mu$ and $\delta$ (2.1.4a and b), and then find $c_1$ and $\lambda$ (2.1.3).

$$\frac{hc_1}{ac_0} = \frac{2rM \exp\left(\frac{s\pi}{r}\right)}{3\left(r^2 + \frac{9}{4}\right)} \left\{1 - (-1)^s \exp\left(-\frac{3s\pi}{2r}\right)\right\} , \qquad (2.3.4a)$$

$$\frac{a\lambda^2}{h^3} = \frac{3\left(r^2 + \frac{9}{4}\right)}{2rM(r^2 + 1)} \frac{\left\{\exp\left(\frac{s\pi}{r}\right) + 1\right\}}{\left\{\exp\left(\frac{s\pi}{r}\right) - 1\right\}^2 \left\{1 - (-1)^s \exp\left(-\frac{3s\pi}{2r}\right)\right\}} . \qquad (2.3.4b)$$

These expressions can be shown to agree with those obtained by Maslowe and



Reproduced with permission of the copyright owner. Further reproduction prohibited without permission.

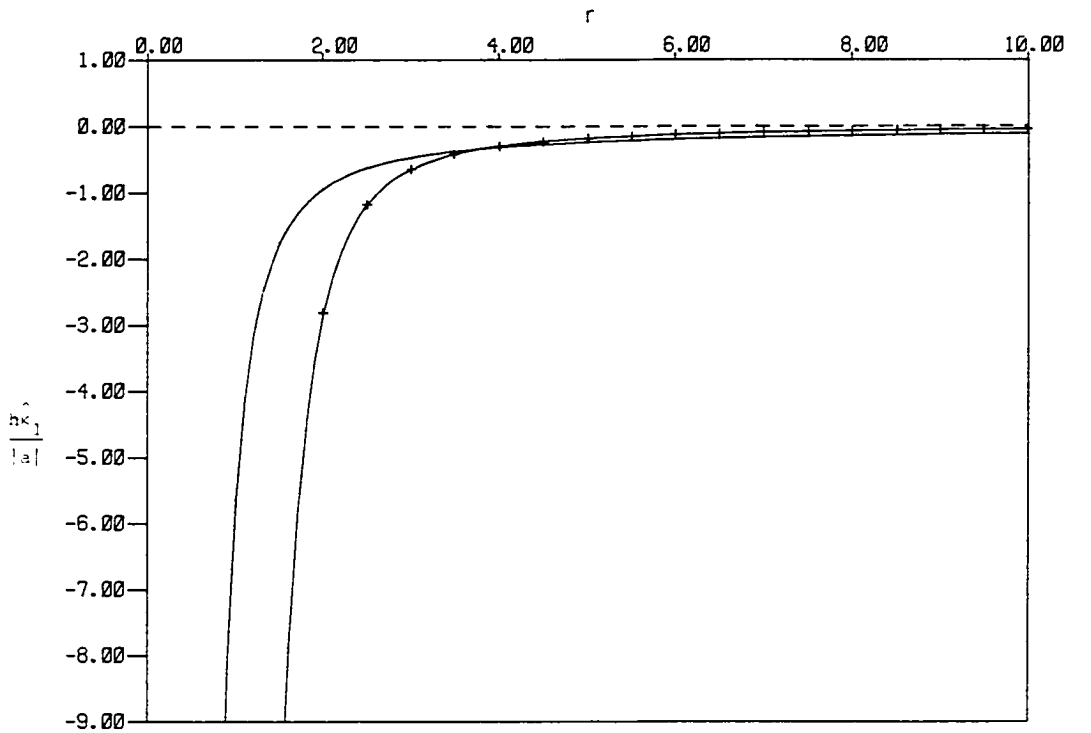


Figure 2.4: A plot of $h\hat{\kappa}_1/|a|$ as a function of r, in case (I), for modes s = ±1 ——; and s = ±2 —+—+—.

Redekopp (1980) and Tung, Ko and Chang (1981), where a comprehensive discussion of the effect of a basic linear shear flow on the first order solitary waves may be found. It is readily shown from (2.3.4a and b) that a is positive or negative according as s is positive or negative. Thus for s positive, the solitary wave is a wave of elevation and propagates against the basic flow, while for s negative, it is a wave of depression and propagates with the basic flow. Figure 2.2 is a plot of $c_1/c_0$ as a function of r. For large Richardson numbers, $r \to \infty$, and it is found that

$$\frac{hc_1}{|a|c_0} = \frac{4}{3r}\left\{1 + \frac{(2s + 1 - |s|)\pi}{4r} + O\left(\frac{s^2}{r^2}\right)\right\} \qquad \text{for } s = \pm 1, \pm 3, \ldots , \tag{2.3.5a}$$

or



Reproduced with permission of the copyright owner. Further reproduction prohibited without permission.

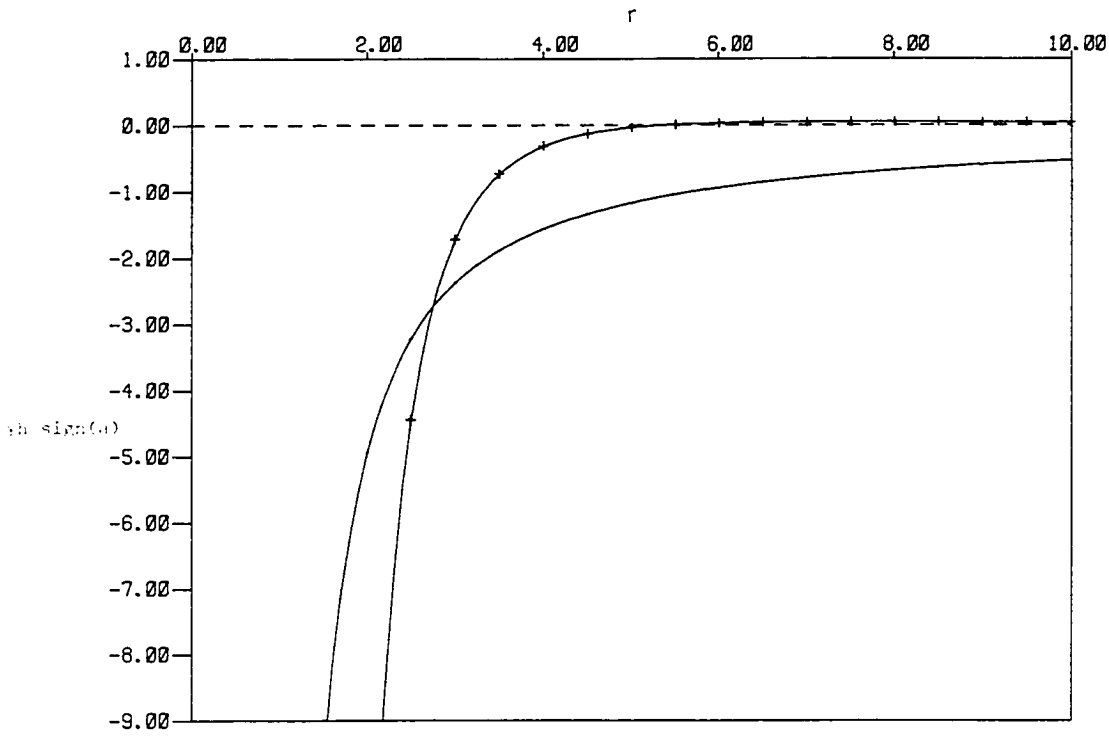


Figure 2.5: A plot of γh sign(a) as a function of r, in case (I), for modes s = ±1 ——; and s = ±2 —+—+—.

$$\frac{hc_1}{|a|c_0} = \frac{|s\pi|}{r^2}\left\{1 + \frac{(2s + 1 - |s|)\pi}{4r} + O\left(\frac{s^2}{r^2}\right)\right\} \qquad \text{for } s = \pm 2, \pm 4, \ldots , \tag{2.3.5b}$$

and

$$\frac{|a|\lambda^2}{h^3} = \frac{3r}{2(s\pi)^2}\left\{1 - \frac{(1 - |s|)\pi}{4r} + O\left(\frac{s^2}{r^2}\right)\right\} \qquad \text{for } s = \pm 1, \pm 3, \ldots , \tag{2.3.5c}$$

or

$$\frac{|a|\lambda^2}{h^3} = \frac{2r^2}{|s\pi|^3}\left\{1 - \frac{(1 - |s|)\pi}{4r} + O\left(\frac{s^2}{r^2}\right)\right\} \qquad \text{for } s = \pm 2, \pm 4, \ldots , \tag{2.3.5d}$$

It is apparent from these expressions that $c_1 \to 0$ and $\lambda \to \infty$ as $r \to \infty$ for a fixed value of the amplitude a. This is a result of the well known fact that the nonlinear coefficient μ (2.1.4a) is zero for uniform strati-



Reproduced with permission of the copyright owner. Further reproduction prohibited without permission.

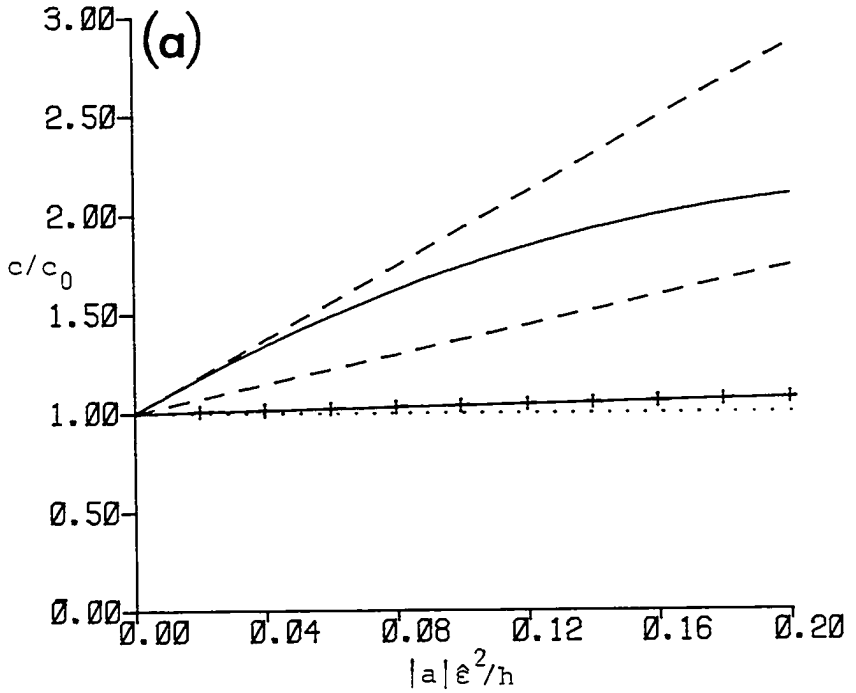


Figure 2.6: $c/c_0$ as a function of wave amplitude, $|a|\hat{\varepsilon}^2/h$ for the modes (a) s = 1 and (b) s = -1, when r = 1.0 and 5.0, in case (I); – – –, first order theory; ———, second order theory for r = 1.0; –+–+–, second order theory for r = 5.0. For s = -1 and r = 5.0 the first and second order theories are indistinguishable.

fication in the absence of any basic shear flow, and in the Boussinesq approximation. The consequences of this are explored further in §2.4.

Proceeding to the second order, first evaluate the functions $\alpha_1$ and $\alpha_2$ (2.2.11b and c), where $\phi$ is given by (2.3.1a). Then the particular solutions $\beta_1$ and $\beta_2$ (2.2.12b and c) can be evaluated. It is found that

$$u^{1/2}\beta_1 = \frac{M}{c_0}\frac{\exp(-\frac{s\pi}{r})}{(1+\exp(\frac{s\pi}{r}))}(u^2-1)(r\cos v - \sin v)$$

$$+\frac{M}{2c_0}(\frac{1}{u}-1)(2r\cos v - \sin v) + \frac{M}{c_0}\{1 - \frac{\exp(-\frac{s\pi}{r})}{(1+\exp(\frac{s\pi}{r}))}\}\sin v\ , \quad (2.3.6a)$$



Reproduced with permission of the copyright owner. Further reproduction prohibited without permission.

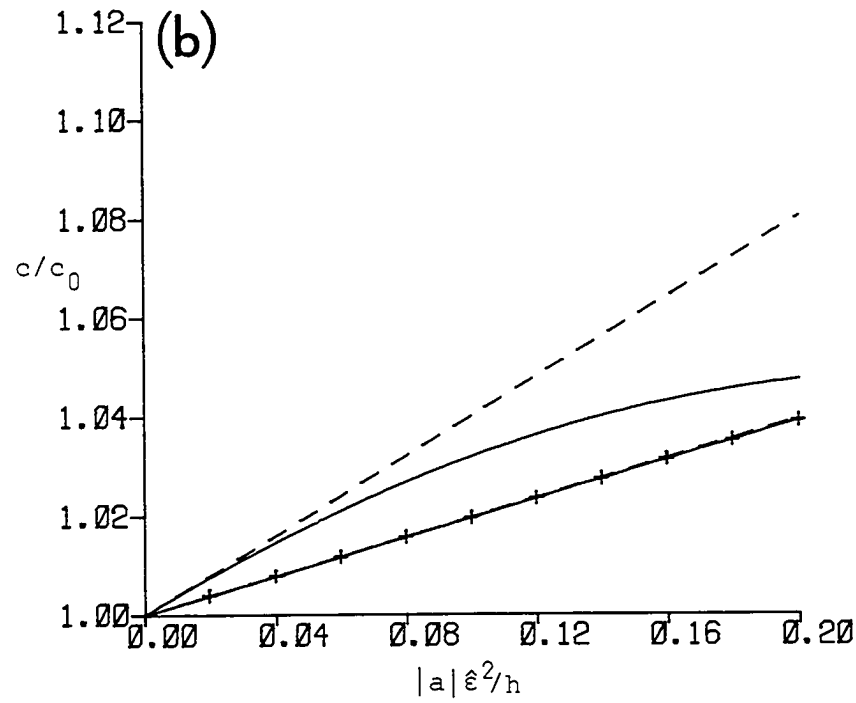


$$u^{1/2}\beta_2 = -\frac{kM^2}{c_0}\frac{r}{(r^2+\frac{9}{4})}\left\{\frac{1-(-1)^s\exp(-\frac{3s\pi}{2r})}{\exp(\frac{2s\pi}{r})-1}\right\}(u^2-1)(r\cos v - \sin v)$$

$$+\frac{kM^2}{2c_0}\frac{(2r\cos v - \sin v)}{(r^2+\frac{9}{4})}\left[u^{-3/2}\left\{(r^2+\frac{3}{4})\sin v - r\cos v\right\} + r\right]$$

$$+\frac{kM^2}{2c_0}\frac{2r}{(r^2+\frac{9}{4})}\left[\left\{\frac{1-(-1)^s\exp(-\frac{3s\pi}{2r})}{\exp(\frac{2s\pi}{r})-1}\right\} - \frac{1}{2}\right]\sin v\ , \qquad (2.3.6b)$$

where $u = 1 + \frac{kz}{c_0}$, and $v = r \log u$ . (2.3.6c)

The coefficients $\sigma_1$, $\sigma_2$ and $\sigma_3$ can now be evaluated from (2.2.14a,b and c), and finally expressions for $\hat{c}_2$ (2.2.22b), $\hat{\kappa}_1$ (2.2.23b) and $\gamma$ (2.2.25b) can be found. These expressions are extremely complicated and shall not be displayed explicitly. Instead in Figures 2.3, 2.4 and 2.5 graphs of $\hat{c}_2/c_0$, $\hat{\kappa}_1$ and $(a\gamma)$ are displayed as functions of r. Note that $\hat{c}_2/c_0$ is negative and $\hat{\kappa}_1$ is negative for all positive values of r (i.e. for all Richardson



Reproduced with permission of the copyright owner. Further reproduction prohibited without permission.

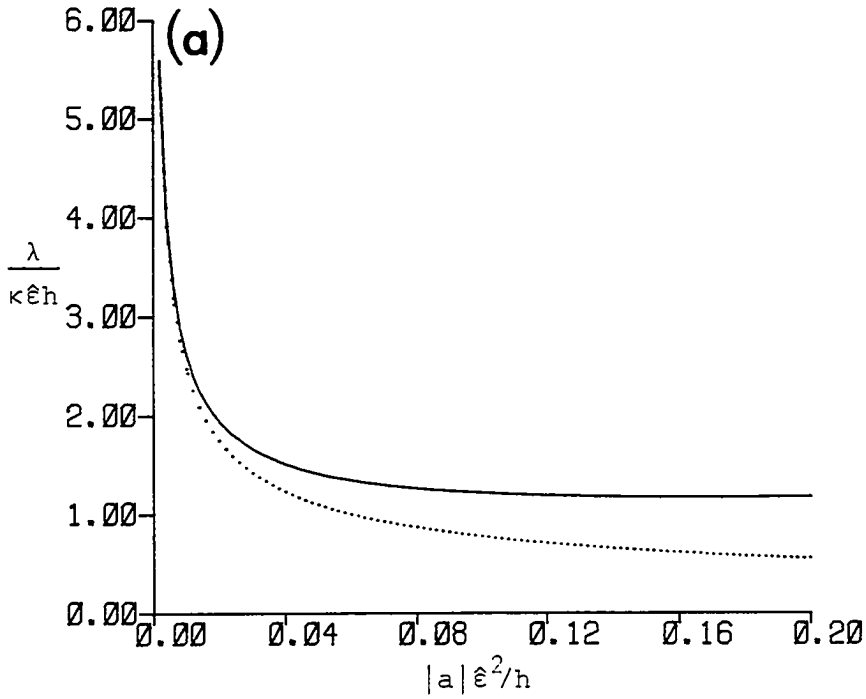


Figure 2.7: $\lambda/\kappa\hat{\varepsilon}h$ as a function of wave amplitude, $|a|\hat{\varepsilon}^2/h$ for the modes $s = \pm 1$, when (a) $r = 1.0$ and (b) 5.0, in case (I); ····· , first order theory; ——— , second order theory.

numbers greater than 1/4). Thus all these second order solitary waves have smaller phase speeds than those predicted by the first order theory; their wavelengths are increased above that predicted by the first order theory. The coefficient $(a\gamma)$ is negative for all odd numbered modes, whose wave shapes are thus narrower than the first order theory; for the even numbered modes $(a\gamma)$ is positive for large values of r, giving thicker wave shapes, but is negative for small values of r. Figure 2.6 is a graph of $c/c_0$ (2.2.22a) as a function of wave amplitude for $r = 1$, 5 and $s = \pm 1$; it is seen that as r increases with s and the wave amplitude fixed, $c/c_0$ decreases and it may be shown that $c/c_0 \to 1$ as $r \to \infty$. Figure 2.7 is a graph of $\lambda(\kappa\varepsilon)^{-1}$ (2.2.23a) as a function of wave amplitude for $r = 1$, 5 and $s = \pm 1$; it is seen that as r increases with s and the wave amplitude fixed, the wavelength increases. Figure 2.8 shows graphs of $\eta(z = z_m)$



Reproduced with permission of the copyright owner. Further reproduction prohibited without permission.

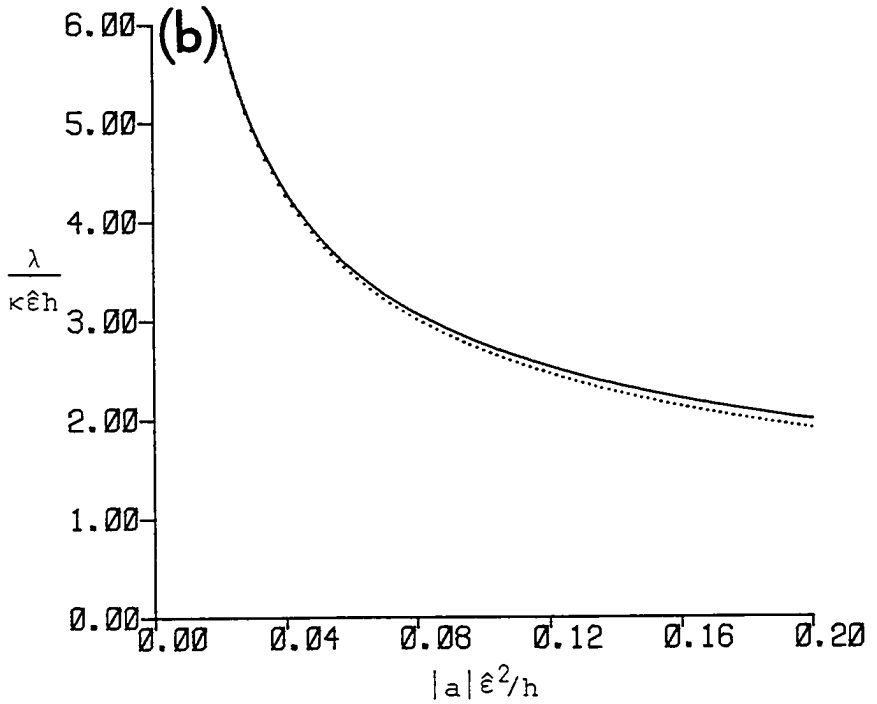


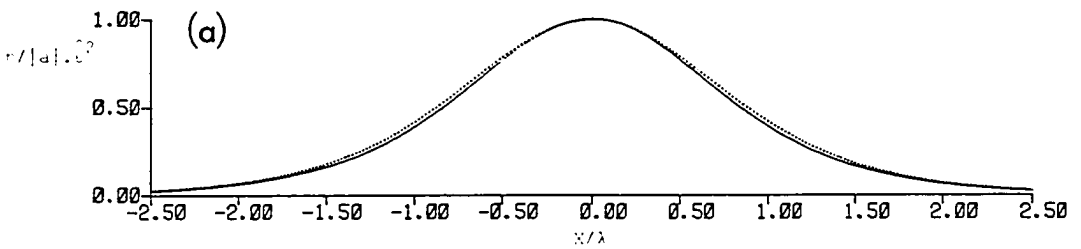


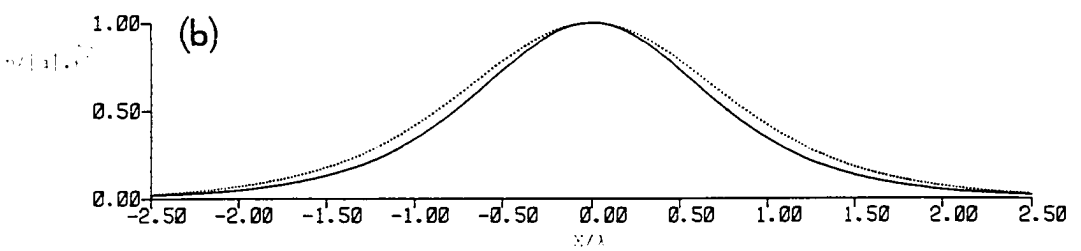


Figure 2.8: $\eta(X, z_m)$ as a function of $X/\lambda$ for (a) s = 1, r = 5.0 and $|a|\hat{\varepsilon}^2/h = 0.1$, and (b) s = 1, r = 1.0 and $|a|\hat{\varepsilon}^2/h = 0.01$, in case (I); ····, first order theory; ———, second order theory.



Reproduced with permission of the copyright owner. Further reproduction prohibited without permission.

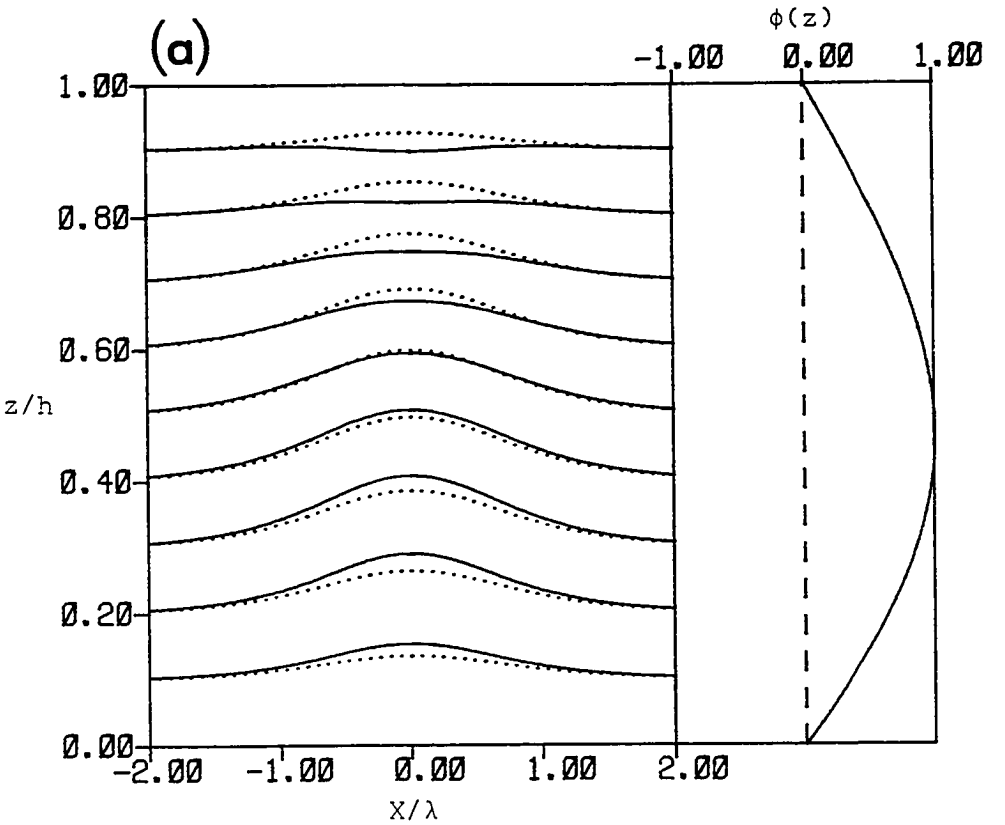


Figure 2.9: The streamlines as a function of $X/\lambda$ and $z/h$ for the modes (a) $s = 1$ and (b) $s = 2$, when $r = 5.0$ and $|a|\hat{\varepsilon}^2/h = 0.01$, in case (I); ·····, first order theory; ———, second order theory.

(2.2.25a) for $s = 1$, $r = 1$, 5 and $|a|\hat{\varepsilon}^2 h^{-1} = 10^{-2}$, $10^{-1}$ respectively; it is seen that the second order theory acts to narrow the wave. Also as r decreases it is found that $|a|\hat{\varepsilon}^2 h^{-1}$ must be correspondingly decreased in order that the second order term should remain small relative to the first order term; as $r \to 0$, $|a|\hat{\varepsilon}^2 h^{-1} \to 0$ and the theory fails in this limit. Figure 2.9 shows graphs of the streamlines given by $\eta(X, z)$ (2.2.24a) for $r = 5.0$, $|a|\hat{\varepsilon}^2 h^{-1} = 10^{-1}$ and $s = 1, 2$; it is seen that the second order theory may give a quite different picture of the streamlines than the first order theory even for moderate wave amplitudes. Also, as the mode number increases, it is found that the amplitude $|a|\hat{\varepsilon}^2 h^{-1}$ must be correspondingly



Reproduced with permission of the copyright owner. Further reproduction prohibited without permission.

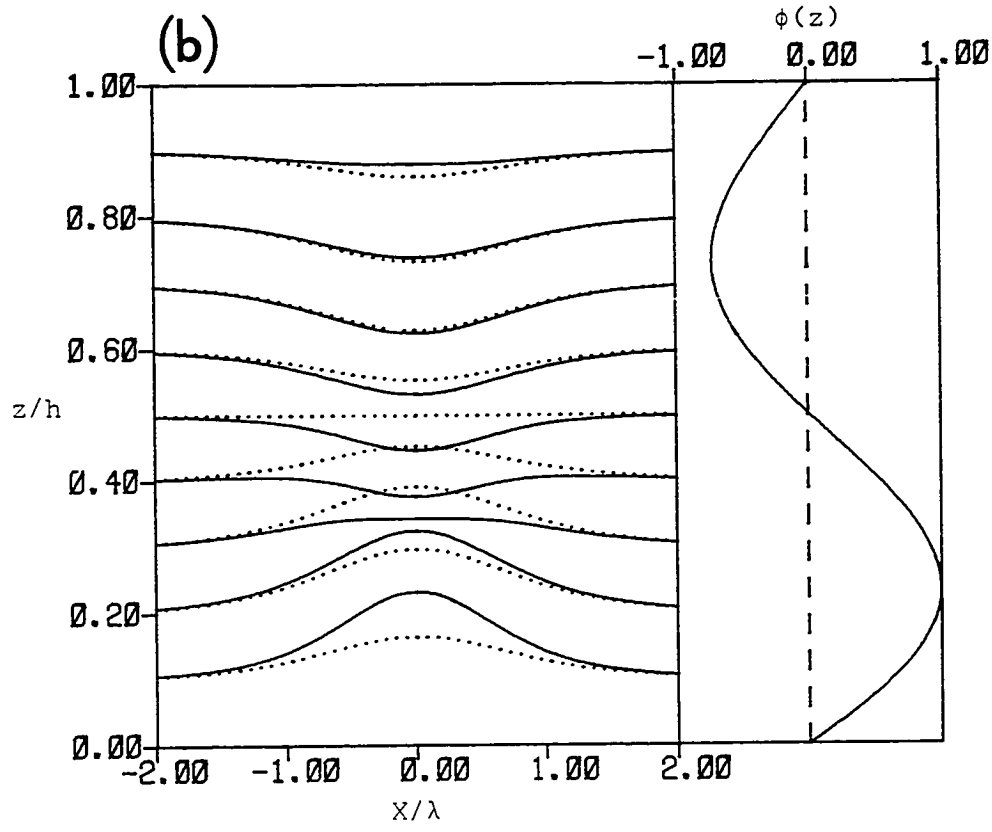


reduced in order that the second order corrections should remain small relative to the first order term.

As $r \to \infty$, it is found that

$$\frac{h^2\hat{c}_2}{a^2c_0} = -\frac{2}{9r^2}\left\{1 + \frac{\pi}{2r}(s + 3 - 3|s|) + O\left(\frac{s^2}{r^2}\right)\right\} \quad \text{for} \quad s = \pm 1, \pm 3, \ldots , \tag{2.3.7a}$$

or

$$\frac{h^2\hat{c}_2}{a^2c_0} = -\frac{(s\pi)^2}{8r^4}\left\{1 + \frac{\pi}{2r}(s + 3 - 3|s|) + O\left(\frac{s^2}{r^2}\right)\right\} \quad \text{for} \quad s = \pm 2, \pm 4, \ldots , \tag{2.3.7b}$$

$$\frac{h\hat{\kappa}_1}{|a|} = -\frac{13}{12r}\left\{1 + \frac{17\pi}{52r}(1 - |s|) + O\left(\frac{s^2}{r^2}\right)\right\} \quad \text{for} \quad s = \pm 1, \pm 3, \ldots , \tag{2.3.7c}$$

or



Reproduced with permission of the copyright owner. Further reproduction prohibited without permission.

$$\frac{\hat{h\kappa}_1}{|a|} = -\frac{13}{16}\frac{|s\pi|}{r^2}\left\{1 + \frac{17\pi}{52r}(1 - |s|) + O\left(\frac{s^2}{r^2}\right)\right\} \quad \text{for} \quad s = \pm 2, \pm 4, \ldots , \tag{2.3.7d}$$

$$\gamma h \operatorname{sign}(a) = -\frac{31}{6r}\left\{1 + \frac{43\pi}{124r}(1 - |s|) + O\left(\frac{s^2}{r^2}\right)\right\} \text{ for } s = \pm 1, \pm 3, \ldots , \tag{2.3.7e}$$

or

$$\gamma h \operatorname{sign}(a) = \frac{19}{24}\frac{|s|\pi}{r^2}\left\{1 + \frac{17\pi}{16r}(1 - |s|) + O\left(\frac{s^2}{r^2}\right)\right\} \quad \text{for} \quad s = \pm 2, \pm 4, \ldots , \tag{2.3.7f}$$

Like $c_1$ and $\lambda^{-1}$ all these expressions tend to zero as $r \to \infty$. It is apparent that this limit requires a different scaling for the amplitude and wavelength than that which has been used so far, and this aspect is taken up in §2.4.



Reproduced with permission of the copyright owner. Further reproduction prohibited without permission.

(II) Uniform stratification: $u_0 = 0$, $N^2 = N_0^2$.

Here $N_0$ is a constant, and so in the Boussinesq approximation $\sigma \to 0$, the nonlinear coefficient $\mu$ (2.1.4a) is identically zero. It is thus necessary to retain the terms neglected in the Boussinesq approximation, and the results of this calculation are presented in this subsection. When $N^2$ is a constant, the density is given by

$$\rho_0(z) = \rho_1 \exp(-\sigma N_0^2 z) , \tag{2.3.8}$$

and it follows readily from (2.1.1a,b and c) that

$$\phi = M\rho_0^{-1/2} \sin(\gamma_s z) , \tag{2.3.9a}$$

$$c_0^2 = \frac{N_0^2}{\gamma_s^2 + \frac{1}{4}\sigma^2 N_0^4} , \tag{2.3.9b}$$

where $$\tan \gamma_s h = \frac{p\sigma\gamma_s N_0^2}{\gamma_s^2 - \frac{1}{4}\sigma^2 N_0^4} , \qquad s = 0, 1, 2, \ldots . \tag{2.3.9c}$$

Here recall that $p = O(1)$ corresponds to a rigid (free) upper boundary condition. For each mode number s there are two solutions for $c_0$ representing waves travelling to the right and left respectively. For a rigid upper boundary condition $\gamma_s h = s\pi$, and the $s = 0$ mode is excluded. For a free upper boundary condition

$$c_0^2 = \left(\frac{N_0 h}{s\pi}\right)^2 \left\{1 - \frac{2\sigma N_0^2 h}{(s\pi)^2} + O(\sigma^2)\right\} , \quad s = 1, 2, \ldots, \tag{2.3.10a}$$



Reproduced with permission of the copyright owner. Further reproduction prohibited without permission.

and $$c_0^2 = \frac{h}{\sigma}\left\{1 - \frac{1}{6}\sigma N_0^2 h + O(\sigma^2)\right\}, \qquad s = 0 . \tag{2.3.10b}$$

The $s = 0$ mode is the free surface mode, while the remaining modes are internal; for all modes the effect of the Boussinesq parameter $\sigma$ is to decrease the phase speed. M is a constant chosen so that the maximum value of $|\phi(z)|$ is 1. This value is attained at $z_m$, where $\phi(z_m) = 1$; it is found that

$$(h - z_m)\gamma_s = \frac{\pi}{2} + 2(p - \tfrac{1}{2})\tan^{-1}\left(\frac{\sigma N_0^2}{2\gamma_s}\right) , \tag{2.3.11a}$$

and $$M\rho_1^{-1/2} = (-1)^{s+1}\left(1 + \frac{\sigma^2 N_0^4}{4\gamma_s^2}\right)^{1/2} \exp\left(-\tfrac{1}{2}\sigma N_0^2 z_m\right) , \tag{2.3.11b}$$

for the internal modes ($s = 1, 2, \ldots$). For the free surface mode ($s = 0$), and sufficiently small $\sigma$ ($\sigma N_0^2 < \pi$), the maximum is attained at $z_m = h$, and M is chosen so that $\phi(h) = 1$.

Next, from (2.3.9a,b and c) $\mu$ and $\delta$ (2.1.4a and b) can be evaluated, and hence $c_1$ and $\lambda$ (2.1.3) can be found. Then

$$\frac{hc_1}{ac_0} = \frac{M\sigma N_0^2 \gamma_s^3\{1 + (-1)^s(9p - 1)\exp(\frac{1}{2}\sigma N_0^2 h)\}}{\rho_1^{1/2}(9\gamma_s^2 + \frac{1}{4}\sigma^2 N_0^4)(\gamma_s^2 + \frac{1}{4}\sigma^2 N_0^4 + p\sigma N_0^2/h)} , \tag{2.3.12a}$$

$$\frac{a\lambda^2}{h^3} = \frac{2\rho_1^{1/2}(9\gamma_s^2 + \frac{1}{4}\sigma^2 N_0^4)\{1 - \frac{p\sigma N_0^2}{h}\frac{(\gamma_s^2 - \frac{1}{4}\sigma^2 N_0^4)}{(\gamma_s^2 + \frac{1}{4}\sigma^2 N_0^4)}\}}{Mh^2\sigma N_0^2\gamma_s^3\{1 + (-1)^s(9p - 1)\exp(\frac{1}{2}\sigma N_0^2 h)\}} . \tag{2.3.12b}$$



Reproduced with permission of the copyright owner. Further reproduction prohibited without permission.

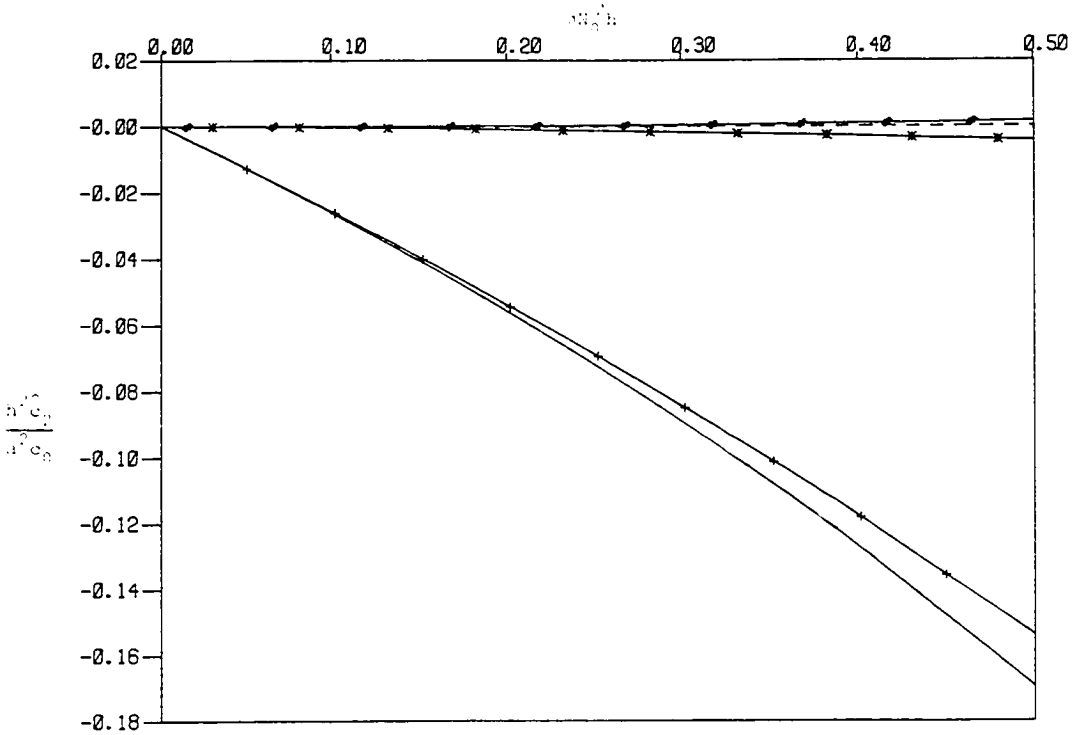


Figure 2.10: A plot of $\hat{hc}_2/a^2c_0$ as a function of $\sigma N_0^2 h$ in case (II), for modes s = 1, p = 1 ——; s = 2, p = 1 —+—+—; s = 1, p = 0 —#—; and s = 2, p = 0 —*—.

When p = 0 these expressions agree with those obtained by Benney (1966). It is readily shown from these expressions that the amplitude a is positive (negative) for the mode numbers s = 1, 2, ... for the rigid (free) upper boundary condition. However, the amplitude a is positive for the free surface mode, s = 0. Thus the internal modes are waves of elevation (depression) at $z = z_m$ when p = 0(1), and the free surface mode (p = 1, s = 0) is a wave of elevation. As $\sigma \to 0$, for the internal modes

$$\frac{hc_1}{ac_0} = \frac{2\sigma N_0^2 h}{9s\pi}\left\{1 - \frac{\sigma N_0^2 h}{4s}(s-1) + O(\sigma^2)\right\} \qquad \text{for } p = 0,\ s = 1,3,\ldots, \tag{2.3.13a}$$

or



Reproduced with permission of the copyright owner. Further reproduction prohibited without permission.

$$\frac{hc_1}{ac_0} = \frac{(\sigma N_0{}^2 h)^2}{18s\pi}\left\{1 - \frac{\sigma N_0{}^2 h}{4s}(s-1) + O(\sigma^2)\right\} \qquad \text{for } p = 0,\ s = 2,4,\ldots, \tag{2.3.13b}$$

or

$$\frac{hc_1}{ac_0} = -(8 + (-1)^s)\frac{\sigma N_0{}^2 h}{9s\pi}\left\{1 + \sigma N_0{}^2 h\left(\frac{1}{4s} - \frac{2}{(s\pi)^2} + \frac{(1 - 8(-1)^s)}{126}\right) + O(\sigma^2)\right\}$$

$$\text{for } p = 1,\ s = 1,2,3,\ldots, \tag{2.3.13c}$$

and

$$\frac{a\lambda^2}{h^3} = \frac{9}{s\pi\sigma N_0{}^2 h}\left\{1 + \frac{\sigma N_0{}^2 h}{4s}(s-1) + O(\sigma^2)\right\} \qquad \text{for } p = 0,\ s = 1,3,\ldots, \tag{2.3.13d}$$

or

$$\frac{a\lambda^2}{h^3} = \frac{36}{s\pi(\sigma N_0{}^2 h)^2}\left\{1 + \frac{\sigma N_0{}^2 h}{4s}(s-1) + O(\sigma^2)\right\} \quad \text{for } p = 0,\ s = 2,4,\ldots, \tag{2.3.13e}$$

or

$$\frac{a\lambda^2}{h^3} = -\frac{2(8 - (-1)^s)}{7s\pi\sigma N_0{}^2 h}\left\{1 - \sigma N_0{}^2 h\left(\frac{1}{4s} + \frac{2}{(s\pi)^2} + \frac{(1 - 8(-1)^s)}{126}\right) + O(\sigma^2)\right\}$$

$$\text{for } p = 1,\ s = 1,2,3,\ldots, \tag{2.3.13f}$$

These expressions show that $c_1/c_0 \to 0$ and $\lambda \to \infty$ as $\sigma \to 0$ for a fixed value of the amplitude a. This is a result of the vanishing of the nonlinear coefficient $\mu$ (2.1.4a) in this limit, and the consequences of this are explored further in §2.4. For the free surface mode p = 1, s = 0, as $\sigma \to 0$

$$\frac{hc_1}{ac_0} = \frac{1}{2}\{1 + O(\sigma^2)\}\ , \tag{2.3.14a}$$



Reproduced with permission of the copyright owner. Further reproduction prohibited without permission.

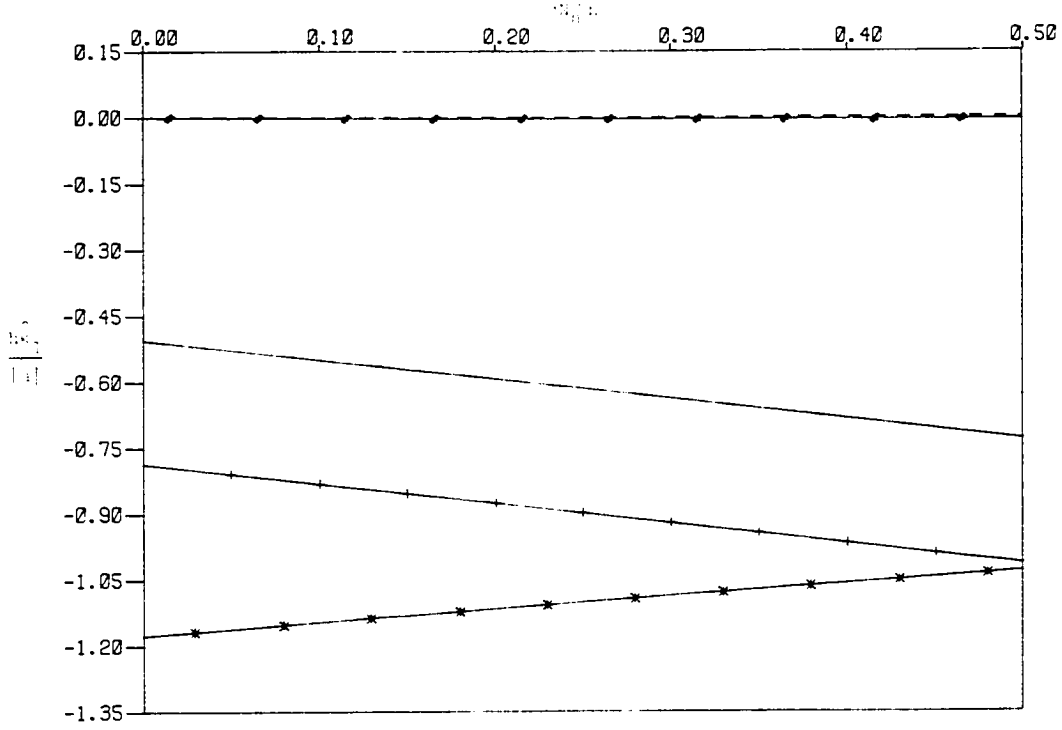


Figure 2.11: A plot of $h\hat{\kappa}_1/|a|$ as a function of $\sigma N_0^2 h$ in case (II), for modes s = 1, p = 1 ———; s = 2, p = 1 —+—+—; s = 1, p = 0 —#—; and s = 2, p = 0 —*—.

and
$$\frac{a\lambda^2}{h^3} = \frac{4}{3}\{1 - \frac{11\sigma N_0^2 h}{30} + O(\sigma^2)\} . \qquad (2.3.14b)$$

In the limit $\sigma \to 0$, these expressions reduce to the well known results for the surface solitary wave on a homogeneous fluid.

Proceeding to the second order, first evaluate the functions $\alpha_1$ and $\alpha_2$ (2.2.11b and c), so that the particular solutions $\beta_1$ and $\beta_2$ (2.2.12b and c) can be evaluated. It is found that

$$\sqrt{\rho_0}\,\beta_1 = -\frac{M}{2\gamma_s^2}\left(\frac{2N_0^2}{c_0^3} - \frac{1}{\delta}\right)\{(\gamma_s z)\cos\gamma_s z - \sin\gamma_s z\} , \qquad (2.3.15a)$$



Reproduced with permission of the copyright owner. Further reproduction prohibited without permission.

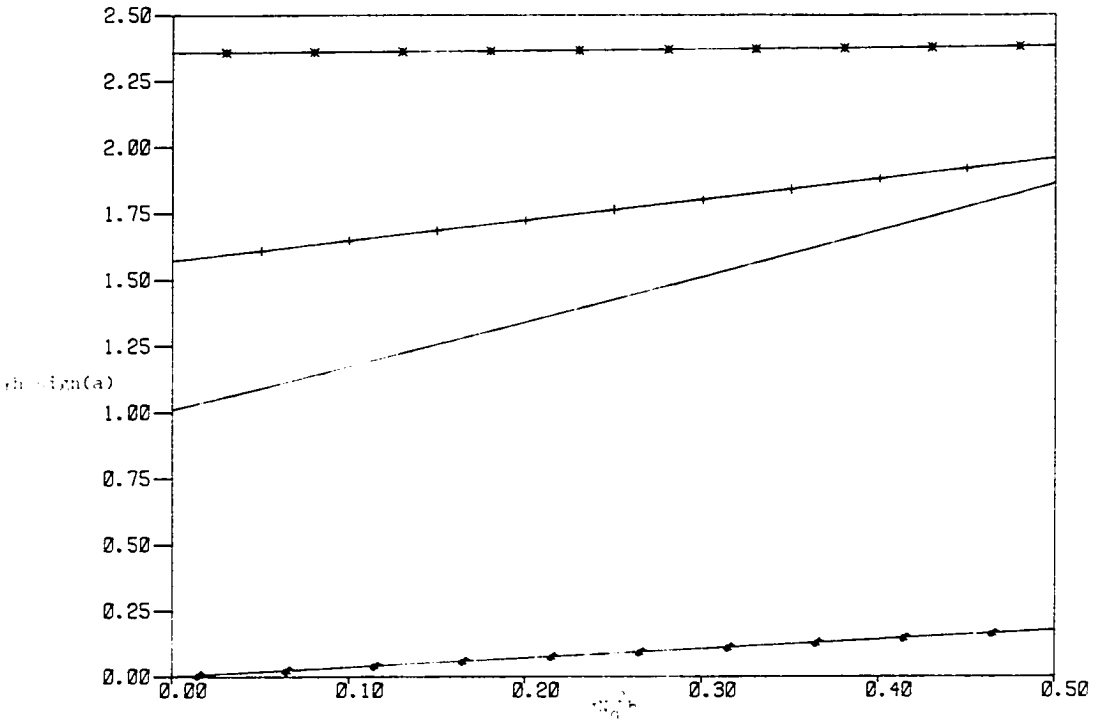


Figure 2.12: A plot of $\gamma h\ \mathrm{sign}(a)$ as a function of $\sigma N_0^2 h$ in case (II), for modes s = 1, p = 1 ———; s = 2, p = 1 —+—+—; s = 1, p = 0 —#—; and s = 2, p = 0 —*—.

$$\sqrt{\rho_0}\,\beta_2 = -\frac{M\mu}{4\delta\gamma_s^2}\{(\gamma_s z)\cos\gamma_s z - \sin\gamma_s z\}$$

$$+\frac{3M^2\gamma_s^2}{2\sqrt{\rho_0}\left(9\gamma_s^2+\frac{1}{4}\sigma^2N_0^4\right)}\{-6\gamma_s\sin\gamma_s z + \sigma N_0^2\cos\gamma_s z\}$$

$$+\frac{3M^2\gamma_s^2}{2\sqrt{\rho_0}\left(9\gamma_s^2+\frac{1}{4}\sigma^2N_0^4\right)}\{(3\gamma_s^2+\tfrac{1}{4}\sigma^2N_0^4)\sin 2\gamma_s z - \sigma N_0^2\gamma_s\cos 2\gamma_s z\}\ . \qquad (2.3.15b)$$

Note that if the rigid upper boundary condition is applied then $\delta = c_0^3/2N_0^2$ and $\beta_1$ is identically zero.



Reproduced with permission of the copyright owner. Further reproduction prohibited without permission.

The coefficients $\sigma_1$, $\sigma_2$ and $\sigma_3$ can now be evaluated (2.2.14a,b and c) and expressions for $\hat{c}_2$ (2.2.22b), $\hat{\kappa}_1$ (2.2.23b) and $\gamma$ (2.2.25b) obtained. These expressions are extremely complicated and shall not be displayed explicitly. Figures 2.10, 2.11 and 2.12 display graphs of $\hat{c}_2/c_0$, $\hat{\kappa}_1$ and $\gamma$ respectively as functions of $(\sigma N_0{}^2 h)$, for the internal modes s = 1, 2. Note that $h^2\hat{c}_2/a^2c_0$ is negative for all modes except for the first mode with a rigid upper lid (s = 1, p = 0); for this mode the second order solitary wave has a larger phase speed than that predicted by the first order theory, but for all other modes the phase speed is smaller than that predicted by first order theory. The quantity $h\hat{\kappa}_1/|a|$ is negative and the coefficient ($h\gamma$ sign a) is positive for all the internal modes. Thus the second order solitary waves have a larger wavelength and are wider at $z = z_m$ than the solitary waves predicted by first order theory. As $\sigma \to 0$,

$$\frac{h^2\hat{c}_2}{a^2c_0} = -\frac{\sigma N_0{}^2 h}{4} + O(\sigma^2) \qquad \text{for } p = 1 , \qquad (2.3.16a)$$

or

$$\frac{h^2\hat{c}_2}{a^2c_0} = (\sigma N_0{}^2 h)^2 \left\{-\frac{1}{48} + \frac{(1 - (-1)^s)}{81s^2\pi^2}(3s\pi - 5)\right\} + O(\sigma^3) \quad \text{for } p = 0 , \qquad (2.3.16b)$$

$$\frac{h\hat{\kappa}_1}{|a|} = -\frac{s\pi}{56}\{8 - (-1)^s\} + O(\sigma) \qquad \text{for } p = 1 , \qquad (2.3.16c)$$

or

$$\frac{h\hat{\kappa}_1}{|a|} = -s\pi\sigma N_0{}^2 h \left\{\frac{3}{64} + \frac{(7 - 12s\pi)}{72s^2\pi^2}\right\} + O(\sigma^2) \qquad \text{for } p = 0,\ s = 1,3,\ldots, \qquad (2.3.16d)$$

or



Reproduced with permission of the copyright owner. Further reproduction prohibited without permission.

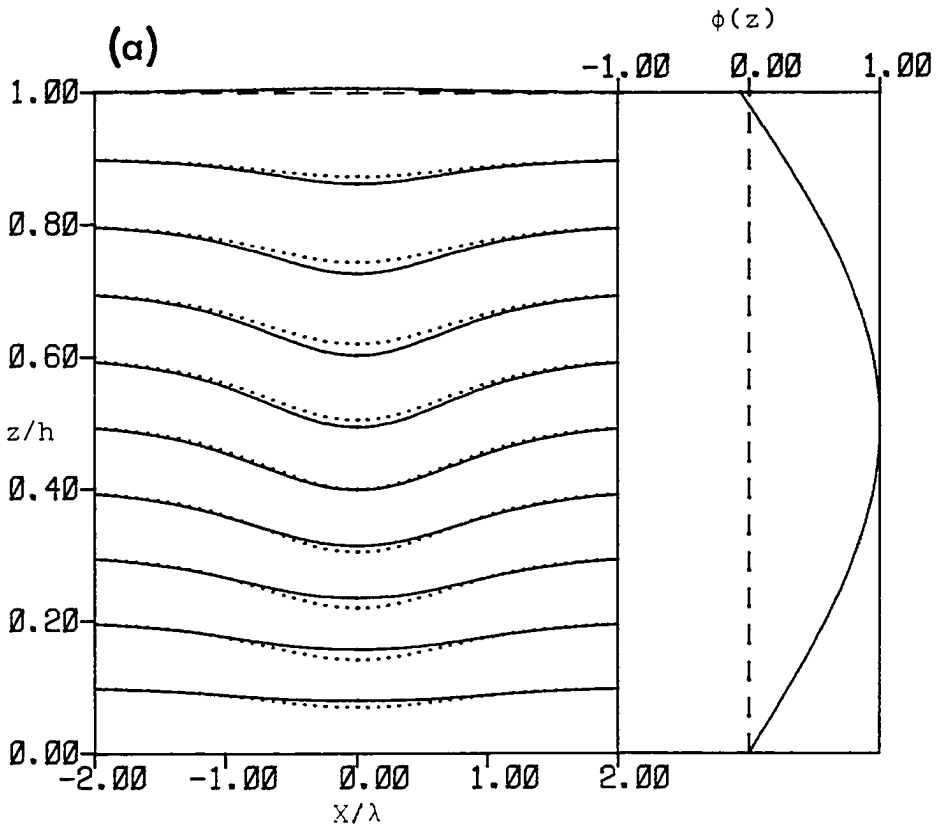


Figure 2.13: The streamlines as a function of $X/\lambda$ and $z/h$ for the mode $s = 1$, $\sigma N_0^2 h = 0.2$, $|a|\hat{\varepsilon}^2/h = 0.1$ when (a) $p = 1$ and (b) $p = 0$ for case (II); ····· , first order theory; ——— second order theory.

$$\frac{h\hat{\kappa}_1}{|a|} = -\frac{3}{16}s\pi + O(\sigma) \qquad \text{for } p = 0,\ s = 2,4,\ldots, \tag{2.3.16e}$$

$$h\gamma = -\frac{s\pi}{28}(8 - (-1)^s) + O(\sigma) \qquad \text{for } p = 1\ , \tag{2.3.16f}$$

or

$$h\gamma = s\pi\sigma N_0^2 h\left\{\frac{3}{32} + \frac{(12s\pi - 31)}{36s^2\pi^2}\right\} + O(\sigma^2) \qquad \text{for } p = 0,\ s = 1,3,\ldots, \tag{2.3.16g}$$

or



Reproduced with permission of the copyright owner. Further reproduction prohibited without permission.

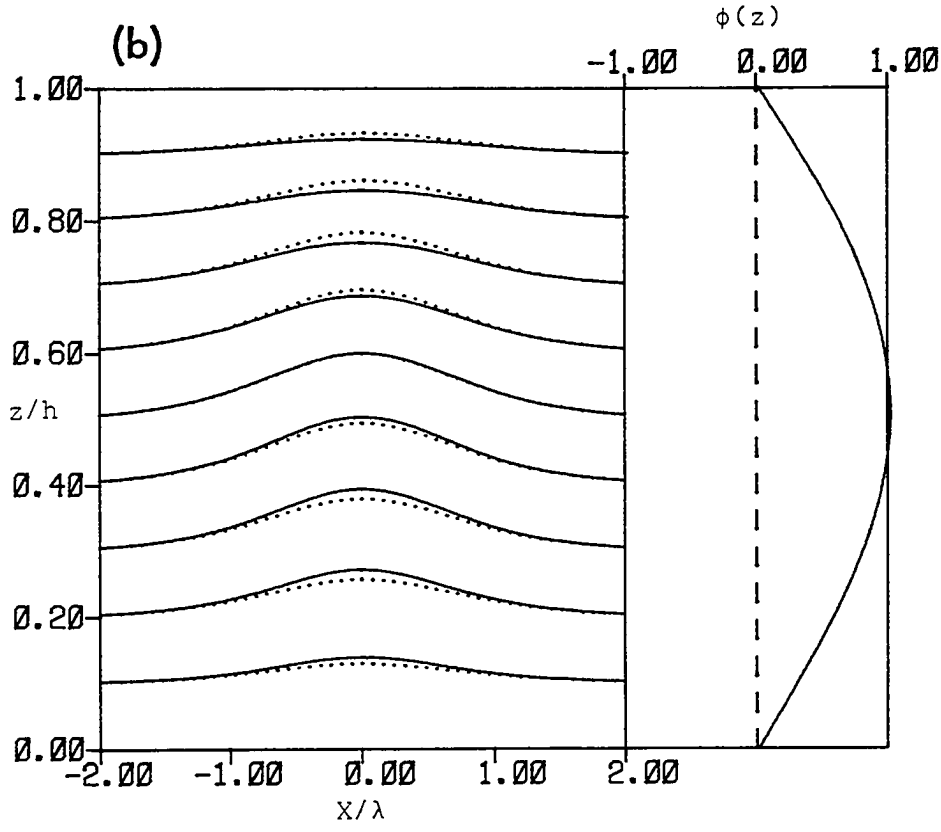


$$h\gamma = \frac{3}{8}s\pi + O(\sigma) \qquad \text{for } p = 0,\ s = 2,4,\ldots . \tag{2.3.16h}$$

For the free surface mode $s = 0$, as $\sigma \to 0$,

$$\frac{h^2\hat{c}_2}{a^2c_0} = -\frac{3}{20}\left\{1 + \frac{1219}{20160}(\sigma N_0{}^2h) + O(\sigma^2)\right\}, \tag{2.3.17a}$$

$$\frac{h\hat{\kappa}_1}{a} = -\frac{5}{8}\left\{1 - \frac{51}{5600}(\sigma N_0{}^2h) + O(\sigma^2)\right\}, \tag{2.3.17b}$$

$$h\gamma = -\frac{3}{4}\left\{1 + \frac{6233}{10080}(\sigma N_0{}^2h) + O(\sigma^2)\right\}. \tag{2.3.17c}$$

Finally, Figure 2.13 displays graphs of the streamlines for $s = 1$, $|a|\hat{\varepsilon}^2/h = 0.1$, $\sigma N_0{}^2h = 0.2$ and $p = 0,\ 1$. Note that when $p = 0$



Reproduced with permission of the copyright owner. Further reproduction prohibited without permission.

(rigid upper lid) the solitary wave is a wave of elevation, and when $p = 1$ (free upper surface) it is a wave of depression. In this latter case the amplitude at the free surface is always positive. Figure 2.13 also shows both first and second order theories. Also note that, for fixed $\sigma$ and amplitude the second order effect increases as the mode number increases.



Reproduced with permission of the copyright owner. Further reproduction prohibited without permission.

(III) Inversion layer: $u_0 \equiv 0$, $N^2 \equiv N_0^2 H(d - z)$.

Here H is the Heaviside function, so that N takes the constant value $N_0$ below the inversion level $z = d$ $(0 < d < h)$, and is zero above this level. For this case the Boussinesq approximation $\sigma \to 0$ is taken, so that $\rho_0$ in (2.1.1a) and similar subsequent equations is regarded as a constant. Then it follows from (2.1.1a,b and c) that

$$\phi(z) = \begin{cases} (-1)^{s-1} \sin \gamma_s z & \text{for } 0 \leq z \leq d , \\ (-1)^{s-1} \frac{(h - z)}{(h - d)} \sin \gamma_s d & \text{for } d \leq z \leq h . \end{cases} \qquad (2.3.18a)$$

where $$c_0 = \pm N_0 \gamma_s^{-1} , \qquad (2.3.18b)$$

and $$\tan \gamma_s d = -\gamma_s (h - d) , \qquad s = 1,2,3, \ldots . \qquad (2.3.18c)$$

For each mode number s there are two solutions for $c_0$ representing waves travelling to the right and left respectively. For mode number s, $(s - \frac{1}{2})\pi < \gamma_s d < s\pi$, and $\gamma_s d \to (s - \frac{1}{2})\pi$ as $s \to \infty$. As in the previous two cases choose $z_m$ so that $\phi(z_m) = 1$; here there is more than one choice for $z_m$, so the value closest to $z = d$ has been chosen. This ensures that $\phi(d)$ is positive.

Next, from (2.3.18a,b and c) $\mu$ and $\delta$ (2.1.4a and b) can be evaluated hence $c_1$ and $\lambda$ (2.1.3) can be found. It then follows that

$$\frac{hc_1}{ac_0} = \frac{2(-1)^{s-1} \gamma_s^2 (h - d)^2 \sin \gamma_s d}{3\left\{1 + \frac{\gamma_s^2 (h - d)^2 d}{h}\right\}} , \qquad (2.3.19a)$$



Reproduced with permission of the copyright owner. Further reproduction prohibited without permission.

| | s = 1 | | | s = 2 | | |
|---|---|---|---|---|---|---|
| d/h | $\gamma_s d$ | $\hat{c}_1 h/ac_0$ | $a\lambda^2/h^3$ | $\gamma_s d$ | $\hat{c}_1 h/ac_0$ | $a\lambda^2/h^3$ |
| 0.1 | 1.6385 | 6.3590 | 78.9157 | 4.7359 | 6.6284 | 9.3731 |
| 0.2 | 1.7155 | 2.9819 | 19.4330 | 4.7648 | 3.2836 | 2.4350 |
| 0.3 | 1.8040 | 1.8197 | 8.6649 | 4.8014 | 2.1562 | 1.1245 |
| 0.4 | 1.9071 | 1.2051 | 5.0364 | 4.8490 | 1.5766 | 0.6592 |
| 0.5 | 2.0288 | 0.8049 | 3.4985 | 4.9132 | 1.2066 | 0.4438 |
| 0.6 | 2.1746 | 0.5101 | 2.8738 | 5.0037 | 0.9257 | 0.3324 |
| 0.7 | 2.3522 | 0.2811 | 2.9367 | 5.1386 | 0.6699 | 0.2817 |
| 0.8 | 2.5704 | 0.1119 | 4.4029 | 5.3540 | 0.3932 | 0.3044 |
| 0.9 | 2.8363 | 0.0183 | 16.9035 | 5.7173 | 0.1058 | 0.7280 |

Table 2.1: $\gamma_s d$, $h\hat{c}_1/ac_0$ and $a\lambda^2/h^3$ as a function of d/h for the modes s = 1, 2 in case (III).

$$\frac{a\lambda^2}{h^3} = \frac{3 + \gamma_s{}^2(h - d)^2(2 + \frac{d}{h})}{(-1)^{s-1}\gamma_s{}^4 h^2(h - d)^2 \sin \gamma_s d} . \qquad (2.3.19b)$$

It is readily seen from these expressions that the amplitude a is positive for all modes. Thus these are waves of elevation; note, in particular that the inversion layer z = d is displaced upwards by the wave. Table 2.1 displays the values of $hc_1/ac_0$ and $a\lambda^2/h^3$ for some selected values of d/h for the first two modes. It is apparent that $c_1 \to 0$ and $\lambda \to \infty$ as $d \to h$; this agrees with the results of §2.3 (II) when $\sigma \to 0$.

Proceeding to the second order again following the procedure of §2.3 (I) and (II) the functions $\alpha_1$ and $\alpha_2$ (2.2.11b and c) can be evaluated, then the particular solutions $\beta_1$ and $\beta_2$ (2.2.12b and c) can be found, the coefficients $\sigma_1$, $\sigma_2$ and $\sigma_3$ are then evaluated and so find



Reproduced with permission of the copyright owner. Further reproduction prohibited without permission.

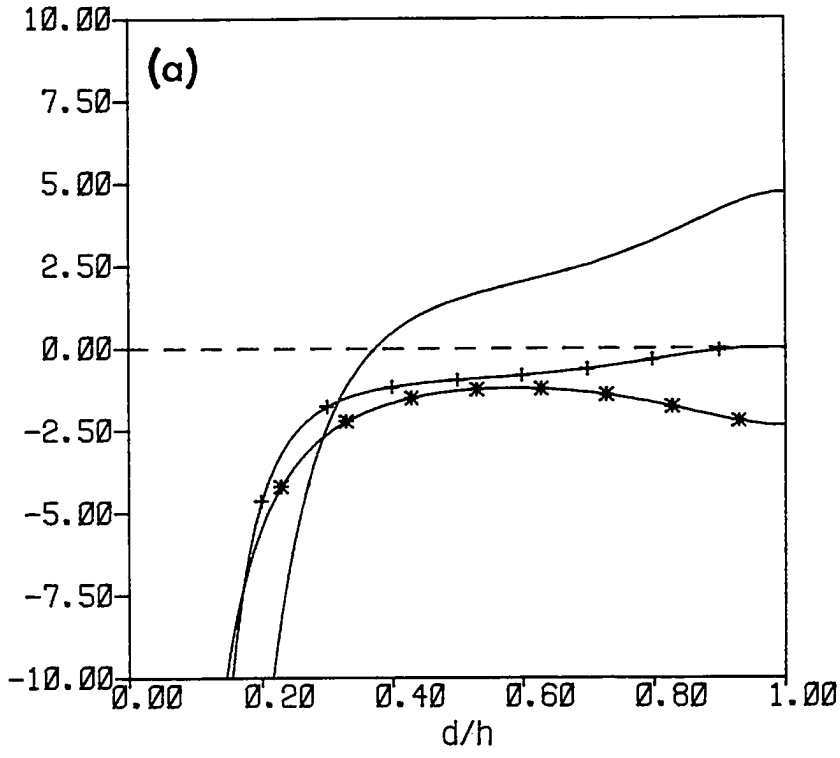


Figure 2.14: A plot of $\gamma h$ ——; $h^2\hat{c}_2/a^2c_0$ —+—+—; and $h\hat{\kappa}_1/a$ —*—; as a function of d/h for the modes (a) s = 1 and (b) s = 2, in case (III).

expressions for $\hat{c}_2$ (2.2.22b), $\hat{\kappa}_1$ (2.2.23b) and $\gamma$ (2.2.25b). Figure 2.14 displays graphs of $\hat{c}_2/c_0$, $\hat{\kappa}_1$ and $\gamma$ as functions of d/h. Note that $\hat{c}_2/c_0$ and $\hat{\kappa}_1$ are negative for all values of d/h. Thus all the second order solitary waves have smaller phase speeds and larger wavelengths than those predicted by the first order theory. For small values of d/h, the coefficient $\gamma$ is negative and the second order solitary waves are narrower at $z = z_m$ than those predicted by first order theory. When d/h is close to one, $\gamma$ is positive and the second order solitary waves are now wider.



Reproduced with permission of the copyright owner. Further reproduction prohibited without permission.

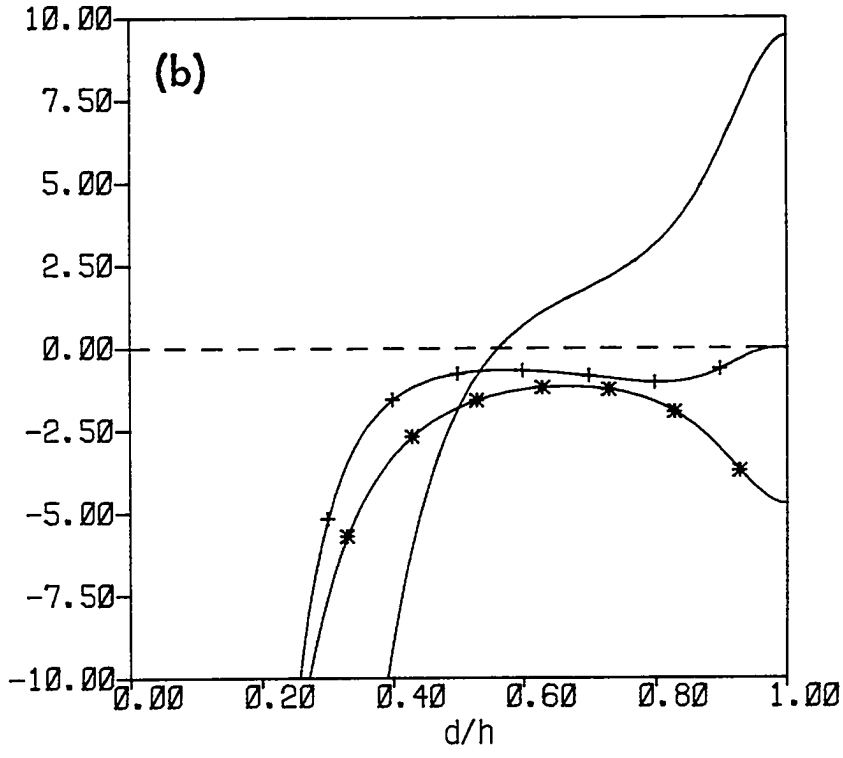




Reproduced with permission of the copyright owner. Further reproduction prohibited without permission.

(IV) Two-layer fluid: $u_0 = 0$, $\rho_0 = \rho_1 H(z - d) + \rho_2 H(d - z)$.

Here H is the Heaviside function, so that the equilibrium position of the interface is $z = d$ $(0 < d < h)$, and the upper (lower) fluid has density $\rho_1$ $(\rho_2)$. The Boussinesq parameter $\sigma$ is here defined to be $2(\rho_2 - \rho_1)/(\rho_2 + \rho_1)$. The Brunt-Väisälä frequency has a delta-function singularity at $z = d$, and is zero elsewhere. Hence, from (2.1.1a,b and c) the modal function is

$$\phi(z) = M \begin{cases} z/d , & 0 \leq z \leq d , \\ 1 - (z - d)(h - d - p\sigma c_0^{\,2})^{-1}, & d \leq z \leq h , \end{cases} \tag{2.3.20a}$$

and $$pc_0^{\,4}\sigma(1 + \tfrac{1}{2}\sigma) - c_0^{\,2}\{h(1 + \tfrac{1}{2}\sigma) + \sigma d(p - 1)\} + d(h - d) = 0. \tag{2.3.20b}$$

Here recall that $p = 0$, or 1, according as the upper boundary is rigid, or free. In the latter case there are two solutions for $c_0^{\,2}$ corresponding to an interfacial mode and free surface mode respectively, with a right and left propagating wave in each case. As $\sigma \to 0$,

$$c_0^{\,2} = \frac{d(h - d)}{h}\left[1 - \sigma\left\{\frac{1}{2} - \frac{d}{h} + p\,\frac{d^2}{h^2}\right\} + O(\sigma^2)\right]$$

for the interfacial mode, (2.3.21a)

or $$c_0^{\,2} = \frac{h}{\sigma}\left[1 - \sigma\,\frac{d(h - d)}{h^2} + O(\sigma^2)\right]$$

for the free surface mode. (2.3.21b)



Reproduced with permission of the copyright owner. Further reproduction prohibited without permission.

Note that for both modes the effect of increasing the Boussinesq parameter $\sigma$ is to decrease the phase speed. For a rigid upper boundary condition, $M = 1$ as the maximum value of $\phi(z)$ is attained at $z = d$. For a free upper boundary condition again choose $M = 1$ for the interfacial mode; for the free surface mode, choose $M = (d - h + \sigma c_0^2)/\sigma c_0^2$ so that $\phi(h) = 1$.

Next, from (2.3.20a,b) $\mu$ and $\delta$ (2.1.4a and b) can be evaluated, and hence $c_1$ and $\lambda$ (2.1.3) can be found. Then

$$\frac{hc_1}{ac_0} = \frac{Mh}{2d} \frac{1}{(h - d - p\sigma c_0^2)} \left\{ \frac{\rho_2(h - d - p\sigma c_0^2)^3 - \rho_1 d^2(h - d)}{\rho_2(h - d - p\sigma c_0^2)^2 - \rho_1 d(h - d)} \right\} , \qquad (2.3.22a)$$

$$\frac{a\lambda^2}{h^3} = \frac{4d^2(h-d-p\sigma c_0^2)}{3Mh^3} \left\{ \frac{\rho_2 d(h-d-p\sigma c_0^2)^2 + \rho_1[(p\sigma c_0^2)^3 + (h-d-p\sigma c_0^2)^3]}{\rho_2(h - d - p\sigma c_0^2)^3 - \rho_1 d^2(h - d)} \right\} . \qquad (2.3.22b)$$

When $p = 0$, these results agree with those obtained by Long (1956). The amplitude $a$ is positive for the surface mode which is thus a wave of elevation. For the interfacial mode $a$ is positive (negative) according as

$$\rho_2(h - d - p\sigma c_0^2)^3 \gtrless \rho_1 d^2(h - d) , \qquad (2.3.23)$$

or

$$h \gtrless 2d\{1 - \tfrac{1}{8}\sigma(2 - 3p) + O(\sigma^2)\} ,$$

and thus the interfacial mode is a wave of elevation (depression) at the interface. As $\sigma \to 0$, for the interfacial mode

$$\frac{hc_1}{ac_0} = \frac{h}{2d(h - d)} \{h - 2d + \sigma d\left(1 - \frac{d}{h} + p\frac{d^2}{h^2} - 2p\frac{d}{h}\right) + O(\sigma^2)\} , \qquad (2.3.24a)$$



Reproduced with permission of the copyright owner. Further reproduction prohibited without permission.

$$\frac{a\lambda^2}{h^3} = \frac{4d^2(h-d)^2}{3h^3}\left\{h - 2d + \sigma\left[h + (p-3)d + \frac{3d^2}{h}(1-p) - p\,\frac{d^3}{h^2}\right] + O(\sigma^2)\right\}^{-1} . \qquad (2.3.24b)$$

These expressions show that $hc_1/ac_0 \to 0$ and $a\lambda^2/h^3 \to \infty$ when equality is attained in (2.2.23); this is because the coefficient $\mu$ (2.1.4a) is zero in this limit, the consequences of this are explored further in §2.4. For the free surface mode

$$\frac{hc_1}{ac_0} = \frac{1}{2}\{1 + O(\sigma^2)\} , \qquad (2.3.25a)$$

$$\frac{a\lambda^2}{h^3} = \frac{4}{3}\left\{1 - \frac{\sigma d(h-d)(2h-d)(h+d)}{h^4} + O(\sigma^2)\right\} . \qquad (2.3.25b)$$

Proceeding to the second order again following a similar procedure to the previous three subsections eventually expressions for $\hat{c}_2$, $\hat{\kappa}_1$ and $\gamma$ are obtained. Figures 2.15, 2.16 and 2.17 respectively, display graphs of these quantities as functions of d/h for $\sigma = 0,\ 0.1,\ 0.5$. Note that for all values of d/h, $\hat{c}_2/c_0$ and $\hat{\kappa}_1$ are negative. Thus all the second order solitary waves have smaller phase speeds and larger wavelengths than those predicted by the first order theory. The coefficient $\gamma a$ is positive for $\frac{1}{4} < \frac{d}{h} < \frac{3}{4}$ in the limit $\sigma \to 0$, and so the interfacial waves are broader at the crest than the first order theory would predict; for $\frac{d}{h} < \frac{1}{4}$ or $\frac{d}{h} > \frac{3}{4}$ in the limit $\sigma \to 0$, $\gamma a$ is negative and the waves are now narrower at the crest. Note that $\hat{\kappa}_1 \to -\infty$ and $\gamma a \to \infty$ when equality is attained in (2.3.23) (i.e. the coefficient $\mu$ is zero). Also $\hat{c}_2/c_0$, $\hat{\kappa}_1$ and $a\gamma \to -\infty$ as $d \to 0$ or $d \to h$. In both of these limits the assumption that the amplitude of the solitary wave is small compared to the depth of fluid layer fails. A



Reproduced with permission of the copyright owner. Further reproduction prohibited without permission.

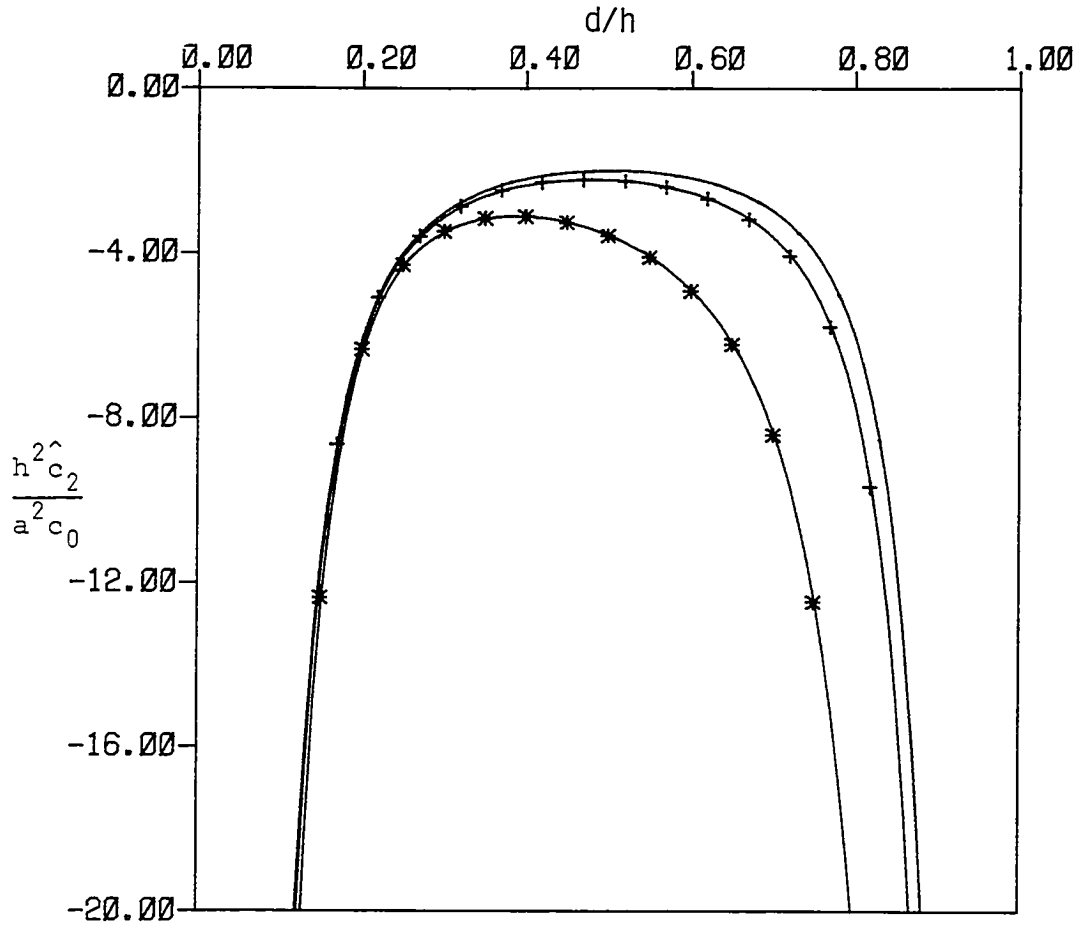


Figure 2.15: A plot of $h^2\hat{c}_2/a^2c_0$ as a function of d/h for the internal mode when $\sigma$ = 0 ———; 0.1 —+—+—; and 0.5 —*—; in case (IV).

different scaling is required and the outcome would be the second order theory for solitary waves in deep fluids (see Grimshaw (1981a)).

Finally, the theory shall be compared the experimental results of Koop and Butler (1982) and Segur and Hammack (1982), who both investigated internal solitary waves in a two-layer fluid and compared their results with existing solitary wave theories; that is, the shallow water theory which leads to a Kortweg-de Vries equation at first order, or the infinite depth theory which leads to the Benjamin-Ono equation



Reproduced with permission of the copyright owner. Further reproduction prohibited without permission.

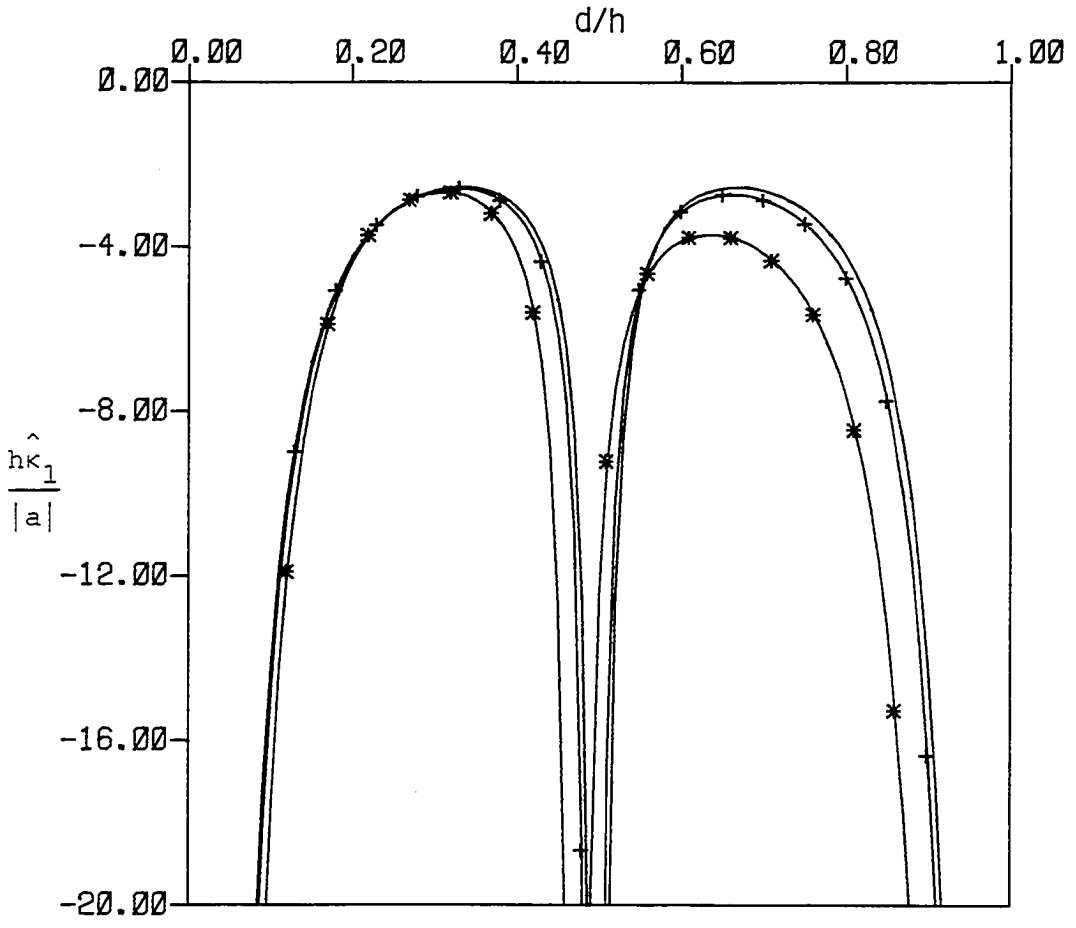


Figure 2.16: A plot of $h\hat{\kappa}_1/|a|$ as a function of d/h for the internal mode when $\sigma$ = 0 ——; 0.1 —+—+—; and 0.5 —*—; in case (IV).

(Benjamin (1967), Davis and Acrivos (1967) and Ono (1975)) or the finite depth theory which is intermediate between these two (Kubota, Ko and Dobbs (1978)). In the experiments of Koop and Butler (1982) $\sigma$ = 0.45 and d/h = 0.1645; they plotted the wave profile $\eta(x, d)/a\hat{\varepsilon}^2$ for seven wave realizations in the amplitude range $0.006 < |a|\hat{\varepsilon}^2/h < 0.11$ against $x/\lambda_{1/2}$ where $\lambda_{1/2}$ is a measure of wavelength, defined so that at $x = \lambda_{1/2}$ the wave is exactly one-half of its maximum amplitude. Note that this introduces the artificial constraint of requiring the theory and experiment to agree



Reproduced with permission of the copyright owner. Further reproduction prohibited without permission.

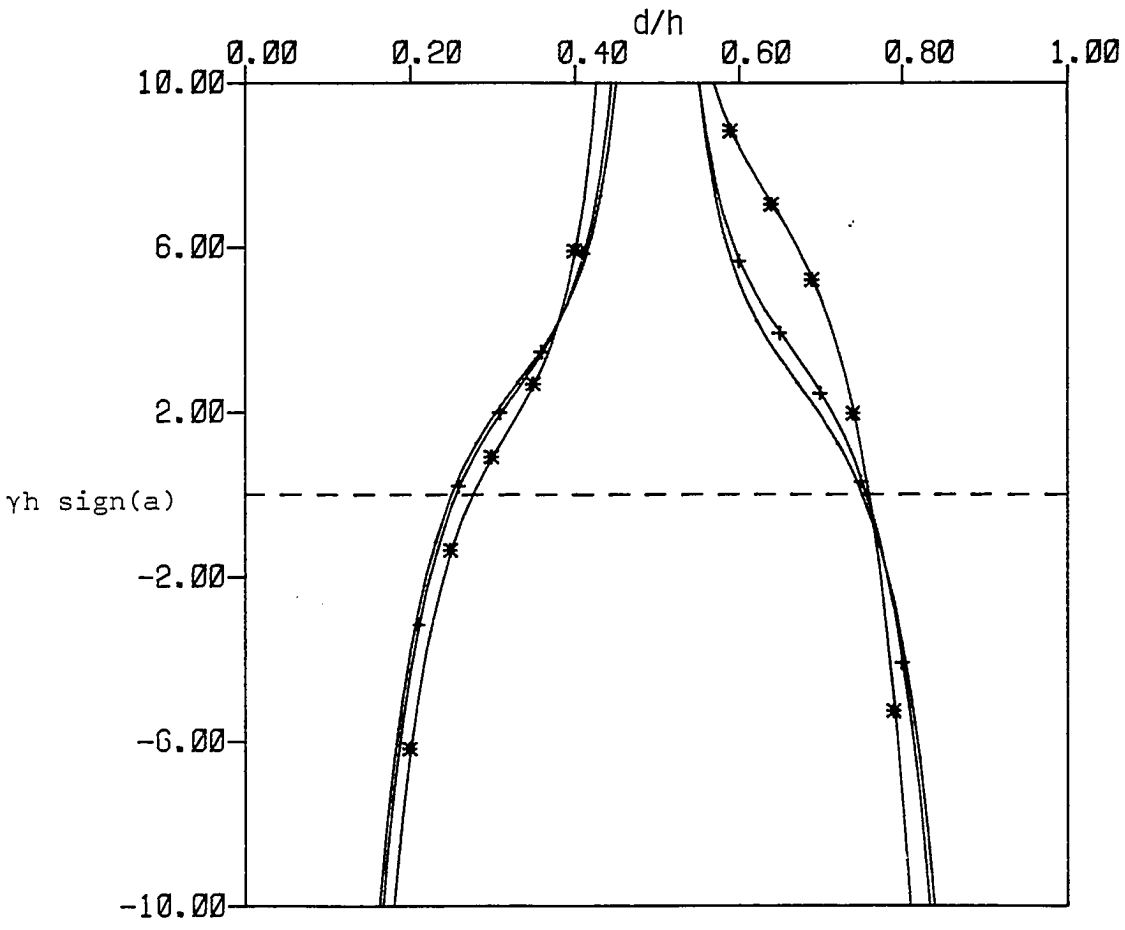


Figure 2.17: A plot of γh sign(a) as a function of d/h for the internal mode when σ = 0 ———; 0.1 —+—+—; and 0.5 —*—; in case (IV).

at both x = 0 and x = $\lambda_{1/2}$. In the experiments of Segur and Hammack (1982) σ = 0.05 and d/h = 0.1; they plotted the wave profile $\eta(x, d)/a\hat{\varepsilon}^2$ for five wave realizations in the amplitude range $0.01 < |a|\hat{\varepsilon}^2/h < 0.02$ against X/λ where λ is the theoretically determined wavelength given by the first order theory (i.e. 2.3.22b). In both cases it was found there was good agreement between the measured wave profiles and the first order shallow water theory (that is, the equations (2.1.2) and (2.1.3)). If the second order theory developed here is compared with the experimentally measured wave profiles



Reproduced with permission of the copyright owner. Further reproduction prohibited without permission.

it is found that there is good agreement when the amplitude is sufficiently small in comparison to the depth of the interface (typically $|a|\hat{\varepsilon}^2/h$ should be less than 0.06 for the experiments of Koop and Butler (1982), or 0.013 for the experiments of Segur and Hammack (1982)). However, in the range where there is agreement the difference between the first and second order theory is less that the experimental scatter. When the amplitude is increased to the point where a distinction can be made between the first and second order theories, it is found that the second order theory predicts a wave profile somewhat below that observed. Remarkably the experimental results continue to show some agreement with first order theory. Note that a similar phenomenon occurs with free surface solitary waves (see Miles (1980)), where it is known that continuation of the expansion to third order gives a wave profile close to the first order "$\text{sech}^2$"-profile (Fenton (1972)). This may be the explanation of the discrepancy here, although also note that the experimental values of d/h are rather small if shallow water theory is to be used.

As another test of the shallow water theory Koop and Butler (1982) compared the theoretically predicted amplitude-wavelength relationship with their experimental results. Using an integrated measure of wavelength $\lambda_I$ (proportional to $\int_0^h \eta(x, d)\, dx$) they found no agreement with the infinite depth theory, finite depth theory, or first order shallow water theory. However, they also calculated the amplitude-wavelength relationship for the second order shallow water theory (their theoretical results agree completely with this theory) and found excellent agreement with their experimental results.



Reproduced with permission of the copyright owner. Further reproduction prohibited without permission.

## §2.4 Regularization when $\mu \to 0$.

In §2.3 it was shown that under special circumstances the nonlinear coefficient $\mu$ (2.1.4a) may vanish. For instance in §2.3 (I) $\mu \to 0$ as $r \to \infty$, the asymptotic behaviour being $r^{-1}$ for the odd modes and $r^{-2}$ for the even modes, where r (2.3.1c) is an inverse measure of the shear. Similarly in §2.3 (II) $\mu \to 0$ as $\sigma \to 0$, where $\sigma$ is the Boussinesq parameter; the asymptotic behaviour is $\sigma$ for the odd modes and $\sigma^2$ for the even modes when the rigid upper boundary condition pertains; for a free upper boundary condition $\mu \propto \sigma$ as $\sigma \to 0$ for all modes. Again in §2.3 (III) $\mu \to 0$ when d (the inversion level ) $\to$ h; the asymptotic behaviour is $\mu \propto (h - d)^3$. All these cases correspond to the well known fact that $\mu$ vanishes for uniform stratification in the absence of a basic shear flow and in the Boussinesq approximation. In §2.3 (IV) $\mu \to 0$ when equality is attained in (2.3.23); the asymptotic behaviour is $\mu \propto (h - 2d)$, where d is the depth of the interface (in the Boussinesq approximation).

For the two-layer fluid Long (1956) and Kakutani and Yamasaki (1978) have shown that when $\mu \to 0$ cubic and quadratic nonlinearity are of comparable significance; Miles (1979) has argued similarly whenever $\mu$ is small. In this section the limit $\mu \to 0$ shall be considered by modifying the asymptotic expansion of §2.2. In view of the special cases of §2.3 it shall be supposed that there is a parameter $\nu$ such that

$$\mu = \nu\mu' . \qquad (2.4.1)$$

Thus the limit $\mu \to 0$ is achieved by letting $\nu \to 0$ and in this limit $\mu'$ remains finite. From the discussion above the parameter $\nu$ is readily identified; thus in §2.3 (I) $\nu$ is $r^{-1}$ for the odd modes and $r^{-2}$ for the even modes, etc.. Assuming that $\delta$ remains finite as $\nu \to 0$ it follows from



Reproduced with permission of the copyright owner. Further reproduction prohibited without permission.

(2.1.3) that

$$c_1 = \nu c_1' , \qquad \lambda = \lambda' \nu^{-1/2} . \tag{2.4.2}$$

Here and subsequently all primed quantities remain finite as $\nu \to 0$. It now follows from (2.2.14a,b and c) that

$$\sigma_1 = \nu^2 \sigma_1' , \quad \sigma_2 = \nu \sigma_2' , \quad \sigma_3 = \sigma_3' , \tag{2.4.3}$$

and then from (2.2.17a,b) it follows that

$$c_2 = c_2' , \qquad \kappa_1 = \kappa_1' \nu^{-1} . \tag{2.4.4}$$

Note here that $\sigma_3'$ may be $0(\nu)$, with the consequence that $c_2'$ and $\kappa_1'$ are also $0(\nu)$; indeed this is the case for the special cases of §2.3 (I), (II) and (III) for all of which the limit $\nu \to 0$ is the case of a uniform stratification in the absence of a basic shear flow and in the Boussinesq approximation.

The expressions (2.4.2), (2.4.3) and (2.4.4) imply that a rescaling is necessary as $\nu \to 0$. Thus in equation (2.2.10) for the first order solitary wave put

$$X' = \nu^{1/2} X \tag{2.4.5}$$

and then (2.2.10) becomes

$$-c_1' A + \frac{1}{2}\mu' A^2 + \delta A_{X'X'} = 0 . \tag{2.4.6}$$

Similarly, equation (2.2.16a) for the second order term becomes



Reproduced with permission of the copyright owner. Further reproduction prohibited without permission.

$$-c_1'A_2' + \mu'AA_2' + \delta A_{2X'X'}' - \nu^2\sigma_1'A - \nu\sigma_2'A^2 - \sigma_3'A^3 - c_2'A + 2\kappa_1'\delta A_{X'X'} = 0 , \tag{2.4.7a}$$

where
$$A_2' = \nu A_2 . \tag{2.4.7b}$$

It can now be observed that if

$$A' = A + \varepsilon^2\nu^{-1}A_2' , \tag{2.4.8a}$$

then equations (2.4.6) and (2.4.7) may be combined to give

$$-c'A' + \frac{1}{2}\mu'A'^2 - \gamma A'^3 + \delta' A'_{X'X'} = 0 , \tag{2.4.8b}$$

where
$$c' = c_1' + \varepsilon^2\nu^{-1}c_2' , \tag{2.4.8c}$$

$$\delta' = \delta\{1 + \varepsilon^2\nu^{-1}\kappa_1'\}^2 , \tag{2.4.8d}$$

and
$$\gamma = \sigma_3'\varepsilon^2\nu^{-1} . \tag{2.4.8e}$$

Here the terms of relative order $\nu$ have been neglected, so that $\mu'$, $\delta$ and $\sigma_3'$ are evaluated as $\nu \to 0$; also terms of $O(\varepsilon^4\nu^{-2})$ have been neglected. Equation (2.4.8b) has the solitary wave solution (see Kakutani and Yamasaki (1978), or Miles (1979))

$$A' = \frac{a\ \mathrm{sech}^2(X'/\lambda')}{1 - b\ \tanh^2(X'/\lambda')} , \tag{2.4.9a}$$

where
$$c' = \frac{\mu'a}{3} - \frac{\gamma a^2}{2} = \frac{4\delta'}{(\lambda')^2} , \tag{2.4.9b}$$



Reproduced with permission of the copyright owner. Further reproduction prohibited without permission.

and $$b = \frac{3\gamma a}{2\mu' - 3\gamma a} . \qquad (2.4.9c)$$

Note that $|3\gamma a/\mu'|$ is a measure of the importance of cubic nonlinearity relative to quadratic nonlinearity, and for bounded solutions it is required that $b < 1$ whence

$$\frac{3\gamma a}{\mu'} < 1 , \quad \text{or} \quad \frac{3\gamma a}{\mu'} > 2 . \qquad (2.4.10)$$

Also for waves travelling to the right ($c_0 > \max u_0$), $\delta$ is positive, $c'$ is positive and $2\mu' a > 3\gamma a^2$; for waves travelling to the left ($c_0 < \min u_0$), $\delta$ is negative, $c'$ is negative and $2\mu' a < 3\gamma a^2$. When $\varepsilon^2 \ll \nu$, $|b| \ll 1$ and it is readily shown that (2.4.9a) agrees with the expressions (2.1.2) and (2.2.18) for A and $A_2$ respectively. Figure 2.18 shows graphs of A' for various values of b.

If $\sigma_3'$ is $O(\nu)$, then put

$$\sigma_3 = \nu\sigma_3'' , \quad c_2 = \nu c_2'' , \quad \kappa_1 = \kappa_1'' , \qquad (2.4.11a)$$

and $$A'' = A + \varepsilon^2 A_2 . \qquad (2.4.11b)$$

Then proceeding in a similar way to the case described above it is found that

$$-c''A'' + \tfrac{1}{2}\mu''A''^2 - \gamma A''^3 + \delta'' A''_{X'X'} = 0 , \qquad (2.4.12a)$$

where $$c'' = c_1' + \varepsilon^2 c_2'' , \qquad (2.4.12b)$$

$$\mu'' = \mu' - \varepsilon^2 \sigma_2' , \qquad (2.4.12c)$$



Reproduced with permission of the copyright owner. Further reproduction prohibited without permission.

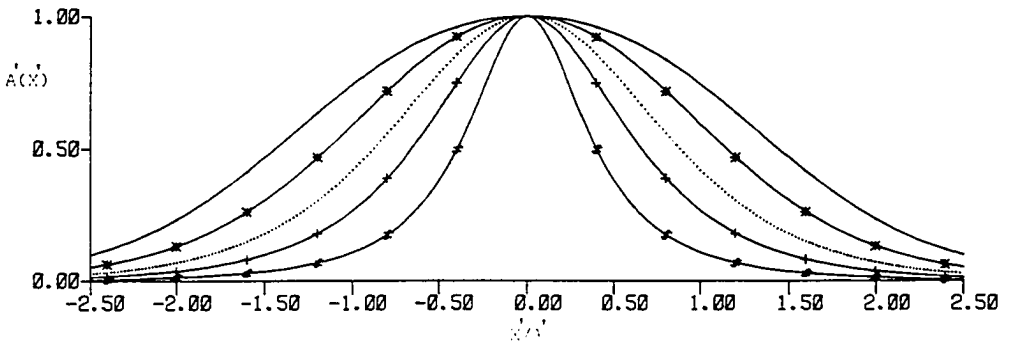


Figure 2.18: A plot of A'(X') as a function of X'/λ' for b = 0 ···; 0.75 ——; 0.50 —*—; -1.0 —+—+—; -5.0 —#—.

$$\delta'' = \delta\{1 + \varepsilon^2\kappa_1''\}^2 , \qquad (2.4.12d)$$

$$\gamma = \varepsilon^2\sigma_3'' . \qquad (2.4.12e)$$

Here the terms of relative order $\varepsilon^2$ and $\nu$ have been neglected. The solutions of (2.4.12a) are identical to those of (2.4.9a) when c" is substituted for c', etc..

The analysis that led to equation (2.4.8b) requires $\varepsilon^2 << \nu << 1$. However, the procedure suggests that equation (2.4.8b) has a more general validity based on the equality of the small parameters $\varepsilon^2$ and $\nu$. Hence it is appropriate to replace (2.2.1a) with the asymptotic expansion

$$\eta = \nu\eta_1(X', z) + \nu^2\eta_2(X', z) + \nu^3\eta_3(X', z) + \ldots , \qquad (2.4.13a)$$

where $$\eta_1 = A(X')\phi(z) \qquad (2.4.13b)$$

and $$X' = \nu\kappa x . \qquad (2.4.13c)$$



Reproduced with permission of the copyright owner. Further reproduction prohibited without permission.

Simultaneously the phase speed c and $\kappa$ are expanded in the form

$$c = c_0 + \nu^2 c_2 + \nu^3 c_3 + \dots , \tag{2.4.14a}$$

$$\kappa = 1 + \nu\kappa_1 + \dots . \tag{2.4.14b}$$

Note here that in (2.4.14a) the absence of the term $\nu c_1$ has been anticipated; this is to ensure that c differs from $c_0$ by a term proportional to the dispersion parameter (here $\nu^2$). This will be confirmed a posteriori.

Upon substitution of (2.4.13a,b,c) and (2.4.14a,b) into (2.1.8a), (2.1.9) and (2.1.10) it is found that at the lowest order in $\nu$, equations (2.1.1a,b,c) are satisfied. Next it is assumed that the basic density $\rho_0(z)$ and the basic shear flow $u_0(z)$ are functions of $\nu$, and can be expanded in $\nu$. Consequently, $\phi(z)$ and $c_0$ also have expansions in $\nu$. Thus write

$$\phi(z) = \phi_0(z) + \nu\phi_1(z) + \dots , \tag{2.4.15a}$$

$$c_0 = c_{00} + \nu c_{01} + \dots , \tag{2.4.15b}$$

$$u_0(z) = u_{00}(z) + \nu u_{01}(z) + \dots , \tag{2.4.15c}$$

$$Q_0(z) \equiv \rho_0(c_0 - u_0)^2 = Q_{00}(z) + \nu Q_{01}(z) + \dots , \tag{2.4.15d}$$

$$R_0(z) \equiv \rho_0 N^2 = R_{00}(z) + \nu R_{01}(z) + \dots . \tag{2.4.15e}$$

The terms $\phi_1(z)$ etc. can in principle be expressed in terms of $\phi_0(z)$ etc. by substitution into (2.1.1a,b,c) but it shall not be necessary to display the results of this calculation. Recalling (2.1.4a), the definition (2.4.1) of $\nu$ then implies that



Reproduced with permission of the copyright owner. Further reproduction prohibited without permission.

$$\int_0^h Q_{00}\phi_{0z}^3\,dz = 0 . \qquad (2.4.16)$$

At the next two orders in $\nu$, for $i = 2, 3$ it is found that

$$(Q_{00}\eta_{iz})_z + R_0\eta_i + f_i = 0 , \qquad (2.4.17a)$$

$$\eta_i = 0 \quad \text{on} \quad z = 0 , \qquad (2.4.17b)$$

$$\eta_i - p\sigma(c_{00} - u_{00})^2\eta_{iz} + p\sigma g_i = 0 \quad \text{on} \quad z = h . \qquad (2.4.17c)$$

Here the inhomogeneous terms are given by

$$f_2 = -A^2\{\tfrac{3}{2}Q_{00}\phi_{0z}^2\}_z , \qquad (2.4.18a)$$

$$f_3 = Q_{00}\phi_0 A_{X'X'} + A\{2c_2\rho_{00}(c_{00} - u_{00})\phi_{0z}\}_z + \{Q_{00}(2A^3\phi_{0z}^3 - 3A\phi_{0z}\eta_{2z} - 3A^2\phi_{0z}\phi_{1z})\}_z + \{Q_{01}(\eta_{2z} - \tfrac{3}{2}A^2\phi_{0z}^2)\}_z + R_{01}\eta_2 , \qquad (2.4.18b)$$

$$g_2 = A^2\,\tfrac{3}{2}(c_{00} - u_{00})^2\phi_{0z}^2 , \qquad (2.4.18c)$$

$$g_3 = -2c_2(c_{00} - u_{00})A\phi_{0z} - (c_{00} - u_{00})^2(2A^3\phi_{0z}^3 - 3A\phi_{0z}\eta_{2z} - 3A^2\phi_{0z}\phi_{1z}) - 2(c_{00} - u_{00})(c_{01} - u_{01})(\eta_{2z} - \tfrac{3}{2}A^2\phi_{0z}^2) . \qquad (2.4.18d)$$

The compatibility condition for equations (2.4.17a,b,c) is derived in a manner identical to that described in §2.2 which led to (2.2.9). Hence

$$\int_0^h \phi_0 f_i\,dz + \{p\sigma Q_{00}\phi_{0z}g_i\}_{z=h} = 0 . \qquad (2.4.19)$$



Reproduced with permission of the copyright owner. Further reproduction prohibited without permission.

Putting i = 2 in (2.4.19) it is readily shown from (2.4.18a and c) that the compatibility condition is satisfied identically in A. Also, using the results of §2.2 (see (2.2.7a) and (2.2.12a) in particular) in the limit $\nu \to 0$, it follows that

$$\eta_2 = A_2(X')\phi_0(z) + A^2\beta_{20}(z) , \tag{2.4.20}$$

where $\beta_{20}(z)$ is the limit of $\beta_2(z)$ as $\nu \to 0$.

Next, applying the compatibility condition (2.4.19) with i = 3, using (2.4.18b and d). The result is

$$-c_2 A + \tfrac{1}{2}\mu_0' A^2 - \sigma_{30}' A^3 + \delta_0 A_{X'X'} = 0 . \tag{2.4.21}$$

Here $\delta_0$ is the value of $\delta$ (2.1.4b) use $\nu \to 0$, $\mu_0'$ is the value of $\mu'$ (2.4.1) as $\nu \to 0$, and $\sigma_{30}'$ is the value of $\sigma_3$ (2.2.14c) as $\nu \to 0$. Equation (2.4.21) agrees completely with (2.4.8b) which was obtained on the more restrictive hypothesis that $\varepsilon^2 \ll \nu$. Allowing for the change of notation (c' replaced by $c_2$, etc.) it has the solitary wave solution (2.4.9a). Note, in particular, that

$$\sigma_{30}' = \frac{\int_0^h Q_{00}\left(2\phi_{0z}^4 - 3\beta_{20z}\phi_{0z}^2\right) dz}{2\int_0^h \rho_{00}(c_{00} - u_{00})\phi_{0z}^2 \, dz} . \tag{2.4.22}$$

This differs from the expression obtained by Miles (1979) by the inclusion of the term involving the particular solution $\beta_{20}$; Miles used a variational argument which assumed that $\eta$ was proportional to $\phi_0(z)$ to $O(\nu^2)$.



Reproduced with permission of the copyright owner. Further reproduction prohibited without permission.

This asymptotic expansion shows that this is not correct, and the particular solution $\beta_{20}$ enters at $O(\nu^2)$. Note that $A_2(X')$ is not determined at this stage and can be found by considering the compatibility condition for $i = 4, 5$.

For the special case of the two-layer fluid considered in §2.3 (IV) the coefficients $\mu_0'$, $\sigma_{30}'$ and $\delta_0$ can be found from the work of Long (1956) and Kakutani and Yamasaki (1978). The parameter $\nu$ is defined so that $\nu \to 0$ gives equality in (2.3.23). Thus put

$$\nu = \left| \frac{\rho_2 (h - d - p\sigma c_0^2)^3}{\rho_1 d^2 (h - d)} - 1 \right| , \tag{2.4.23}$$

and let $d_0$ be the value of d for which $\nu$ is zero. Then

$$\mu_0' = - \frac{3 \ \mathrm{sign}(d - do) c_{00}}{2(h - p\sigma c_{00}^2)} , \tag{2.4.24a}$$

$$\sigma_{30}' = \frac{c_{00}}{d_0 (h - d_0 - p\sigma c_{00}^2)} , \tag{2.4.24b}$$

$$\delta_0 = \frac{c_{00} d_0}{6} \frac{\{d_0^3 + (h - d_0 - p\sigma c_{00}^2)[(h - d_0)^2 - 3p\sigma c_{00}^2 (h - d_0 - p\sigma c_{00}^2)]\}}{(h - d_0)(h - p\sigma c_{00}^2)} . \tag{2.4.24c}$$

When the Boussinesq parameter $\sigma \to 0$, it is seen that $d_0 \simeq \frac{1}{2}h$, and $\nu \simeq h \, |h - 2d| \, d^{-2}$, and there are corresponding simplifications in these expressions. It may be shown from (2.4.24b) that $\sigma_{30}'$ has the same sign as $c_{00}$, and that $\mu_0'$ has the same (opposite) sigh as $c_{00}$ according as $d < d_0$ ($d > d_0$). It follows from the expresssions (2.4.9a,b,c) and (2.4.10) that

$$0 < b < 1, \tag{2.4.25a}$$



Reproduced with permission of the copyright owner. Further reproduction prohibited without permission.

$$0 < |a| < \left|\frac{\mu_0'}{3\sigma_{30}'}\right| , \tag{2.4.25b}$$

and
$$\text{sign } a = -\text{sign}(d - d_0) . \tag{2.4.25c}$$

Thus the solitary wave (2.4.9a) is a wave of elevation (depression) when $d < d_0$ ($d > d_0$).

For the special cases of §2.3 (I), (II) and (III), $\sigma_{30}'$ is zero, and the remaining coefficients can be readily obtained from the results of §2.3. For instance, in §2.3 (I) identify $\nu$ with $r^{-1}$ for the odd modes, and $r^{-2}$ for the even modes, where r is an inverse measure of the shear. It is readily shown that for $s = \pm 1, \pm 2, \ldots,$

$$c_{00} = \frac{N_0 h}{s\pi} \text{ sign } a , \tag{2.4.26a}$$

$$\phi_0(z) = (-1)^{\frac{s-|s|}{2}} \sin\left(\frac{s\pi z}{h}\right) , \tag{2.4.26b}$$

$$\delta_0 = \frac{h^2 c_0}{2(s\pi)^2} , \tag{2.4.26c}$$

and
$$\mu_0' = \begin{cases} \dfrac{4N_0 \text{ sign } a}{|s\pi|} & \text{for } s = \pm 1, \pm 3, \ldots , \\ \dfrac{1}{3}N_0 \text{ sign } a & \text{for } s = \pm 2, \pm 4, \ldots . \end{cases} \tag{2.4.26d}$$

Note that for the even modes, $\nu$ is $r^{-2}$ but $\phi(z)$, $c_0$ etc. have expansions in



Reproduced with permission of the copyright owner. Further reproduction prohibited without permission.

powers of $r^{-1}$; this requires modification of the expansion procedure described above. Details shall not be given as the end result is again (2.4.21). These results show that in the presence of a weak shear flow there are solitary waves of the classical form (2.1.2) (or (2.4.9a) with $b = 0$) whose amplitudes scale with $r^{-1}$ for the odd modes, and $r^{-2}$ for the even modes.

For the special case of §2.3 (II), identify $\nu$ with $\sigma$ (the Boussinesq parameter) for the odd modes and $\sigma^2$ for the even modes when the rigid upper boundary condition pertains; for a free upper boundary condition identify $\nu$ with $\sigma$ for all modes. This case has been considered by Long (1965) (see also Weidman (1978)) when $\varepsilon^2 \ll \nu$, the results presented here agree completely with his. For the benefit of the reader the relevant formulas shall be quoted for $s = 1, 2, \ldots$ . For a rigid upper boundary condition it is found that

$$c_{00}^2 = \frac{N_0^2 h^2}{(s\pi)^2} , \tag{2.4.27a}$$

$$\phi_0(z) = (-1)^{s+1} \sin\left(\frac{s\pi z}{h}\right) , \tag{2.4.27b}$$

and

$$\mu_0' = \begin{cases} \frac{2}{3} \frac{N_0^2 c_0}{s\pi} & \text{for } s = 1, 3, \ldots , \quad (2.4.27c) \\ \\ \frac{1}{6} \frac{N_0^4 h c_0}{s\pi} & \text{for } s = 2, 4, \ldots , \quad (2.4.27d) \end{cases}$$

and $\delta_0$ is again given by (2.4.26c). For a free upper boundary condition $c_{00}$ and $\phi_0(z)$ are again given by (2.4.27a) and (2.4.27b) respectively, while

$$\mu_0' = -\frac{(8 + (-1)^s)}{3s\pi} N_0^2 c_0 . \tag{2.4.28}$$



Reproduced with permission of the copyright owner. Further reproduction prohibited without permission.

It should be noted, however, that the above discussion is based on the expansion (2.4.13a) and equation (2.4.21) with $\sigma_3'$ equal to zero. Thus the solitary wave solution is just the classical solitary wave solution (2.1.2) or (2.4.9a) (with b = 0). However when $\sigma_3'$ is $O(\nu)$ (i.e. $\sigma_{30}' = 0$) it has been indicated previously that a further re-scaling is possible which leads to an equation like (2.4.12a) in which a cubic nonlinearity is recovered. Indeed the scaling which leads to (2.4.12a) suggest there may be a finite amplitude solitary wave for which the asymptotic expansion (2.4.13a,b and c) is replaced by

$$\eta = \eta_1(X', z) + \nu\eta_2(X', z) + \dots , \qquad (2.4.29a)$$

$$c = c_0 + \nu c_1 + \dots , \qquad (2.4.29b)$$

where X' is again defined by (2.4.13c). Benney and Ko (1978) have shown that this is so for the special case of §2.3 (II) and the governing equation is of the form (2.4.12a). However substitution of (2.4.29a) into (2.1.8a), (2.1.9) and (2.1.10) leads to a nonlinear equation for $\eta_1$; this is a consequence of the use of quasi-Lagrangian co-ordinates. As shown by Benney and Ko (1978) the corresponding expansion in terms of Eulerian co-ordinates and z* leads to a linear equation at the leading order. This case shall not be pursued any further except to comment that in the limit $\varepsilon^2 \ll 1$ which led to (2.4.12a) the results of Benney and Ko (1978) agree with those derived from this theory.



Reproduced with permission of the copyright owner. Further reproduction prohibited without permission.

# Chapter 3: STRONG INTERACTIONS BETWEEN INTERNAL SOLITARY WAVES.

## §3.1 INTRODUCTION

Recently there has been some interest in the interaction and resonant transfer of energy between weakly nonlinear long internal gravity waves. Eckart (1961) discussed the linear internal wave problem for two well separated pycnoclines, and showed that resonant transfer of energy between waves in each of the two pycnoclines was possible when the waves possessed similar phase speeds. This energy transfer is also possible between solitary waves. Liu et al (1980,1982) have considered the interaction between weakly nonlinear internal gravity waves in neighboring pycnoclines for the case when the pycnoclines are widely separated. They found that the interactions were governed by a pair of coupled nonlinear equations, each equation having the form of the intermediate depth equation (Joseph (1977) or Kubota et al (1978)) and a dispersive coupling term. They investigated these equations numerically and analytically and demonstrated the existence of time periodic solitary waves, which alternate their relative phase relationship as a result of the oscillation of wave amplitudes. Also Weidman and Johnson (1982) have experimentally investigated the interactions between internal gravity waves on widely separated pycnoclines. Their experimental results agree quantitatively with the numerical and analytical results of Liu et al (1980,1982). Here it is proposed to study the interaction between internal solitary waves associated with different modes, when the total depth of the fluid is shallow with respect to the wavelength.

As in §2.1 consider waves propagating horizontally in an inviscid, incompressible fluid, with the x-axis in the direction of propagation. The horizontal waveguide is now characterized by a basic



Reproduced with permission of the copyright owner. Further reproduction prohibited without permission.

density profile $\rho_0(z)$ and zero basic flow, bounded below by a rigid boundary $z = -h$, and above either by a free surface whose equilibrium position is at $z = 0$, or by a rigid boundary at $z = 0$. Weakly nonlinear long internal gravity waves in shallow stratified fluids can be characterized by the equality of the two small parameters $\varepsilon^2$ and $\alpha$; here $\varepsilon^2$ is a measure of dispersion and is given by $\varepsilon = H/L$ where H is a vertical scale typically the fluid depth and L is the horizontal scale of the waves, while $\alpha$ is a measure of the characteristic amplitude of the vertical displacement $\eta$ due to the waves.

Long waves in shallow stratified fluids of amplitude $\alpha A$ are normally defined by $\eta \simeq \alpha A \phi_k(z)$, where $\phi_k(z)$ is the solution of the following linear eigenvalue problem for a certain critical value $c_k$, of the wave phase speed (c.f. (2.2.1a,b,c)).

$$\frac{\partial}{\partial z}\left(\rho_0 c_k^2 \frac{\partial \phi_k}{\partial z}\right) + \rho_0 N^2 \phi_k = 0 , \quad \text{for } 0 > z > -h , \qquad (3.1.1a)$$

$$\phi_k = 0 , \quad \text{on } z = -h , \qquad (3.1.1b)$$

$$\phi_k = p\sigma c_k^2 \frac{\partial \phi_k}{\partial z} , \quad \text{on } z = 0 , \qquad (3.1.1c)$$

where $N^2 = -(\sigma\rho_0)^{-1}\rho_{0z}$ is the Brunt-Väisälä frequency, and the number p in (3.1.1c) takes the value 0 or 1 according as the upper boundary is rigid or free. These equations are expressed in non-dimensional co-ordinates based on a length scale H, a time scale $N_1^{-1}$ where $N_1$ is a typical value of the Brunt-Väisälä frequency and a pressure scale $\rho_1 gH$ where $\rho_1$ is typical value of the density. Then the parameter $\sigma$ is $HN_1^2 g^{-1}$ and is small in the Boussinesq approximation. This eigenvalue problem is essentially identical with that which appears in the formulations of Benjamin (1966) and Benney



Reproduced with permission of the copyright owner. Further reproduction prohibited without permission.

(1966). In the weakly nonlinear long wave theory for shallow fluids, the equation which describes the evolution of the amplitude A is the Korteweg-de Vries equation

$$\frac{\partial A}{\partial \tau} + \mu_k A \frac{\partial A}{\partial \theta} + \delta_k \frac{\partial^3 A}{\partial \theta^3} = 0 . \qquad (3.1.2)$$

Here A is a function of a phase variable $\theta = \varepsilon(x - c_k t)$ and the long time variable $\tau = \varepsilon^3 t$. The coefficients $\mu_k$ and $\delta_k$ are known in terms of the modal functions $\phi_k(z)$ and are given by (Benney (1966), or Grimshaw (1981b))

$$I_k \mu_k = 3\int_{-h}^{0} \rho_0 c_k^2 \left(\frac{\partial \phi_k}{\partial z}\right)^3 dz , \qquad (3.1.3a)$$

$$I\kappa\delta_k = \int_{-h}^{0} \rho_0 c_k^2 \phi_k^2 \, dz , \qquad (3.1.3b)$$

and

$$I_k = 2\int_{-h}^{0} \rho_0 c_k^2 \left(\frac{\partial \phi_k}{\partial z}\right)^2 dz . \qquad (3.1.3c)$$

In this chapter the strong interaction between two waves belonging to different modes shall be discussed. It shall be supposed that both waves are propagating in the positive x-direction with phase speeds $c_n$ and $c_m$, corresponding to the modes $\phi_n$ and $\phi_m$, with $n \neq m$. Strong interactions between modes occur when $c_n \simeq c_m$ (i.e. $c_n$ differs from $c_m$ by an $O(\varepsilon^2)$ quantity), while weak interactions between modes occur when $c_n \neq c_m$ (i.e. $c_n$ differs from $c_m$ by an O(1) quantity with respect to the small parameter $\varepsilon$, (c.f. Gear and Grimshaw (1984)). Note, that the terminology used here is adapted from Miles (1977a,b) who considered the oblique interaction of surface solitary waves. Also note that the strong interaction case discussed here differs from the direct resonance recently



Reproduced with permission of the copyright owner. Further reproduction prohibited without permission.

discussed by Akylas and Benney (1980,1982). Direct resonance requires $c_n \simeq c_m$ and $\phi_n \simeq \phi_m$. The latter condition cannot occur here, due to the orthogonality of the solutions of (3.1.1a,b,c). For certain density and velocity profiles, it has been shown by Eckart (1961) that it is possible for $c_n \simeq c_m$ with $n \neq m$ (i.e. for different modes). In such resonant cases, the coupling between these modes must be considered. In §3.2 the equations of motion will be formulated for an inviscid, incompressible, stably stratified fluid. To simplify the analytical work Lagrangian variables are used, where the fluid particle displacements and the pressure act as the dependent variables. Then by expanding in powers of $\varepsilon^2$, it is shown that the strong interaction between modes is described by two coupled Korteweg-de Vries equations, with both dispersive and nonlinear coupling terms. In §3.3 it is shown that these two coupled equations possess three conserved quantities and an exact analytic solution involving the characteristic "sech$^2$" profile of the Korteweg- de Vries equation (3.1.2). Also it is shown that when the coefficients satisfy some special conditions, the coupled nonlinear equations possess an n-soliton solution in terms of the Korteweg-de Vries n-soliton solution. In §3.4 it is shown that the coupled equations are not generally amenable to solution by inverse scattering technique, and thus a numerical method must be employed to solve the equations. In §3.5 numerical solutions of the coupled equations are discussed for several special cases. One case considers two pycnoclines of constant Brunt-Väisälä frequency separated by a region of constant density, while other cases consider only dispersive coupling between the equations or only nonlinear coupling.



Reproduced with permission of the copyright owner. Further reproduction prohibited without permission.

## §3.2 FORMULATION

Consider long wave perturbations relative to a two dimensional basic state which is a function only of the vertical co-ordinate. As in Grimshaw (1980/81,1981b), it is convenient to cast the equations of motion in terms of Lagrangian variables. Thus, let x, z be the Lagrangian co-ordinates of a particle of fluid in the basic state, then define particle displacements $\xi(x,z;t)$, $\eta(x,z;t)$ relative to this basic state, such that Eulerian cartesian co-ordinates are defined as

$$x^* = x + \xi \quad , \quad z^* = z + \eta \ . \tag{3.2.1}$$

The basic state consists of the density $\rho_0(z)$, the pressure $P_0(z)$ and zero basic flow. Before displaying the Lagrangian equations, it is convenient to define a pressure perturbation by

$$P = P_0 + \sigma P^* - \eta \rho_0 \ . \tag{3.2.2}$$

Where $P^*$ is the Eulerian pressure perturbation correct to first order in an expansion in powers of $\xi$ and $\eta$, while P is the pressure associated with the particle displacements.

In an inviscid, incompressible, stably stratified two dimensional fluid in hydrastatic equilibrium, the Lagrangian equations of motion for the pressure $P^*$ and the particle displacements $\xi$ and $\eta$, are given by (Lamb (1932), Yih (1969) and Grimshaw (1980/81,1981b))

$$\frac{\partial \xi}{\partial x} + \frac{\partial \eta}{\partial z} + \frac{\partial \xi}{\partial x}\frac{\partial \eta}{\partial z} - \frac{\partial \xi}{\partial z}\frac{\partial \eta}{\partial x} = 0 \ , \tag{3.2.3a}$$



Reproduced with permission of the copyright owner. Further reproduction prohibited without permission.

$$\rho_0 \frac{\partial^2 \xi}{\partial t^2} + \frac{\partial P^*}{\partial x} + \rho_0 \frac{\partial^2 \xi}{\partial t^2}\frac{\partial \xi}{\partial x} + \rho_0 \frac{\partial^2 \eta}{\partial t^2}\frac{\partial \eta}{\partial x} = 0 , \qquad (3.2.3b)$$

and

$$\rho_0 \frac{\partial^2 \eta}{\partial t^2} + \frac{\partial P^*}{\partial z} + \rho_0 N^2 \eta + \rho_0 \frac{\partial^2 \xi}{\partial t^2}\frac{\partial \xi}{\partial z} + \rho_0 \frac{\partial^2 \eta}{\partial t^2}\frac{\partial \eta}{\partial z} = 0 . \qquad (3.2.3c)$$

It will be assumed that the fluid is bounded below by a rigid boundary $z = -h$, where

$$\eta = 0 \quad \text{on} \quad z = -h . \qquad (3.2.4)$$

If $P_0$ is set to zero on $z = 0$, then the Lagrangian pressure P is also zero on $z = 0$, thus using (3.2.2) the boundary condition on the free surface is

$$\eta = p \frac{\sigma P^*}{\rho_0} \quad \text{on} \quad z = 0 . \qquad (3.2.5)$$

The position of the free surface is a constant in the Lagrangian formulation and the constant p, is 0 or 1 according as the upper boundary is rigid or free.

It is proposed to investigate the modulation of weakly nonlinear long waves in shallow stratified fluids, where the horizontal scale, based on a typical wavelength, is much greater than the vertical scale. If $\varepsilon$ is a small parameter representing the ratio of vertical to horizontal scales it is appropriate to introduce the new variables

$$\theta = \varepsilon(x - c_n t) , \quad \tau = \varepsilon^3 t \qquad (3.2.6)$$

and to suppose that $\xi$, $\eta$ and $P^*$ are functions of $\theta$, $\tau$ and z. Here $\theta$ is the phase of the wave which has phase speed $c_n$ and $\tau$ is a fast time variable, representative of the evolution of long waves. To be consistent with the above rescaling and the shallow water theory it is necessary to make the



Reproduced with permission of the copyright owner. Further reproduction prohibited without permission.

following transformations

$$\eta = \varepsilon^2 \hat{\eta}_\theta \,, \tag{3.2.7a}$$

$$\xi = \varepsilon \hat{\xi} \,, \tag{3.2.7b}$$

and

$$P^* = \varepsilon^2 \hat{P}^* \,. \tag{3.2.7c}$$

Then substitution of (3.2.6) and (3.2.7a,b,c) into the perturbation equations (3.2.3a,b,c) and, into the boundary conditions (3.2.4) and (3.2.5), yields the following system of equations for $\hat{\eta}$

$$c_n^2 \frac{\partial}{\partial z} \{\rho_0 \hat{\eta}_{\theta\theta z}\} + \rho_0 N^2 \hat{\eta}_{\theta\theta} = \varepsilon^2 f_n \quad \text{for} \quad 0 > z > -h \,, \tag{3.2.8a}$$

$$\hat{\eta}_{\theta\theta} = 0 \quad \text{on} \quad z = -h \,, \tag{3.2.8b}$$

and

$$\hat{\eta}_{\theta\theta} - p\sigma c_n^2 \hat{\eta}_{\theta\theta z} = p\sigma\varepsilon^2 g_n \quad \text{on} \quad z = 0 \,. \tag{3.2.8c}$$

Where the inhomogeneous terms $f_n$, $g_n$ are given by

$$f_n = -\rho_0 c_n^2 (\hat{\eta}_{\theta\theta\theta\theta} + (\hat{\eta}_{zz}\hat{\eta}_{\theta\theta z})_\theta) + 2c_n(\rho_0 \hat{\eta}_{\theta z\tau})_z + c_n^2 \{\rho_0 (3\hat{\eta}_{\theta z}\hat{\eta}_{\theta\theta z} - (\hat{\eta}_{\theta\theta}\hat{\eta}_{zz})_\theta)\}_z + O(\varepsilon^2), \tag{3.2.9a}$$

and

$$g_n = \sigma c_n^2 (-3\hat{\eta}_{\theta z}\hat{\eta}_{\theta\theta z} + (\hat{\eta}_{\theta\theta}\hat{\eta}_{zz})_\theta) - 2\sigma c_n \hat{\eta}_{\theta z\tau} + O(\varepsilon^2) \quad \text{on} \quad z = 0. \tag{3.2.9b}$$

At this stage in the analysis it is usual to assume that $\hat{\eta}_{\theta\theta}$ has a power series expansion solution in terms of the small parameter $\varepsilon^2$.



Reproduced with permission of the copyright owner. Further reproduction prohibited without permission.

Consequently it would be found that to leading order in $\varepsilon^2$, the evolution equation for the amplitude of $\hat{\eta}_{\theta\theta}$ is just the Korteweg-de Vries equation (3.1.2). In certain circumstances, there exists the possibility for the wave phase speeds of two distinct modal functions (solutions of (3.1.1a,b and c)) to be approximately the same. In such cases the evolution of the wave amplitudes cannot be described solely by equation (3.1.2), but by a system of equations that take into consideration the coupling between the modal functions. To investigate this interaction between weakly nonlinear, long internal gravity wave modes, it is supposed that, $\phi_n$ and $\phi_m$ are two distinct solutions of the eigenvalue problem (3.1.1a,b and c) and that their phase speeds $c_n$ and $c_m$, differ by a quantity proportional to $\varepsilon^2$. That is

$$c_m = c_n - \varepsilon^2\chi \ . \tag{3.2.10}$$

Simultaneously it is noted that the homogeneous part of equations (3.2.8a,b and c) is identical to the eigenvalue problem (3.1.1a,b and c). Thus a solution of (3.2.8a,b and c) can be found by representing $\hat{\eta}$ as a sum of the modal functions of the system (3.1.1a,b and c), that is

$$\hat{\eta} = \sum_i a_i(\tau,\theta)\phi_i(z) \ . \tag{3.2.11}$$

To determine the form of the amplitudes $a_i(\tau,\theta)$ multiply both sides of (3.2.11) by $\rho_0 N^2\phi_k$ and integrate with respect to z from -h to zero. Then after suitable manipulations it is found that

$$\frac{\partial^2 a_k}{\partial\theta^2}\frac{c_k I_k}{2}\left(1 - \frac{c_n^2}{c_k^2}\right) = \varepsilon^2\left\{\int_{-h}^{0}\phi_k f_n\, dz + \left(p\rho_0\phi_k g_n\right)_{z=0}\right\} \ . \tag{3.2.12}$$

It is readily seen from (3.2.12) that if $c_k^2 - c_n^2$ is an order one quantity,



Reproduced with permission of the copyright owner. Further reproduction prohibited without permission.

then $a_k$ must be an order $\varepsilon^2$ quantity and is thus negligible at leading order. But, if k is m or n, then $c_k^2 - c_n^2$ is an order $\varepsilon^2$ quantity and thus it must be concluded that both $a_n$ and $a_m$ are order one quantities. So to leading order it is sufficient to consider only $a_n$ and $a_m$, thus $\hat{\eta}$ has the expansion

$$\hat{\eta} = a_n(\tau,\theta)\phi_n(z) + a_m(\tau,\theta)\phi_m(z) + O(\varepsilon^2) . \qquad (3.2.13)$$

Now in order that $\hat{\eta}$, given by (3.2.13), should satisfy (3.2.8a,b and c), it is necessary and sufficient that

$$\int_{-h}^{0} \phi_n f_n \, dz + \left(p\rho_0 \phi_n g_n\right)_{z=0} = 0 , \qquad (3.2.14a)$$

and

$$\int_{-h}^{0} \phi_m f_n \, dz + \left(p\rho_0 \phi_m g_n\right)_{z=0} = -\chi I_m a_{m\theta\theta} + O(\varepsilon^2) . \qquad (3.2.14b)$$

Here, (3.2.14a and b) are equation (3.2.12) when k = n, m respectively. Using (3.2.9a,b) and ignoring terms of $O(\varepsilon^2)$ the compatibility conditions (3.2.14a and b) are equivalent to

$$0 = I_n\left(\frac{\partial A_n}{\partial \tau} + \mu_n A_n \frac{\partial A_n}{\partial \theta} + \delta_n \frac{\partial^3 A_n}{\partial \theta^3}\right) + \nu_{nmm} A_m \frac{\partial A_m}{\partial \theta}$$

$$+ \nu_{nnm} \frac{\partial}{\partial \theta}(A_n A_m) + \lambda_{nm} \frac{\partial^3 A_m}{\partial \theta^3} , \qquad (3.2.15a)$$



Reproduced with permission of the copyright owner. Further reproduction prohibited without permission.

$$0 = I_m\left(\frac{\partial A_m}{\partial \tau} - \chi \frac{\partial A_m}{\partial \theta} + \mu_m A_m \frac{\partial A_m}{\partial \theta} + \delta_m \frac{\partial^3 A_m}{\partial \theta^3}\right) + \nu_{nnm} A_n \frac{\partial A_n}{\partial \theta}$$

$$+ \nu_{nmm} \frac{\partial}{\partial \theta}(A_n A_m) + \lambda_{nm} \frac{\partial^3 A_n}{\partial \theta^3} , \qquad (3.2.15b)$$

where $$A_n(\tau,\theta) = \frac{\partial a_n}{\partial \theta} , \quad A_m(\tau,\theta) = \frac{\partial a_m}{\partial \theta} , \qquad (3.2.15c)$$

$$\nu_{skl} = 3\int_{-h}^{0} c_n^2 \rho_0 \frac{\partial \phi_s}{\partial z} \frac{\partial \phi_k}{\partial z} \frac{\partial \phi_l}{\partial z} dz , \qquad (3.2.15d)$$

and $$\lambda_{kl} = \int_{-h}^{0} c_n^2 \rho_0 \phi_k \phi_l \, dz . \qquad (3.2.15e)$$

Here recall that $I_k$, $\mu_k$ and $\delta_k$ are defined by (3.1.3a,b,c). Note also that $I_k\mu_k = \nu_{kkk}$ and $I_k\delta_k = \lambda_{kk}$. The equations (3.2.15a and b) are evolution equations for the amplitudes $A_n(\tau,\theta)$, $A_m(\tau,\theta)$, they may be regarded as coupled Korteweg-de Vries equations. In the absence of the component $A_m$ (or $A_n$) (3.2.15a or b) reduces to the single Korteweg-de Vries equation (3.1.2). Note that the coupling terms are either nonlinear terms whose coefficients are $\nu_{nnm}$ or $\nu_{nmm}$, or dispersive terms whose coefficients are $\lambda_{nm}$.

The complete solution for the vertical displacement $\eta$, can now be constructed from (3.2.7a), (3.2.13) and (3.2.15c),

$$\eta = \varepsilon^2\left(A_n(\tau,\theta)\phi_n(z) + A_m(\tau,\theta)\phi_m(z)\right) + O(\varepsilon^4) . \qquad (3.2.16)$$



Reproduced with permission of the copyright owner. Further reproduction prohibited without permission.

## §3.3 SOME PROPERTIES OF THE EVOLUTION EQUATIONS

Before proceeding to consider numerical solutions of (3.2.15a,b) it is useful to note that these equations possess several properties that can be obtained by analytical techniques. Firstly by integrating (3.2.15a,b) it is readily deduced that the following mass conservation laws are true

$$\frac{d}{d\tau}\int_{-\infty}^{\infty} A_n(\tau,\theta)\, d\theta = 0 , \tag{3.3.1}$$

$$\frac{d}{d\tau}\int_{-\infty}^{\infty} A_m(\tau,\theta)\, d\theta = 0 , \tag{3.3.2}$$

Equations (3.3.1) and (3.3.2) indicate that the area under the amplitude curves for each internal gravity wave mode is a conserved quantity even in the presence of interaction.

If (3.2.15a) is multiplied by $A_n$ and added to $A_m$ times (3.2.15b), then integrating the resultant equation gives

$$\frac{d}{d\tau}\int_{-\infty}^{\infty} \frac{1}{2}\left(I_n A_n^2(\tau,\theta) + I_m A_m^2(\tau,\theta)\right) d\theta = 0 , \tag{3.3.3}$$

Thus the total energy of the combined system is a conserved quantity, while in general the energy of individual modes is not conserved. As in Liu et al (1980), (3.3.1), (3.3.2) and (3.3.3) suggest that one nonlinear wave mode can only increase its energy by increasing its amplitude and contracting its width, while the other nonlinear wave has to reduce its amplitude and increase its width.

An exact analytic solution to (3.2.15a and b) may be found by



Reproduced with permission of the copyright owner. Further reproduction prohibited without permission.

seeking steady progressive stationary wave solutions satisfying

$$A_n(\tau,\theta) = A_n(\theta - V\tau) = A_n(y) \tag{3.3.4a}$$

and

$$A_m(\tau,\theta) = A_m(\theta - V\tau) = A_m(y) \tag{3.3.4b}$$

The introduction of (3.3.4a and b) into (3.2.15a and b) followed by an integration with respect to y leads to

$$0 = I_n\left(-VA_n + \mu_n \frac{A_n^2}{2} + \delta_n \frac{d^2A_m}{dy^2}\right) + \nu_{nmm} \frac{A_m^2}{2} + \nu_{nnm} A_n A_m + \lambda_{nm} \frac{d^2A_m}{dy^2}, \tag{3.3.5a}$$

and

$$0 = I_m\left(-(V + \chi) A_m + \mu_m \frac{A_m^2}{2} + \delta_m \frac{d^2A_m}{dy^2}\right) + \nu_{nnm} \frac{A_n^2}{2} + \nu_{nmm} A_n A_m + \lambda_{nm} \frac{d^2A_n}{dy^2}. \tag{3.3.5b}$$

In order to find a solution to (3.3.5a and b) let $A_m(y)$ be an exact multiple of $A_n(y)$. That is

$$A_m(y) = R\, A_n(y), \tag{3.3.6}$$

where R is a constant, then (3.3.5a and b) give

$$0 = -VI_n A_n + \frac{A_n^2}{2}\left(\nu_{nnn} + 2\nu_{nnm}R + \nu_{nmm}R^2\right) + \left(\lambda_{nn} + R\,\lambda_{nm}\right) \frac{d^2A_n}{dy^2}, \tag{3.3.7a}$$

$$\left(\nu_{nnn} + 2\nu_{nnm}R + \nu_{nmm}R^2\right)\left(\lambda_{mm}R + \lambda_{nm}\right) = \left(\nu_{mmm}R^2 + 2\nu_{nmm}R + \nu_{nnm}\right)\left(\lambda_{nn} + R\lambda_{nm}\right), \tag{3.3.7b}$$



Reproduced with permission of the copyright owner. Further reproduction prohibited without permission.

and $$V = \chi\left(\frac{I_n(\lambda_{mm}R + \lambda_{nm})}{I_m R(\lambda_{nn} + \lambda_{nm}R)} - 1\right)^{-1} , \qquad (3.3.7c)$$

where $I_k\delta_k = \lambda_{kk}$ and $I_k\mu_k = \nu_{kkk}$. Equation (3.3.7a) is an integrated form of the Korteweg-de Vries equation, (3.3.7b) is a cubic polynomial in R which has either one or three real solutions, while (3.3.7c) gives V in terms of R. It is readily verified that (3.3.7a) has the solitary wave solution

$$A_n = A_0 \operatorname{sech}^2(y/\lambda) , \qquad (3.3.8a)$$

with $$A_0 = \frac{3VI_n}{(\nu_{nnn} + 2\nu_{nnm}R + \nu_{nmm}R^2)} , \qquad (3.3.8b)$$

and $$\lambda^2 = \frac{12(\lambda_{nn} + R\lambda_{nm})}{A_0(\nu_{nnn} + 2\nu_{nnm}R + \nu_{nmm}R^2)} . \qquad (3.3.8c)$$

As for the Korteweg-de Vries equation the speed of propagation of this solitary wave is proportional to the amplitude $A_0$, while its width is inversely proportional to the square root of the amplitude. Note, that the soliton solution (3.3.8a) is valid provided $\lambda$ is real. There is thus a restriction on the coefficients $\nu_{nnm}$ etc. to ensure that $\lambda$ is real. For example in the three layer fluid special case of §3.5 it is found that the right hand side of (3.3.8c) is negative and thus the above solution does not exist. Whereas, in the other cases considered in §3.5 the right hand side of (3.3.8c) is positive and thus the solution (3.3.8a) exists in those cases. Note, also that in the solution (3.3.8a), none of the parameters V, $A_0$ or $\lambda$, act as a variable, in fact all three quantities are uniquely determined from R.



Reproduced with permission of the copyright owner. Further reproduction prohibited without permission.

If (3.3.7c) is carefully examined it can be seen that if both the numerator and the denominator in (3.3.7c) are zero, then the speed of propagation of the soliton V, becomes a variable. In fact a special class of solutions are obtained when

$$\chi = 0 , \tag{3.3.9a}$$

$$I_n(\lambda_{mm} R + \lambda_{nm}) = I_m R(\lambda_{nn} + R\lambda_{nm}) , \tag{3.3.9b}$$

$$I_m R(\nu_{nnn} + 2\nu_{nnm} R + \nu_{nmm} R^2) = I_n(\nu_{mmm} R^2 + 2\nu_{nmm} R + \nu_{nnm}) \tag{3.3.9c}$$

and

$$A_m = R A_n . \tag{3.3.9d}$$

Then the evolution equations (3.2.15a and b) reduce to one equation,

$$0 = I_n \frac{\partial A_n}{\partial \tau} + (\nu_{nnn} + 2\nu_{nnm} R + \nu_{nmm} R^2) A_n \frac{\partial A_n}{\partial \theta} + (\lambda_{nn} + R \lambda_{nm}) \frac{\partial^3 A_n}{\partial \theta^3} , \tag{3.3.10}$$

which is just a form of the Korteweg-de Vries equation. Thus if the conditions (3.3.9a,b,c, and d) are satisfied then (3.2.15a and b) have n-soliton solutions derivable from the n-soliton solution of the Korteweg-de Vries equation (Whitham (1974)).

Also it should be noticed that if both the numerator and denominator in (3.3.7c) are infinite then the speed of propagation of the soliton V, becomes a variable. In this case if $\chi = \infty$ then either $R = 0$ or $\lambda_{nn} + \lambda_{nm} R = 0$. If the later condition applies then (3.3.7a) reduces to a



Reproduced with permission of the copyright owner. Further reproduction prohibited without permission.

quadratic equation in $A_n$, which has the solution $A_n = 0$ and thus $A_m = 0$. On the other hand if $R = 0$ then $A_m = 0$ and (3.3.5a) reduces to an integrated form of the Korteweg-de Vries equation for $A_n$. Note that if $\chi = \infty$ then $c_m - c_n$ is not $O(\varepsilon^2)$ and thus the expansion (3.2.13) no longer applies, instead $\hat{\eta} \simeq a_n \phi_n$, and $A_n$ $(= \partial a_n/\partial\theta)$ satisfies a form of the Korteweg-de Vries equation. Finally it should be noted that if $R = \infty$ then $A_n$ should be zero and (3.3.5b) then reduces to an integrated form of the Korteweg-de Vries equation for $A_m$.



Reproduced with permission of the copyright owner. Further reproduction prohibited without permission.

## §3.4 INVERSE SCATTERING AND THE PAINLEVÉ CRITERION

A nonlinear partial differential equation is said to be solvable by an inverse scattering transform if a function of K(x,x;t) solves the partial differential equation, where K(x,y;t) is defined by a linear integral equation of the Gel'fand-Levitan-Marchenko type (Ablowitz and Segur (1981)),

$$K(x,y;t) + F(x,y;t) + \int_x^\infty K(x,z;t)N(z,y;t)\,dz = 0, \qquad (3.4.1)$$

where N is explicitly given in terms of F (for examples see Ablowitz, Ramani and Segur (1978, 1980a,b)), and F satisfies a suitable linear partial differential equation and decays rapidly enough as $x \to +\infty$ for the integral equation to be meaningful.

Using the Fredholm theory of linear integral equations it has been shown by Ablowitz et al (1978, 1980a,b) that the movable singularities of K (if any) are simple poles. Then, K (the solution of the linear integral equation), is said to possess the Painlevé property. A nonlinear ordinary differential equation is of Painlevé type if the solutions of the ODE (ordinary differential equation) do not have movable critical points. A critical point is a branch point or an essential singularity in the solution of the ODE. It is movable if its location in the complex plane depends on the constants of integration.

This information led Ablowitz et al (1978) to conjecture that; a nonlinear PDE (partial differential equation) or system of PDE's is solvable by an inverse scattering transform only if every nonlinear ODE or system of ODE's, obtained by exact reduction is of Painlevé type. Several examples of the connection between nonlinear PDE's solvable by inverse scattering and ODE's of the Painlevé type are given by Ablowitz, Ramani and



Reproduced with permission of the copyright owner. Further reproduction prohibited without permission.

Segur (1980b), Ablowitz and Segur (1981), M$^{c}$Leod and Olver (1983), Weiss, Tabor and Carnevale (1983) and Weiss (1983).

The work of Ablowitz, et al (1978,1980a,b) has been extended by M$^{c}$Leod and Olver (1983), who have shown that a necessary condition that nonlinear PDE or a system of nonlinear PDE's are completely integrable (solvable by inverse scattering) is that all possible ODE's obtained by direct reduction of the PDE's, have solutions that are meromorphic (only singularities are poles) in the complex plane. Thus if an ODE obtained by direct reduction of the given nonlinear PDE, or PDE's is shown not to possess the Painlevé property then the PDE is not solvable by inverse scattering.

Weiss, Tabor and Carnevale (1983) and Weiss (1983) show that a nonlinear PDE can be shown to possess the Painlevé property without having to examine all the ODE's obtained by direct reduction. They say that a PDE has the Painlevé property when the solutions of the PDE are single-valued about the movable singularity manifolds. To be precise, if a singularity manifold is determined by

$$\phi(z_1,---,z_n) = 0 \tag{3.4.2}$$

and $u = u(z_1,---,z_n)$ is a solution of the PDE, then they assume that

$$u = \phi^{\alpha} \sum_{j=0}^{\infty} u_j \phi^j \tag{3.4.3}$$

where $\phi = \phi(z_1,---,z_n)$, $u_j = u_j(z_1,---,z_n)$, $u_0 \neq 0$, are analytic functions of $(z_j)$ in a neighborhood of the manifold (3.4.2) and $\alpha$ is an integer. Substitution of (3.4.3) into the PDE determines the value(s) of $\alpha$ and defines the recursion relations for $u_j$, $j = 0,1,2,---$. When the assumption



Reproduced with permission of the copyright owner. Further reproduction prohibited without permission.

(3.4.3) is correct, the PDE is said to possess the Painlevé property and is conjectured to be integrable.

Given the system of nonlinear PDE's (3.2.15a and b) it remains to determine whether they possess the Painlevé property. This can either be done using the method of Weiss et al (1983) and Weiss (1983) or by using a singular point analysis developed by Ablowitz et al (1980 a,b, 1981)). The method is similar to the method of Kovalevskya (Golubev (1953)), who made major contributions to the theory of the motion of a rigid body about a fixed point after first determining the choices of the parameters for which the equations of motion had no movable singularities. Using the singular point analysis of Ablowitz et al (1980 a,b,1981) it can be determined whether ODE's obtained by an exact reduction of the PDE's, are of the Painlevé type. The easiest reductions occur if the PDE's admit travelling wave or similarity solutions, but these are not the only possibilites. If these ODE's are not of the Painlevé type, then the PDE's (3.2.15a,b) in their present form cannot be solved by inverse scattering.

Due to the simplicity of the singular point analysis it is intended to test whether the ODE's (3.3.5a and b) possess the Painlevé property. (Note that (3.3.5a and b) are an exact reduction of (3.2.15a and b).) Following, Ablowitz, Ramani and Segur (1980a) the first task is to find the dominant behavior of the solutions in a sufficiently small neighborhood of the (movable) singularities. This is affected by making the substitutions

$$A_n = \alpha_1 (y - y_0)^p , \qquad (3.4.4a)$$

$$Am = \alpha_2 (y - y_0)^p , \qquad (3.4.4b)$$

where $Re(p) < 0$ and $y_0$ is arbitrary. Substituting (3.4.4a and b) into



Reproduced with permission of the copyright owner. Further reproduction prohibited without permission.

(3.3.5a and b) shows that at leading order in $(y - y_0)$ the only possible choice for p is -2 and that $\alpha_1$ and $\alpha_2$ satisfy

$$0 = \nu_{nnn}\alpha_1^2 + 2\nu_{nnm}\alpha_1\alpha_2 + \nu_{nmm}\alpha_2^2 + 12(\lambda_{nn}\alpha_1 + \lambda_{nm}\alpha_2) , \quad (3.4.5a)$$

$$0 = \nu_{mmm}\alpha_2^2 + 2\nu_{nmm}\alpha_1\alpha_2 + \nu_{nnm}\alpha_1^2 + 12(\lambda_{mm}\alpha_2 + \lambda_{nm}\alpha_1) , \quad (3.4.5b)$$

Note that if p was not an integer this would signify the presence of an algebraic branch point of order p. The existence of such a branch point means that the equations are not of Painlevé type. Note, also that (3.4.5a and b) possess at least one and possibly three non-trivial solutions for $\alpha_1$ and $\alpha_2$.

Equations (3.4.4a and b) represent the first terms in a Laurent series, valid in a deleted neighborhood of a movable pole. The next step in the singular point analysis is to determine where the remaining constants of integration enter the series solutions of (3.3.5a and b). The powers at which these arbitrary constants enter are called resonances. To determine these resonances two simplified equations are constructed from (3.3.5a and b), that retain only the leading terms, these equations are

$$0 = \nu_{nnn}A_n^2 + 2\nu_{nnm}A_nA_m + \nu_{nmm}A_m^2 + 2\lambda_{nn}\frac{d^2A_n}{dy^2} + 2\lambda_{nm}\frac{d^2A_m}{dy^2} , \quad (3.4.6a)$$

$$0 = \nu_{mmm}A_m^2 + 2\nu_{nmm}A_nA_m + \nu_{nnm}A_n^2 + 2\lambda_{mm}\frac{d^2A_m}{dy^2} + 2\lambda_{nm}\frac{d^2A_n}{dy^2} , \quad (3.4.6b)$$

The resonances are found by making the substitutions

$$A_n = \alpha_1 (y - y_0)^{-2} + \gamma_1 (y - y_0)^{r-2} , \quad (3.4.7a)$$



Reproduced with permission of the copyright owner. Further reproduction prohibited without permission.

$$A_m = \alpha_2 (y - y_0)^{-2} + \gamma_2 (y - y_0)^{r-2} , \qquad (3.4.7b)$$

into the reduced equation (3.4.6a and b). To leading order (3.4.6a and b) reduce to

$$\underline{\underline{Q}}(r) \, [\gamma_1, \gamma_2]^T = 0 \qquad (3.4.8)$$

where $\underline{\underline{Q}}(r) =$

$$\begin{bmatrix} \nu_{nnn}\alpha_1 + \nu_{nnm}\alpha_2 + (r-2)(r-3)\lambda_{nn} & \nu_{nnm}\alpha_1 + \nu_{nmm}\alpha_2 + (r-2)(r-3)\lambda_{nm} \\ \nu_{nnm}\alpha_1 + \nu_{nmm}\alpha_2 + (r-2)(r-3)\lambda_{nm} & \nu_{nmm}\alpha_1 + \nu_{mmm}\alpha_2 + (r-2)(r-3)\lambda_{mm} \end{bmatrix} \qquad (3.4.9)$$

The resonances are the nonnegative roots of

$$\det[\underline{\underline{Q}}(r)] = 0 , \qquad (3.4.10)$$

which are

$$r = -1, \ \frac{5}{2} \pm \frac{1}{2}\sqrt{(4\Lambda - 47)}, \ 6 ,$$

where

$$\Lambda = \{\alpha_1(2\lambda_{nm}\nu_{nnm} - \lambda_{mm}\nu_{nnn} - \lambda_{nn}\nu_{nmm})$$

$$+ \alpha_2(2\lambda_{nm}\nu_{nmm} - \lambda_{mm}\nu_{nnm} - \lambda_{nn}\nu_{mmm})\}/[\lambda_{nn}\lambda_{mm} - \lambda_{nm}^2] . \qquad (3.4.11)$$

The root r = -1 represents the arbitrariness of $y_0$. In order that no movable algebraic branch points exist it is required that the values of r, are only real positive integers (except -1). Generally this requirement is not satisfied (i.e. for the values of r to be real positive integers $\Lambda$ must either be 12 or 14, which only occurs under special circumstances), then



Reproduced with permission of the copyright owner. Further reproduction prohibited without permission.

the solutions of (3.3.5a, b) will contain movable algebraic branch points and thus the ODE's (3.3.5a,b) do not possess the Painlevé property, and the nonlinear evolution equations (3.2.15a,b) in their present form are not amenable to solution by inverse scattering transform. Also note that if $\Lambda = 18$ then a resonance will occur at $r = 0$, as r is not real and positive this suggests that (3.4.4a,b) misses an essential part of the solution (i.e. (3.4.4a and b) cannot be the first terms in a Laurent type series solution of (3.3.5a anb b)). In fact the first terms would now involve logarithms of $y - y_0$ and thus (3.3.5a,b) would not possess the Painlevé property.

It should be noted that if $\Lambda = 12$ or 14, this does not necessarily imply that (3.3.5a,b) possess the Painlevé property, as the method so far has not eliminated the possibility of movable logarithmic branch points. To determine whether logarithmic branch points exist it is necessary to do a Frobenius type expansion about the movable pole $y = y_0$ up to the highest resonance, thus into the full equations (3.3.5a,b) substitute

$$A_n = \alpha_1 (y - y_0)^{-2} + \sum_{j=1}^{6} a_j (y - y_0)^{j-2} , \qquad (3.4.12a)$$

$$A_m = \alpha_2 (y - y_0)^{-2} + \sum_{j=1}^{6} b_j (y - y_0)^{j-2} . \qquad (3.4.12b)$$

The constants $a_j$, $b_j$ can then be determined. At each of the resonances an arbitrary constant enters the expansion and a compatibility condition must be satisfied. If this compatibility condition is not satisfied, there is no solution of the form (3.4.12a,b), and thus logarithmic terms must be used in the expansion. Continuing the expansion to higher orders then



Reproduced with permission of the copyright owner. Further reproduction prohibited without permission.

introduces more and more logarithmic terms. This then signals a movable logarithmic branch point and (3.3.5a,b) will not possess the Painlevé property. If all the compatibility conditions are satisfied then (3.3.5a,b) will possess the Painlevé property and an inverse scattering transform of (3.2.15a,b) may be sought with some confidence.

If $\Lambda = 12$, then the resonances occur at $r = 2$, 3 and 6, and the compatibility conditions at these resonances require

$$\chi = 0 , \tag{3.4.13a}$$

and
$$I_n\alpha_1\left(\nu_{nmm}\alpha_2 + \nu_{nnm}\alpha_1\right) = I_m\alpha_2\left(\nu_{nnn}\alpha_1 + \nu_{nnm}\alpha_2\right) . \tag{3.4.13b}$$

Whereas, if $\Lambda = 14$, then the resonances occur at $r = 1$, 4 and 6, and the compatibility conditions require

$$\chi = 0 , \tag{3.4.14a}$$

and
$$I_n\alpha_1\left(\nu_{nmm}\alpha_2 + \nu_{nnm}\alpha_1 + 2\lambda_{nm}\right) = I_m\alpha_2\left(\nu_{nnn}\alpha_1 + \nu_{nnm}\alpha_2 + 2\lambda_{nn}\right) . \tag{3.4.13b}$$

In both these cases, the conditions (3.4.13a,b) or (3.4.14a,b), with (3.4.5a,b) and (3.4.11) can be shown to reduce to (3.3.9a,b and c), when R represents $\alpha_2/\alpha_1$. It has already been shown (see §3.3) that if (3.3.9a,b,c) are satisfied then (3.2.15a,b) reduce to the Korteweg-de Vries equation which has an inverse scattering transform.



Reproduced with permission of the copyright owner. Further reproduction prohibited without permission.

## §3.5 NUMERICAL SOLUTIONS

In §3.4, it is shown by using the Painlevé criterion (see Ablowitz et al (1980) or Weiss et al (1983)) that the coupled equations (3.2.15a,b) are not generally tractable to solution by the inverse scattering technique. Hence it has been necessary to solve the equations numerically, using an adaptation of the method developed for the Korteweg-de Vries equation by Fornberg and Whitham (1978). A full discussion of the numerical technique can be found in Appendix A. Before proceeding to discuss the numerical results it is useful to transform (3.2.15a and b) as follows, noting that $I_{n,m}$ and $\delta_{n,m}$ (3.1.3b,c) are inherently positive.

$$A_n = \frac{\chi\delta_n A}{r\delta_m\mu_n} \quad , \qquad A_m = \frac{\chi B}{r\mu_m} \quad , \tag{3.5.1a}$$

$$\theta = \left(\frac{r\delta_n}{\chi}\right)^{\frac{1}{2}} \xi \quad , \qquad \tau = \left(\frac{r\delta_m}{\chi}\right)^{\frac{3}{2}} \frac{s}{\delta_n} \, . \tag{3.5.1b}$$

Here r is a non-dimensional disposable parameter which has the same sign as x. On substituting (3.5.1a,b) in (3.2.15a,b) it is found that

$$\frac{\partial A}{\partial s} + A\frac{\partial A}{\partial \xi} + \frac{\partial^3 A}{\partial \xi^3} + a_1 B\frac{\partial B}{\partial \xi} + a_2\frac{\partial}{\partial \xi}(AB) + a_3\frac{\partial^3 B}{\partial \xi^3} = 0 \, , \tag{3.5.2a}$$

$$b_1\frac{\partial B}{\partial s} + B\frac{\partial B}{\partial \xi} + \frac{\partial^3 B}{\partial \xi^3} - r\frac{\partial B}{\partial \xi}$$

$$+ b_2\left(a_1\frac{\partial}{\partial \xi}(AB) + a_2 A\frac{\partial A}{\partial \xi} + a_3\frac{\partial^3 A}{\partial \xi^3}\right) = 0 \, , \tag{3.5.2b}$$



Reproduced with permission of the copyright owner. Further reproduction prohibited without permission.

where

$$a_1 = \frac{\nu_{nmm}\,\nu_{nnn}\,\lambda^2_{mm}}{\nu^2_{mmm}\,\lambda^2_{nn}}\,,$$

$$a_2 = \frac{\nu_{nnm}\,\lambda_{mm}}{\nu_{mmm}\,\lambda_{nn}}\,, \qquad (3.5.2c)$$

$$a_3 = \frac{\nu_{nnn}\,\lambda_{nm}\,\lambda_{mm}}{\nu_{mmm}\,\lambda^2_{nn}}\,,$$

$$b_1 = \frac{\lambda_{nn}}{\lambda_{mm}} \quad \text{and} \quad b_2 = \frac{\lambda^3_{nn}\,\nu^2_{mmm}}{\lambda^3_{mm}\,\nu^2_{nnn}}\,. \qquad (3.5.2d)$$

The coupled equations (3.5.2a,b) thus contain five parameters $a_1$, $a_2$, $a_3$, $b_1$, and $b_2$. In the first two numerical experiments these five parameters are determined from the three-layer model described in Appendix B with $r = 1.0$ and $N_2 = 0.42N_1$ (see Figure B.1); the details are given in Table 3.1. The numerical experiments were performed as an initial value problem, using solitary wave solutions of the Korteweg-de Vries equation (3.1.2) as initial conditions for the wave amplitudes. For Figure 3.1 the initial conditions were a solitary wave profile for A and zero for B. Figure 3.1a shows the evolution of A and Figure 3.1b that for B. Due to the coupling between the modes, B is able to draw energy from the initial waveform in A. As A loses energy the amplitude of its initial waveform decreases and a dispersive wavetrain is developed, in order to satisfy conservation of mass. The system is seen to evolve to a two-soliton state with some trailing radiation. Each soliton, or travelling wave, has both an A and a B component, completely phase-locked. Figure 3.1c is an amplitude-time



Reproduced with permission of the copyright owner. Further reproduction prohibited without permission.

| FIGURE | 3.1 | 3.2 |
|---|---|---|
| MESH POINTS | 256 | 256 |
| $\Delta\xi$ | 1.0 | 1.0 |
| $\Delta s$ | 0.005 | 0.005 |
| TIME STEPS | 40,000 | 30,000 |
| A(s=0) | $\frac{1}{2}S^2(\frac{\sqrt{6}}{12}(\xi-70))$ | $\frac{1}{2}S^2(\frac{\sqrt{6}}{12}(\xi-50))$ $+\frac{1}{4}S^2(\frac{\sqrt{3}}{12}(\xi-90))$ |
| B(s=0) | 0.0 | $S^2(\frac{\sqrt{3}}{6}(\xi-50))$ $+\frac{1}{2}S^2(\frac{\sqrt{6}}{12}(\xi-90))$ |

| | |
|---|---|
| $a_1 = 0.0255778$ | $a_2 = 0.7426849$ |
| $a_3 = 0.1393894$ | $b_1 = 2.2670291$ |
| $b_2 = 21.513946$ | $r = 1.0$ |

Table 3.1: Details of the technical data, initial conditions and coefficients for Figures 3.1 and 3.2. Here $S^2(\xi)$ denotes $\text{sech}^2(\xi)$.

diagram for the time evolution of the nonlinear wave amplitudes and Figure 3.1d is a position-time diagram for the location of the wave crests. These figures show that after an initial period of adjustment each wave travels at a constant speed and constant amplitude. Figure 3.1e is a plot of the wave shapes for both phase-locked solitary like waves, showing the A and B components in each case.

Figures 3.2a and b show the time evolution of (3.4.2a,b) when the initial state contains a 2-soliton profile for A, and a 2-soliton profile for B. So that interactions will occur the solitons have different amplitudes, with the smaller amplitude waves taking the front positions.



Reproduced with permission of the copyright owner. Further reproduction prohibited without permission.

(3.1a)

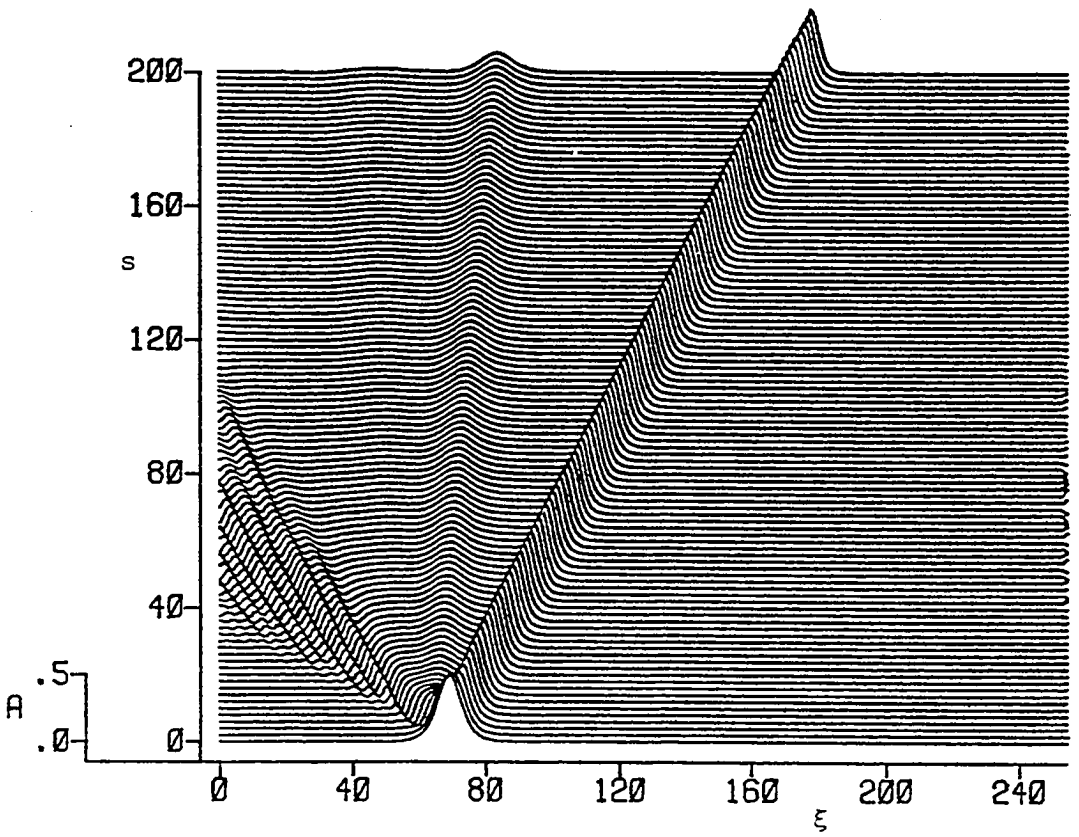


Figure 3.1: A plot of the evolution of the waves for the initial conditions and parameters displayed in Table 3.1. (a) evolution of A; (b) evolution of B; (c) amplitude as a function of time; (d) position of the wave crests as a function of time; ———, first soliton; —+—+—, second soliton; (e) a plot of the wave shapes; ———, A; —+—+—, B.

See Table 3.1 for details of the initial conditions. Figures 3.2a and b show the evolution of A and B respectively. By carefully considering these figures it can be seen that at least four phase-locked solitons as well as a dispersive wave train eventually evolve, and that there appear to be several nonlinear interactions. The most prominent is indicated with an



Reproduced with permission of the copyright owner. Further reproduction prohibited without permission.

(3.1b)

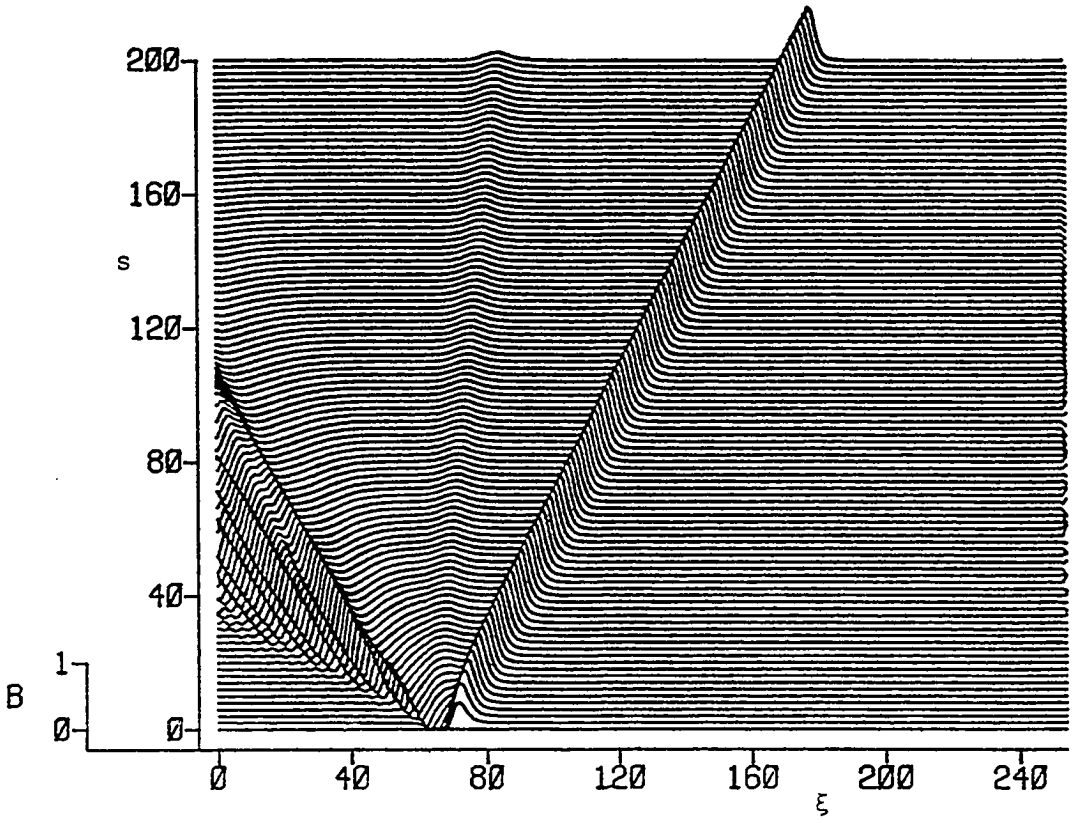


arrow. This interaction is perhaps better illustrated by the amplitude-time diagram Figure 3.2c and the position-time diagram Figure 3.2d. These figures show the amplitudes and positions of only the two largest phase-locked solitons. From these figures it can be seen that initially the second phase-locked soliton has larger amplitudes and moves faster than the soliton in the front position. As the solitons get closer together they begin to interact with each other. During this interaction energy passes from the second soliton to the first soliton. It can be seen that there are always two maxima and that the waves appear to exchange roles; that is the amplitudes of the second phase-locked soliton decrease and it slows down, while the amplitudes of the first soliton increase and it speeds up. After the interaction the solitons propagate apart with



Reproduced with permission of the copyright owner. Further reproduction prohibited without permission.

(3.1c)

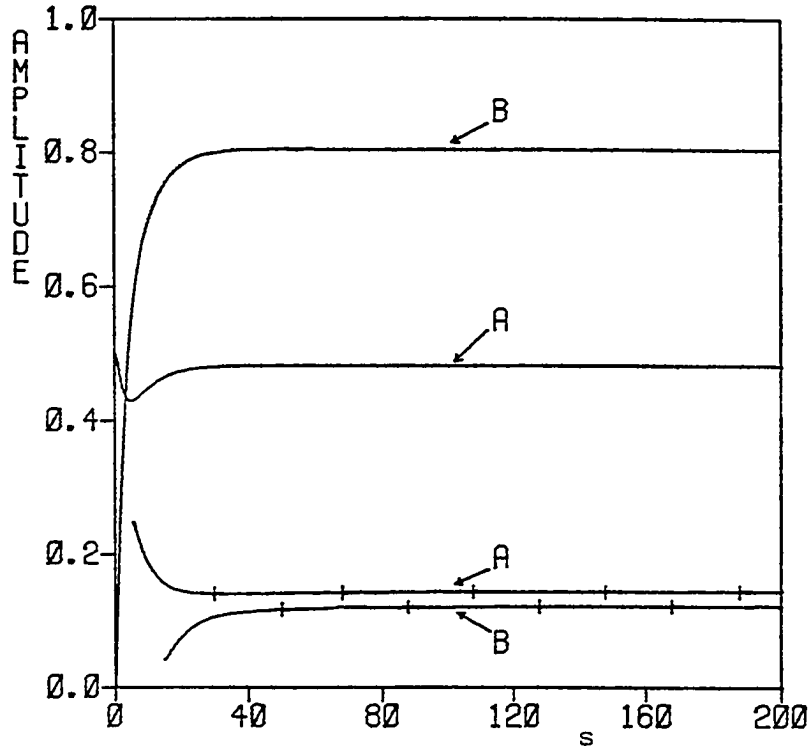


(3.1d)

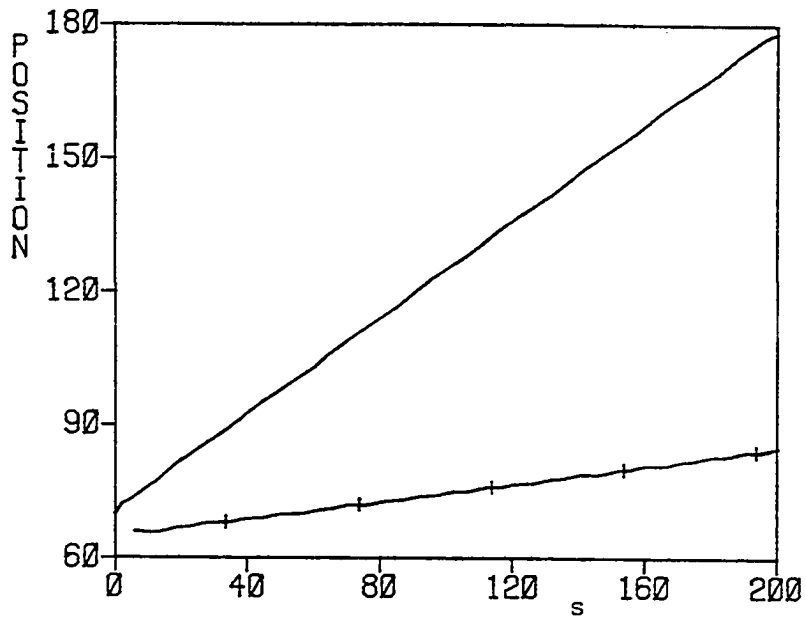




Reproduced with permission of the copyright owner. Further reproduction prohibited without permission.

(3.1e)

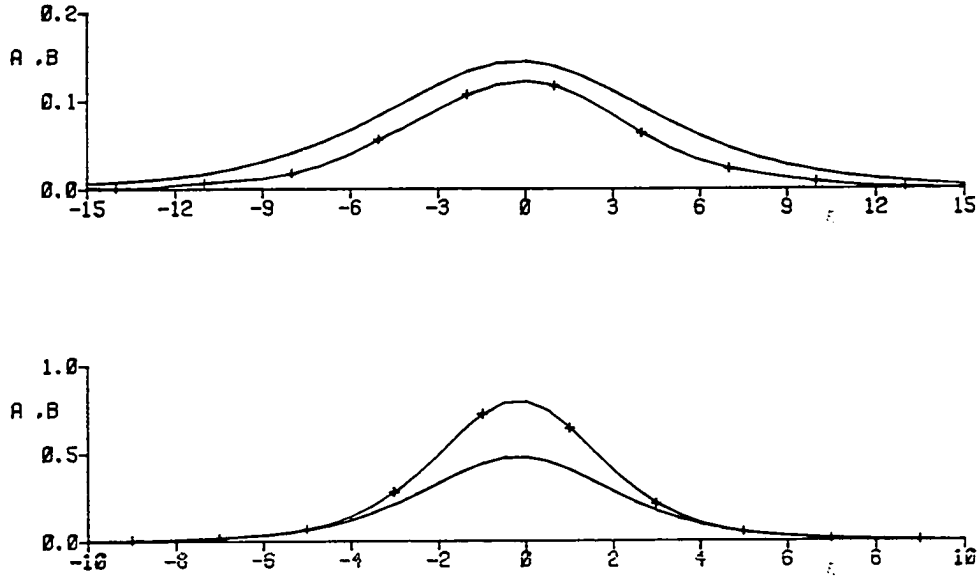


constant speeds and amplitudes. This interaction closely resembles a soliton interaction for the Korteweg-de Vries equation, hence it seems justifiable to call these waves solitons. Note that the amplitudes of the second phase-locked soliton are slightly deviated as it passes through the tail generated by the first soliton, this occurs at about s = 30 to 40 (see Figure 3.2c).

The numerical results of Figures 3.1 and 3.2 contrast strongly with the results of Liu et al (1980,1982) and the corresponding experimental results of Weidman and Johnson (1982). They did not find phase-locked travelling wave solutions such as those shown in Figures 3.1 and 3.2. Instead they demonstrated the existence of time periodic solitary waves which alternate their relative phase relationship as a result of the oscillation of wave amplitudes: the solitary waves leap-frog over each other as they propagate and continually exchange energy in a quasi-periodic manner. In the coupled equations derived by Liu et al (1980), the coupling is solely due to linear dispersive terms of the type found in the intermediate depth equation (see Joseph (1977) or Kubota et al (1978)).



Reproduced with permission of the copyright owner. Further reproduction prohibited without permission.

(3.2a)

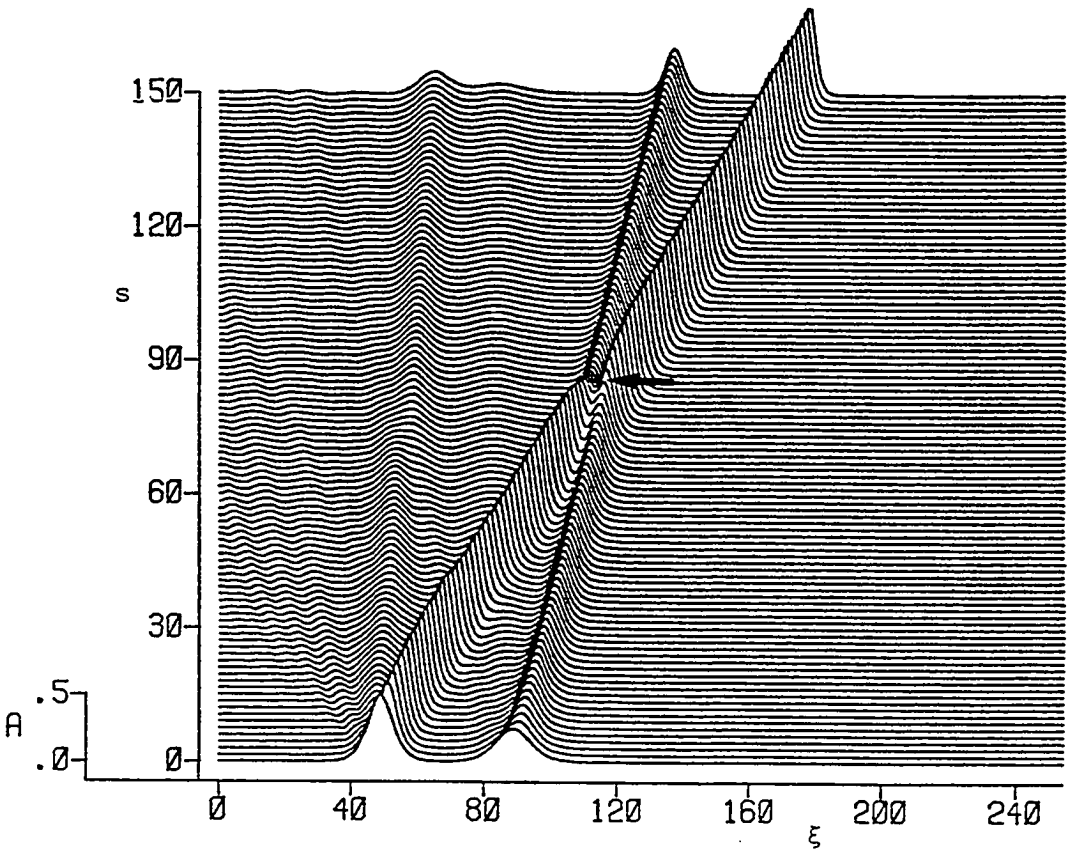


Figure 3.2: A plot of the evolution of the waves for the initial conditions and parameters displayed in Table 3.1. (a) evolution of A; (b) evolution of B; a soliton interaction is marked with an arrow; (c) amplitude as a function of time; (d) position of the wave crests as a function of time; ———, first soliton; —*—, second soliton.

The analogue of their coupled equations for the present system is obtained by setting $a_1 = a_2 = 0$ in (3.4.2a,b). The result of numerical integration for this case is shown in Figure 3.3. Figures 3.3a and b show the time evolution of A and B respectively, when the initial state is a solitary wave profile for A and zero for B. The details of the numerical experiment are set out in Table 3.2. Note, in an attempt to force leap-frogging type



Reproduced with permission of the copyright owner. Further reproduction prohibited without permission.

(3.2b)

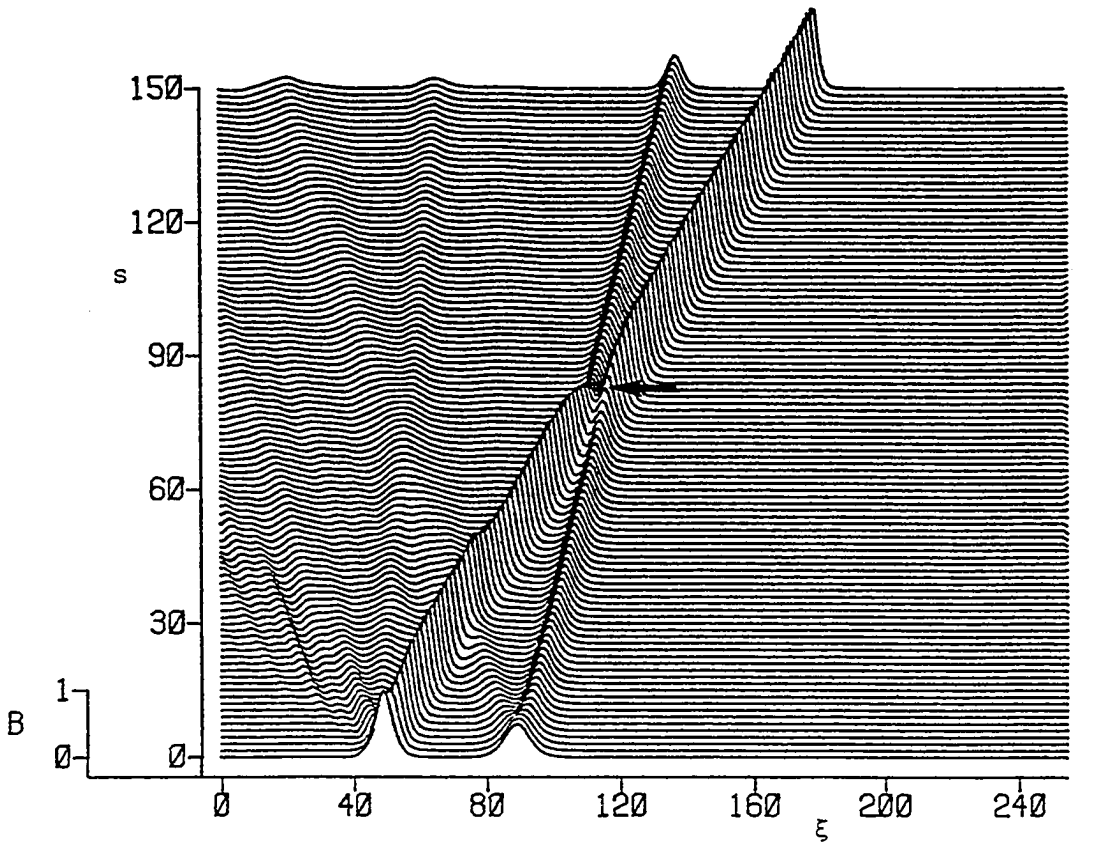


solutions the coefficients $b_1$ and r are chosen in such a way, that if (3.4.2a and b) were uncoupled a solitary wave propagating in the B frame would have twice the speed of a solitary wave of the same amplitude in A. Figure 3.3c is an amplitude-time diagram for the wave amplitudes and Figure 3.3d is a position-time diagram for the wave crests. The dotted line drawn through Figure 3.3d is a least squares straight line fit of the plotted points of the wave crests. This dotted line approximates the trajectory traced out by the systems center of mass. The spatial phase of each wave crest relative to this center of mass is plotted versus time in Figure 3.3e. From these figures it can be seen that initially the wave amplitude of the A waveform decreases rapidly due to the energy transfer to B. As the first B waveform gains amplitude it speeds up until it overtakes the



Reproduced with permission of the copyright owner. Further reproduction prohibited without permission.

(3.2c)

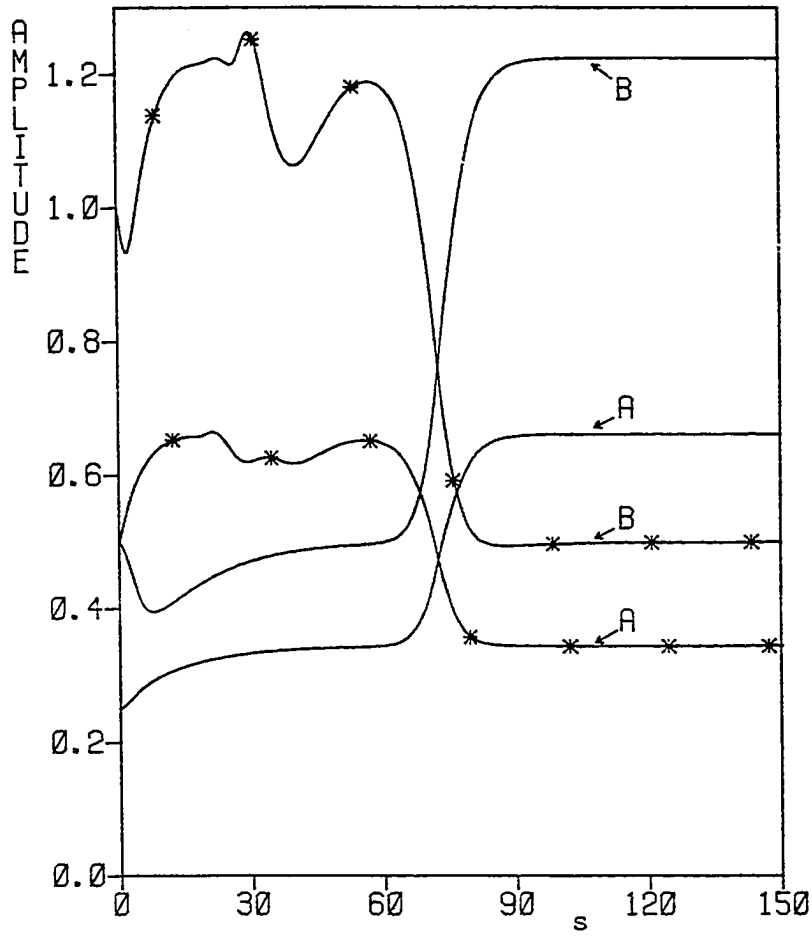


first A wave. Simultaneously a trailing wave in A speeds up and amplifies rapidly due to energy transfer back from B. The system is seen to evolve to a quasi-periodic state with A and B continually exchanging energy, complete periodicity is not attained as some trailing radiation is continually being formed. Notice that in both A and B the trailing waves never catch up with the leading waves before they vanish. Note also that in Figure 3.3c the points indicated with a "1", show deviations in the amplitudes of A and B crests, due to radiation entering the computational domain from the adjacent domain.

As a further investigation of the properties of equation (3.4.2a,b) Figures 3.4a and b show the time evolution of A and B, when



Reproduced with permission of the copyright owner. Further reproduction prohibited without permission.

(3.2d)

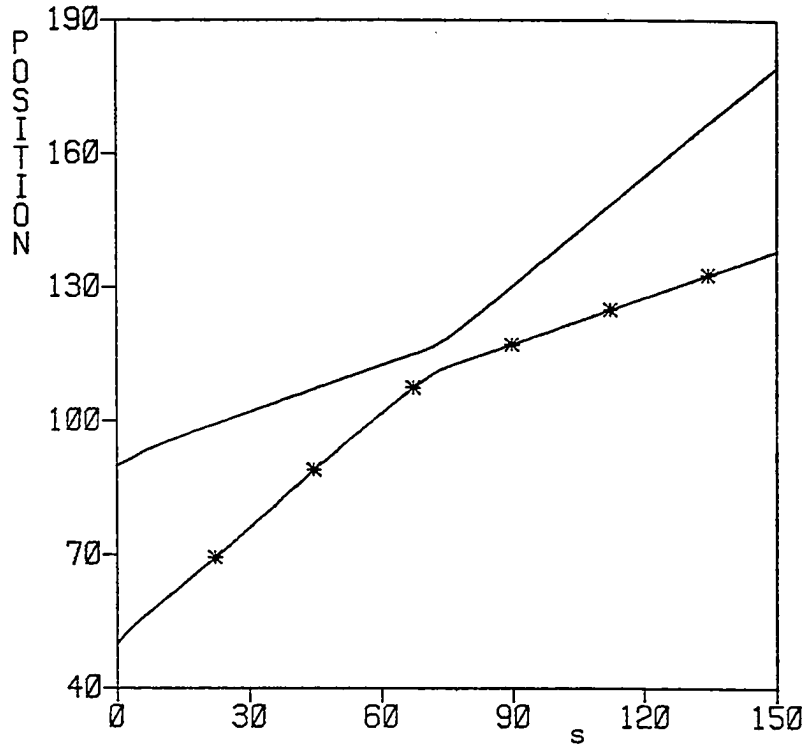


these equation possess only nonlinear coupling. That is $a_3 = 0$, see Table 3.2 for details of the numerical integration. As in the previous case, the initial conditions are a solitary wave profile for A and zero for B. Figure 3.4c is an amplitude-time diagram for the wave amplitudes and Figure 3.4d is a position-time diagram for the wave crests. The numbers "1" to "6" in Figures 3.4c and d indicate the data for the amplitudes and positions of the six main nonlinear waves in B, while the data for A is labelled with a plus sign. Figure 3.4e represents the spatial phase of the A waveform relative to the dotted line shown in Figure 3.4d, this dotted line is a least squares straight line fit of the plotted points for the position of the A wave crest. The system is again seen to evolve to a quasi-periodic state, with A and B continually exchanging energy. As the A waveform loses energy to B its amplitude decreases, its width increases and it slow down energy then passes back from B into the A waveform, and its



Reproduced with permission of the copyright owner. Further reproduction prohibited without permission.

| FIGURE | 3.3 | 3.4 | 3.5 |
|---|---|---|---|
| $a_1$ | 0.0 | 0.25 | 0.25 |
| $a_2$ | 0.0 | 0.25 | 0.25 |
| $a_3$ | 0.5 | 0.0 | 0.5 |
| $b_1$ | 2.0 | 2.0 | 2.0 |
| $b_2$ | 2.0 | 2.0 | 2.0 |
| r | -0.5 | -0.5 | -0.5 |
| MESH POINTS | 128 | 256 | 256 |
| $\Delta\xi$ | 1.0 | 1.0 | 1.0 |
| $\Delta s$ | 0.01 | 0.01 | 0.01 |
| TIME STEPS | 42,000 | 45,000 | 45,000 |
| A(s=0) | $\frac{1}{2}S^2(\frac{\sqrt{6}}{12}(\xi-30))$ | $\frac{1}{2}S^2(\frac{\sqrt{6}}{12}(\xi-40))$ | $\frac{1}{2}S^2(\frac{\sqrt{6}}{12}(\xi-40))$ |
| B(s=0) | 0.0 | 0.0 | 0.0 |

Table 3.2: Details of the coefficients, technical data and initial conditions for Figures 3.3, 3.4 and 3.5. Here $S^2(\xi)$ denotes $\mathrm{sech}^2(\xi)$.

amplitude increases, its width decreases and it speeds up. During this process several nonlinear waves as well as a dispersive tail can be seen to evolve in B. Initially two nonlinear waves develop in B one in front of the A wave crest and one behind. These waves are labelled with a "1" and a "2" in Figures 3.4c and d. The two B waves propagate with the A wave crest until it starts to slow down then the front B wave propagates away while its amplitude gradually decreases. The A waveform then speeds up and as it reaches a maximum in its amplitude, two waves are seen to develop from the original trailing wave (in B). One of these waves propagates in front of



Reproduced with permission of the copyright owner. Further reproduction prohibited without permission.

(3.3a)

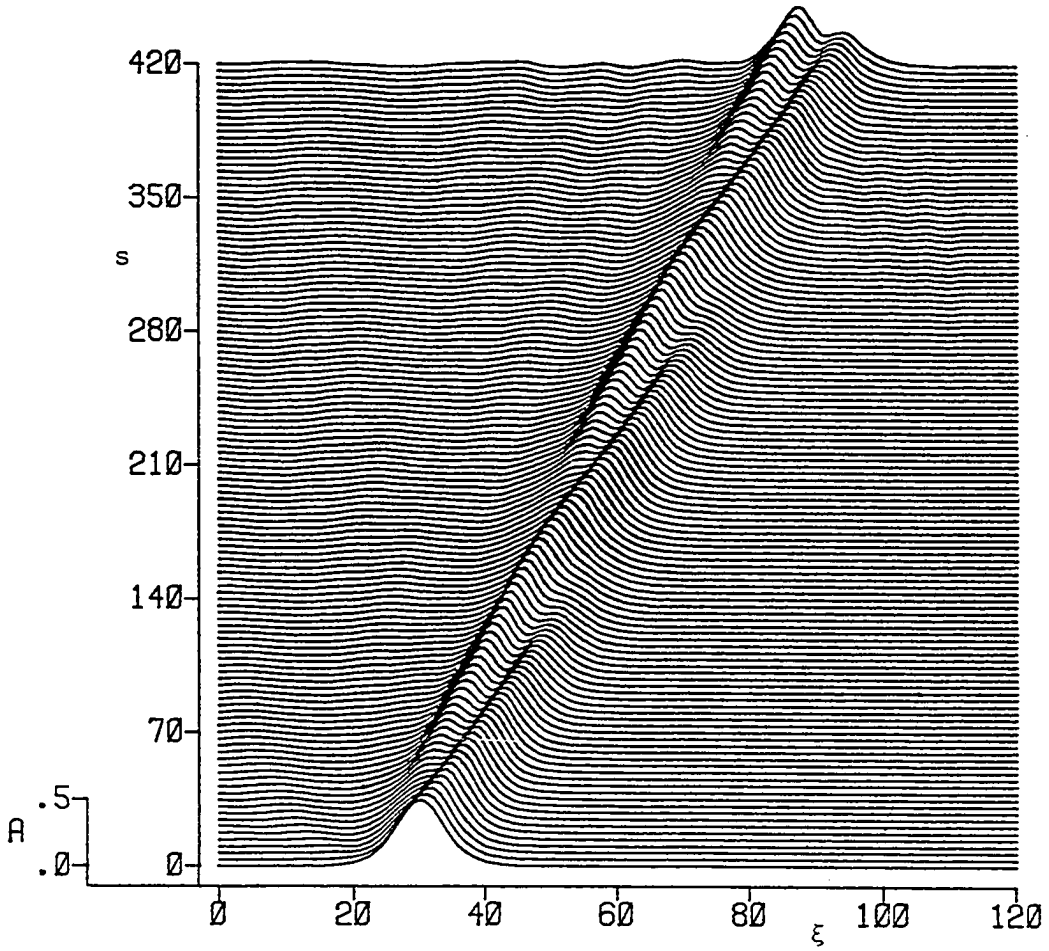


Figure 3.3: A plot of the evolution of the waves for the initial conditions and parameters displayed in Table 3.2. (a) evolution of A; (b) evolution of B; (c) amplitudes as a function of time; (d) position of the wave crests as a function of time; (e) phase of the wave crests relative to the dotted line in Figure 3.3d; ——— A; —+—+—, B.



Reproduced with permission of the copyright owner. Further reproduction prohibited without permission.

(3.3b)

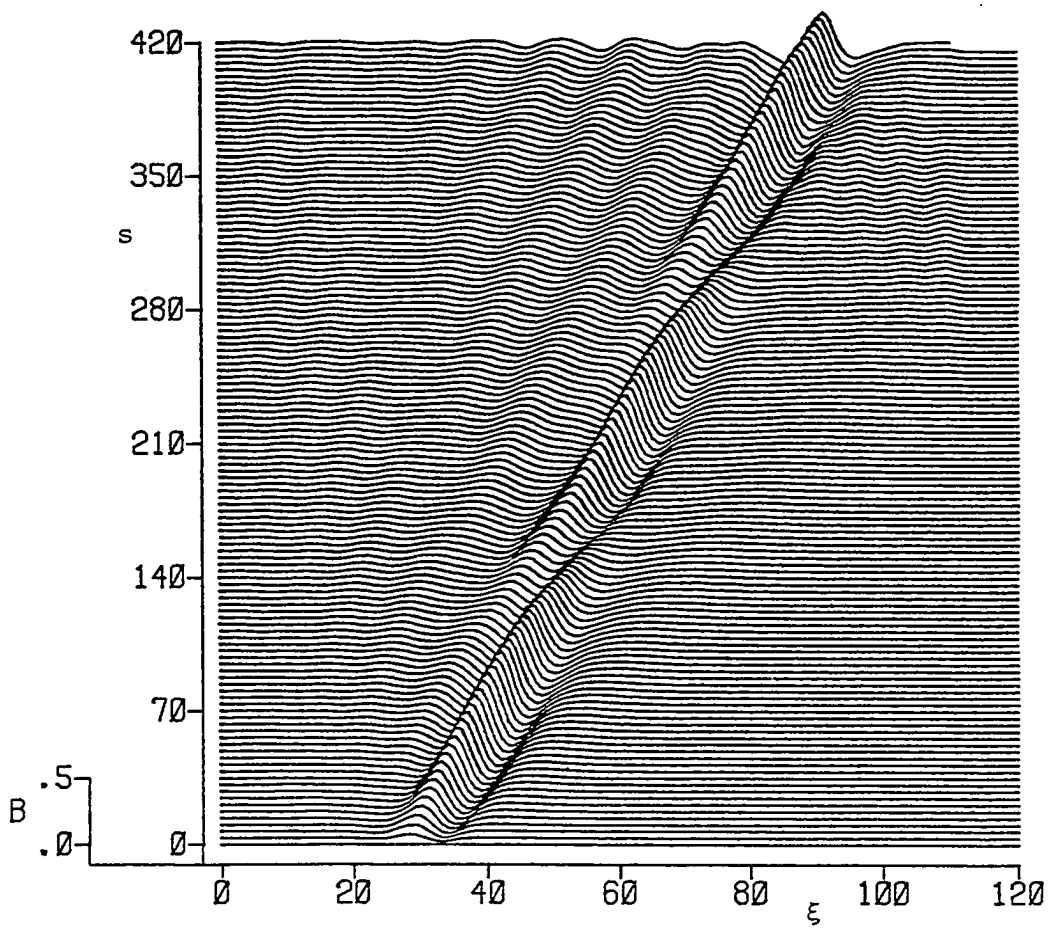


the A wave crest while the other propagates behind. Again the process is repeated, as the A wave slows down the B wave just in front of the position of the A wave crest propagates away and two waves are then seen to develop out of the trailing nonlinear B wave. Note, that the system is not completely periodic as some trailing radiation is continually being formed.

The final numerical integration is a combination of the previous two cases, that is $a_3 = 1/2$ as in Figure 3.1 and $a_1 = a_2 = 1/4$ as in Figure 3.2. The initial conditions are a solitary wave profile for A and zero for B, see Table 3.2 for details of coefficients and the initial conditions. Figures 3.5a and b show the time evolution of A and B,



Reproduced with permission of the copyright owner. Further reproduction prohibited without permission.

(3.3c)

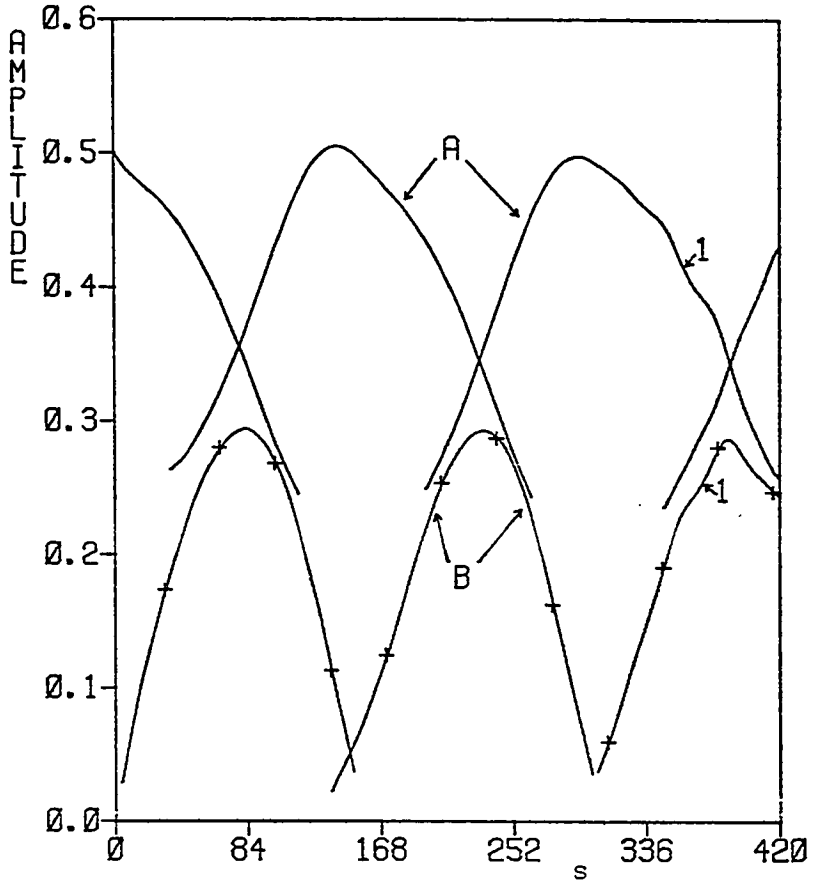


respectively. Figure 3.5c is an amplitude-time diagram for the wave amplitudes and Figure 3.5d is a position-time diagram for the wave crests. The numbers "1" to "4" in Figures 3.5c and d indicate the data for the amplitudes and positions of the main nonlinear waves in B, while the data for A is labelled with a plus sign. Figure 3.5e represents the spatial phase of the A waveform crest relative to a least squares straight line fit of the position of the crest. The system is again seen to evolve to a quasi-periodic state with A and B continually exchanging energy. Initially the amplitude of the A waveform decreases as energy flows from A to B. Two nonlinear waves as well as a dispersive tail are seen to develop in B, one of these nonlinear waves propagates in front of the position of the A wave



Reproduced with permission of the copyright owner. Further reproduction prohibited without permission.

(3.3d)

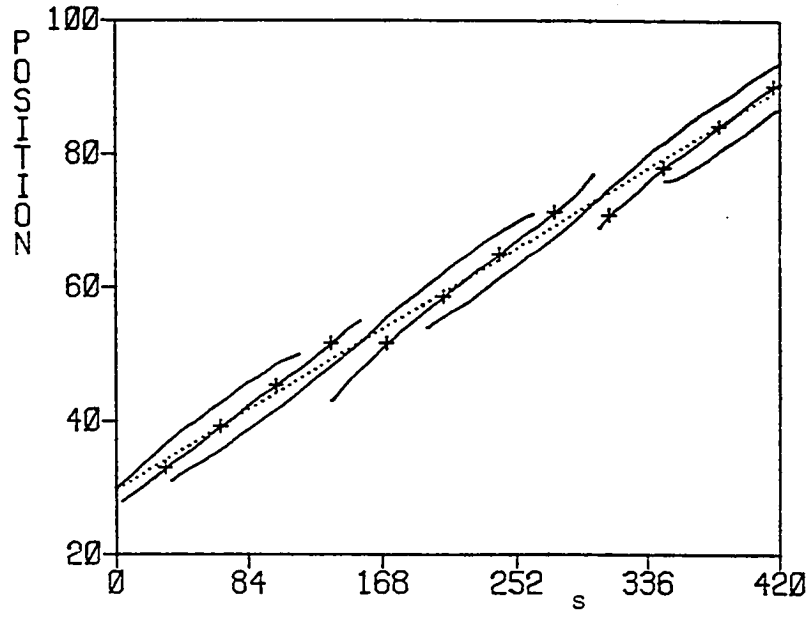


(3.3e)

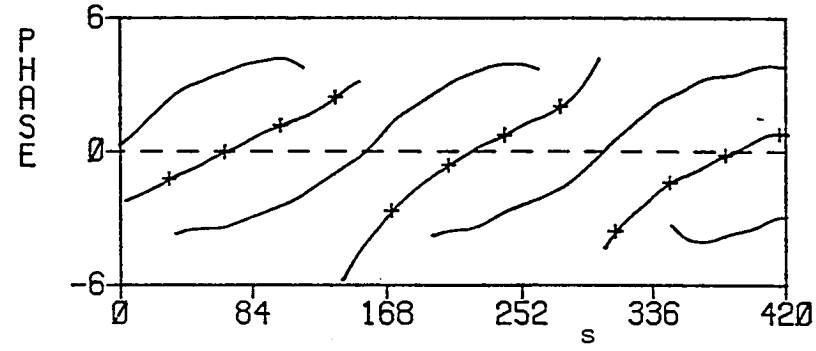


crest while the other propagates behind. These waves are labelled with a "1" and a "2" in Figures 3.5c and d. As in the previous case, as the A waveform loses energy it slows down, and the front B wave propagates away. As the A wave amplitude then increases two nonlinear waves develop out of the original trailing nonlinear wave in B. The system is not completely periodic as radiation is continually being formed, note in the B frame the radiation is of the same amplitude as the nonlinear waves.



Reproduced with permission of the copyright owner. Further reproduction prohibited without permission.

(3.4a)

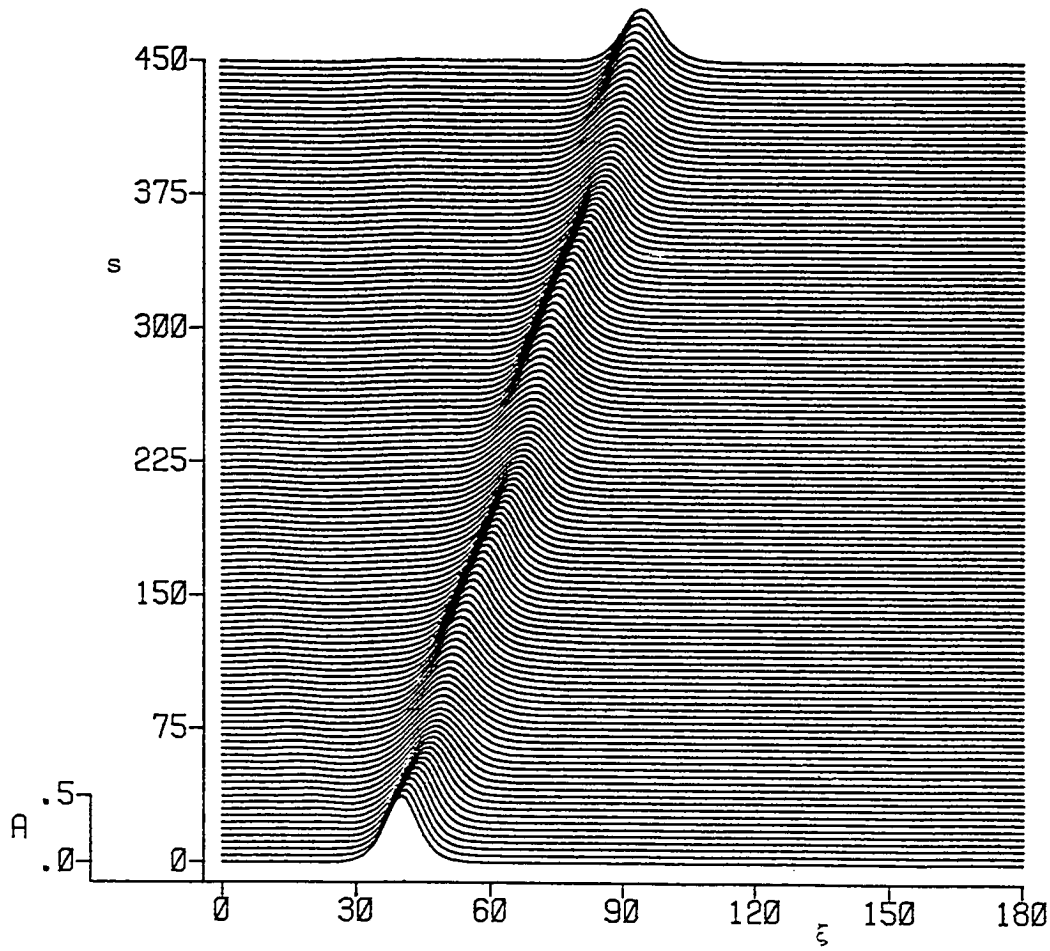


Figure 3.4: A plot of the evolution of the waves for the initial conditions and parameters displayed in Table 3.2. (a) evolution of A; (b) evolution of B; (c) amplitude as a function of time; (d) position of the wave crests as a function of time; —+—+—, A; ———, B; (e) phase of the A-wave relative to the dotted line in Figure 3.4d.



Reproduced with permission of the copyright owner. Further reproduction prohibited without permission.

(3.4b)

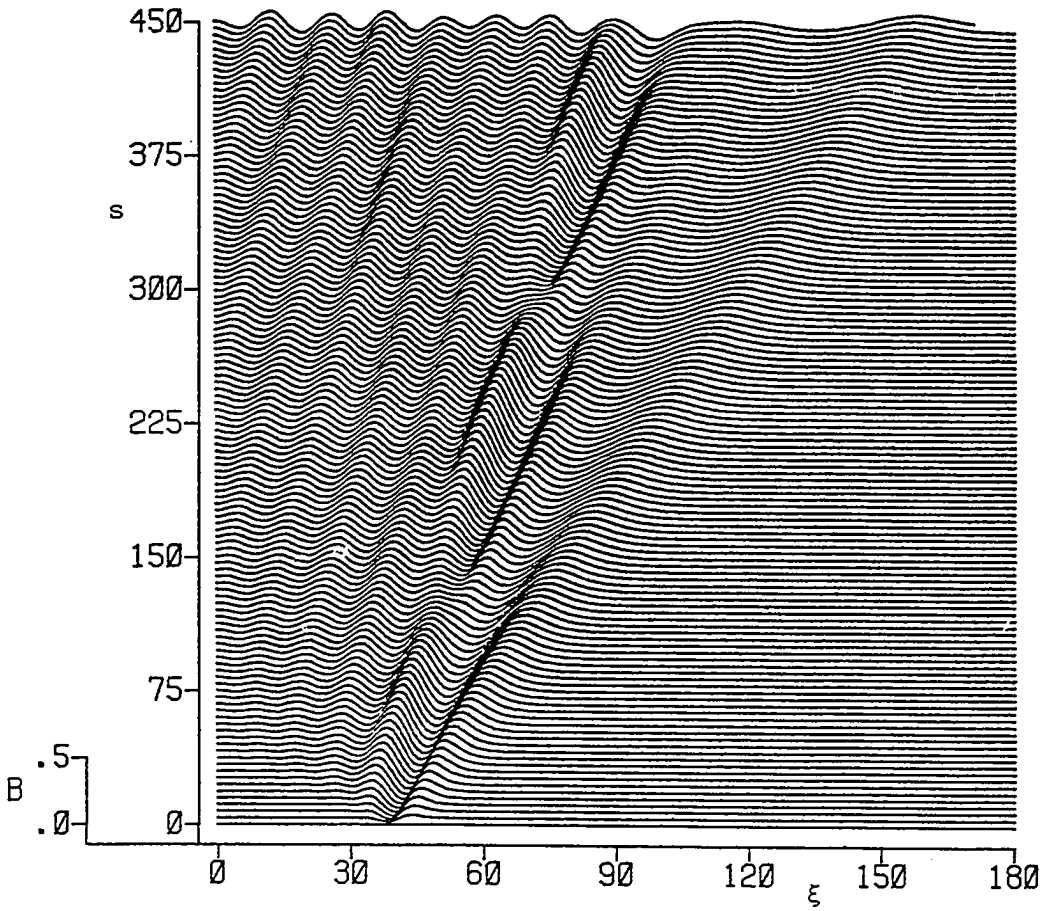




Reproduced with permission of the copyright owner. Further reproduction prohibited without permission.

(3.4c)

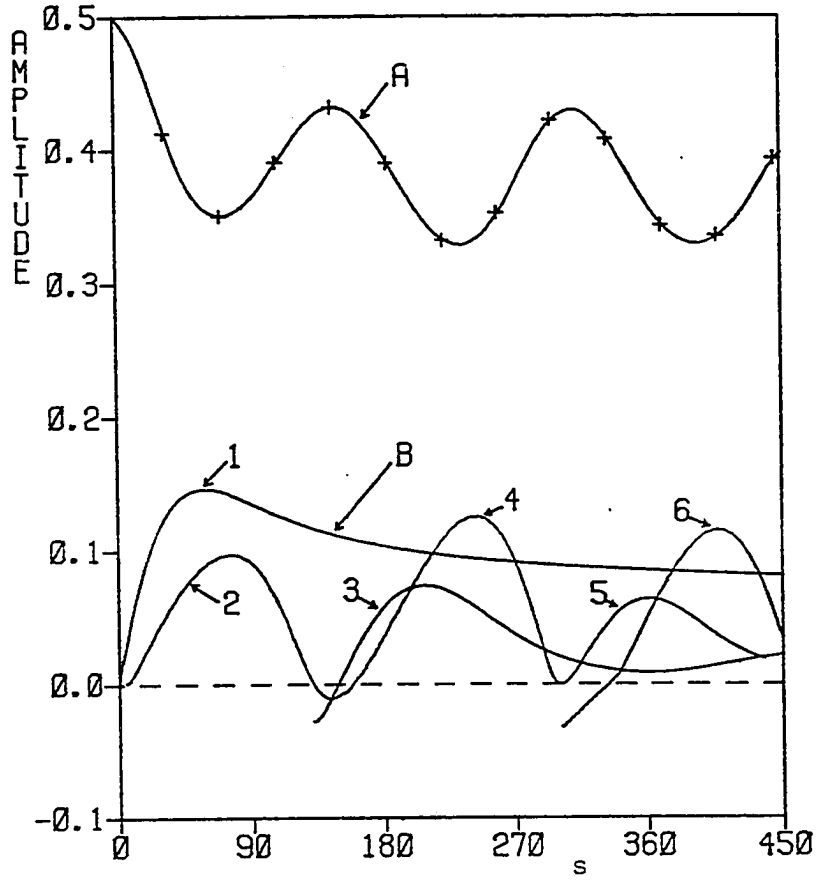




Reproduced with permission of the copyright owner. Further reproduction prohibited without permission.

(3.4d)

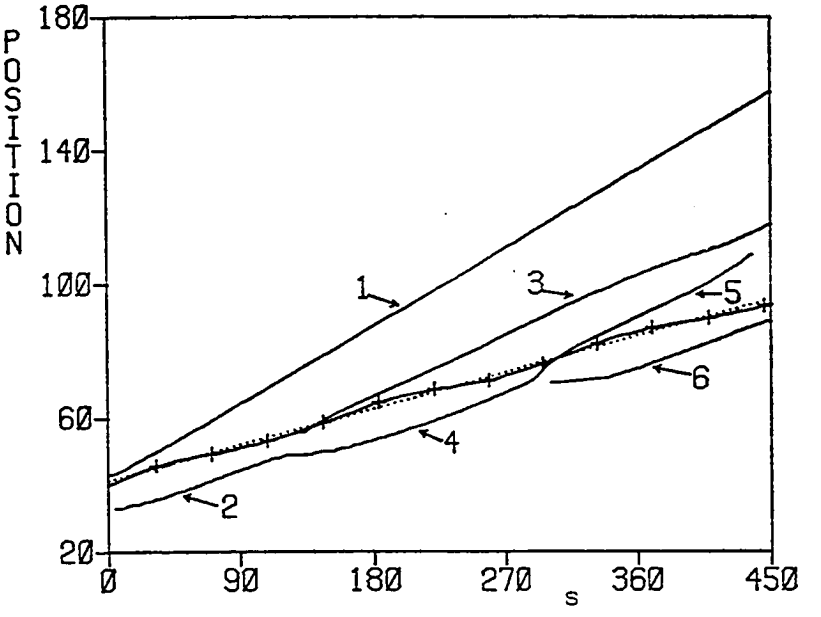


(3.4e)

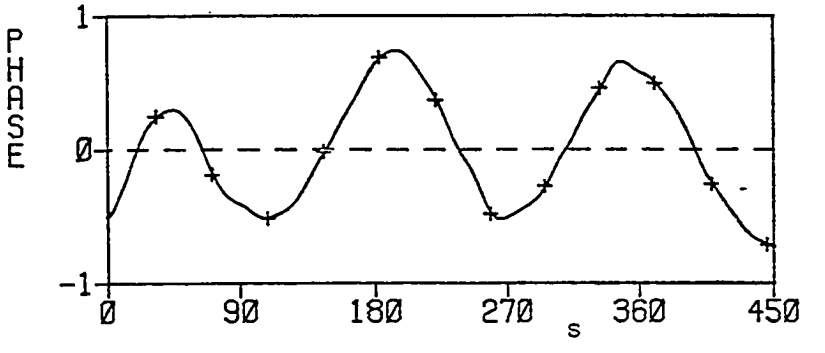




Reproduced with permission of the copyright owner. Further reproduction prohibited without permission.

(3.5a)

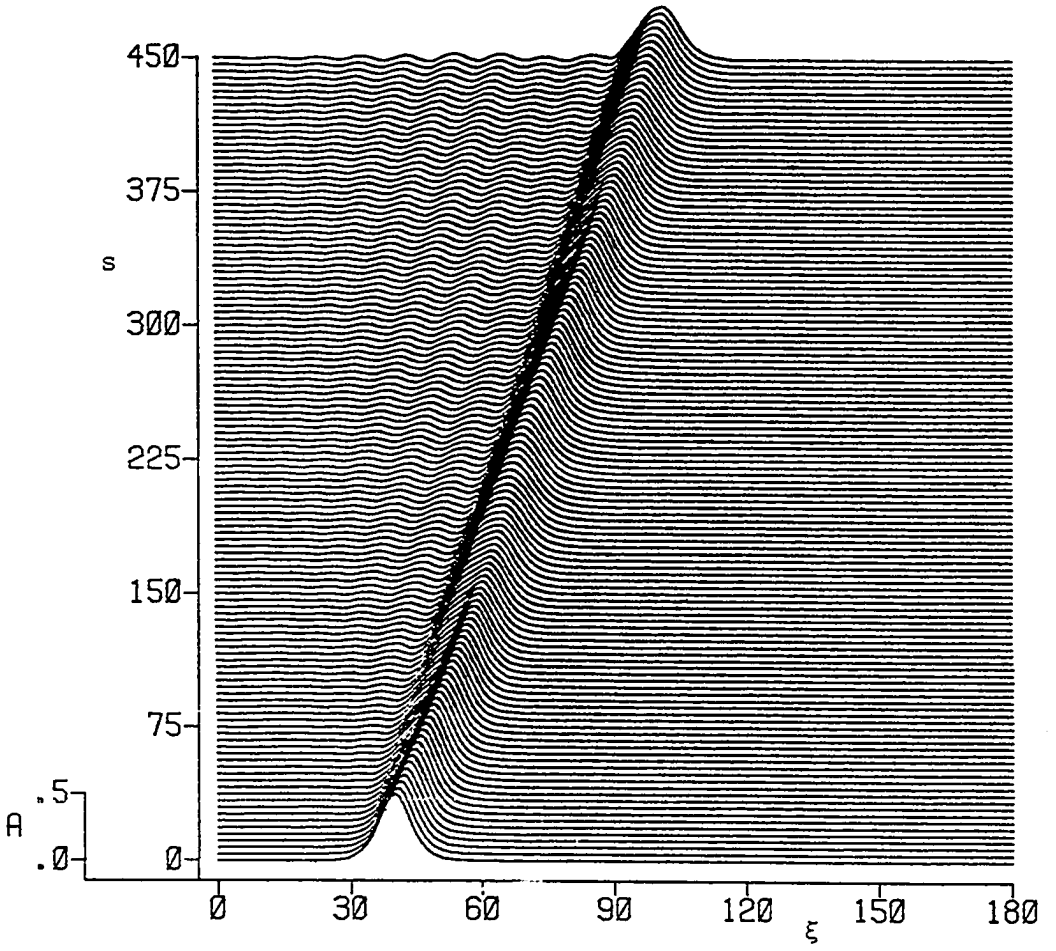


Figure 3.5: A plot of the evolution of the waves for the initial conditions and parameters displayed in Table 3.2. (a) evolution of A; (b) evolution of B; (c) amplitudes as a function of time; (d) position of the wave crests as a function of time; —+—+—, A; ———, B; (e) phase of the a-wave as a function of time.



Reproduced with permission of the copyright owner. Further reproduction prohibited without permission.

(3.5b)

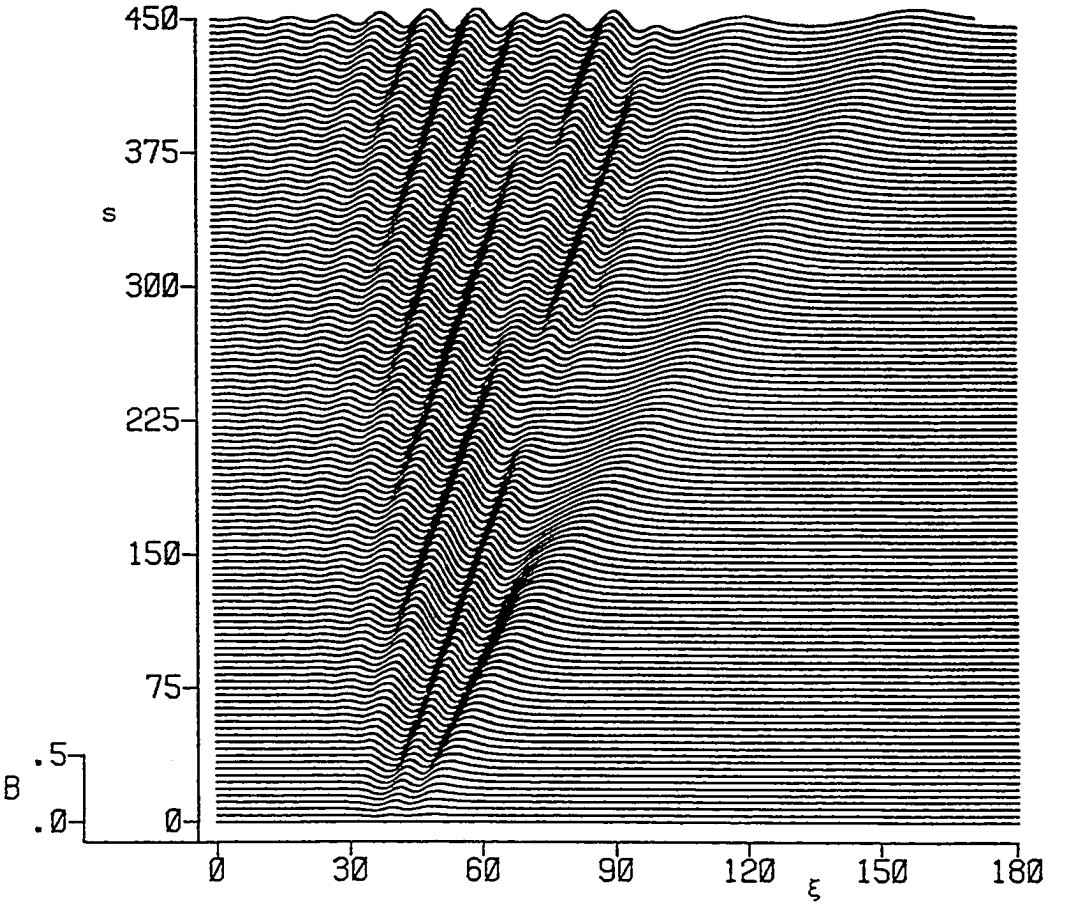




Reproduced with permission of the copyright owner. Further reproduction prohibited without permission.

(3.5c)

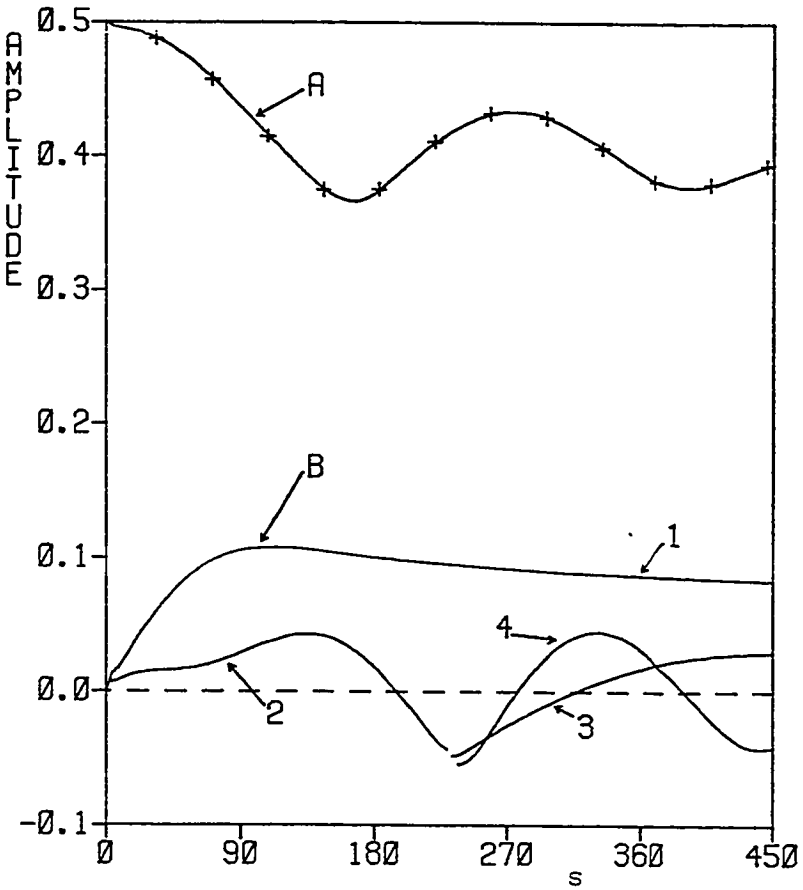




Reproduced with permission of the copyright owner. Further reproduction prohibited without permission.

(3.5d)

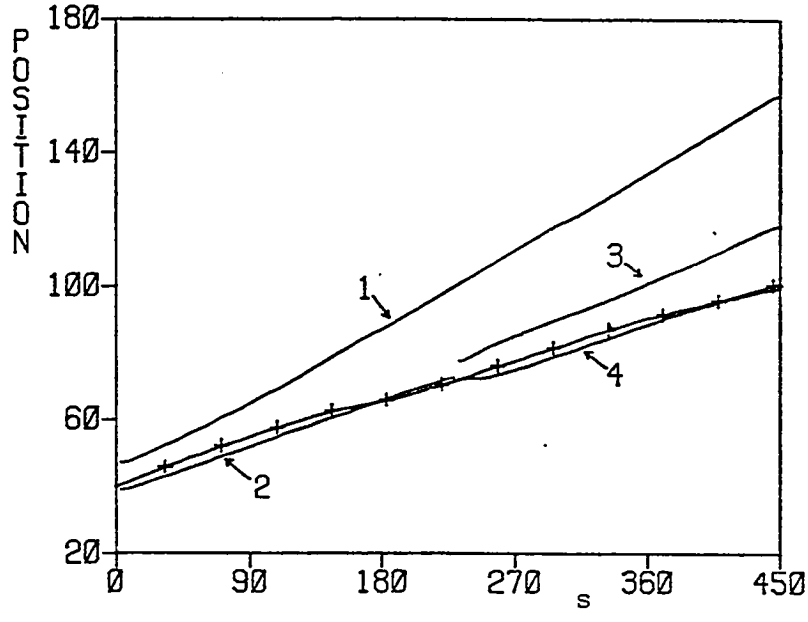


(3.5e)

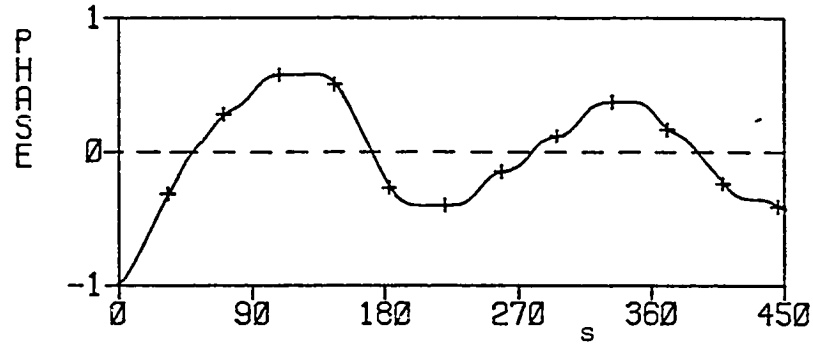




Reproduced with permission of the copyright owner. Further reproduction prohibited without permission.

## APPENDIX A: NUMERICAL METHOD OF CHAPTER THREE.

To investigate the time evolution and energy transfer between two solitary like waves it has been necessary to employ the use of a numerical method. An efficient numerical technique for solving nonlinear wave equations, of the Korteweg-de Vries type, has been developed by Fornberg and Whitham (1978). Their method uses a pseudo-spectral (Fourier transform) treatment of the space dependence together with a leap-frog differencing scheme in the time variable.

The method of Fornberg and Whitham (1978) assumes that the functions $A(s,\xi)$, $B(s,\xi)$ are periodic in $\xi$ outside a basic interval $0 \leq \xi \leq L$. This interval is then discretized by N equidistant points, with spacing $\Delta\xi = L/N$. The functions $A(s,\xi)$, $B(s,\xi)$ numerically defined only on these points can then be transformed to discrete Fourier space (with respect to $\xi$) by use of fast Fourier transform algorithms. If FA represents the discrete Fourier transform of A and $\alpha$ is the transformed variable, $A_\xi$ could then the evaluated as $-iF^{-1}(\alpha FA)$, $A_{\xi\xi\xi}$ as $iF^{-1}(\alpha^3 FA)$ and so on. Following Fornberg and Whitham, it is useful to make a minor modification to the third order derivatives by evaluating them as $iF^{-1}[\sin(\alpha^3\Delta s)FA]/\Delta s$, where $\Delta s$ is the time step chosen in order to maintain numerical stability (see Fornberg and Whitham (1978)). Since $\sin(\alpha^3\Delta s) = \alpha^3\Delta s + O((\Delta s)^3)$ the two methods are identical in the limit $\Delta s$ decreasing to zero, but the new method eliminates the problem of differencing errors at high wavenumbers. Combined with a leap-frog time step the evolution equations (3.5.2a and b) are then approximated by

$$A(s + \Delta s,\xi) - A(s - \Delta s,\xi)$$

$$- 2i\Delta s[AF^{-1}(\alpha FA) + a_1 BF^{-1}(\alpha FB) + a_2\{AF^{-1}(\alpha FB) + BF^{-1}(\alpha FA)\}]$$

$$+ 2iF^{-1}[\sin(\alpha^3\Delta s)(FA + a_3 FB)] = 0 , \qquad (A.1a)$$



Reproduced with permission of the copyright owner. Further reproduction prohibited without permission.

$$b_1[B(s + \Delta s,\xi) - B(s - \Delta s,\xi)] + 2i\Delta s r F^{-1}(\alpha FB)$$

$$- 2i\Delta s[BF^{-1}(\alpha FB) + a_2 b_2 AF^{-1}(\alpha FA) + a_1 b_2\{AF^{-1}(\alpha FB) + BF^{-1}(\alpha FA)\}]$$

$$+ 2iF^{-1}[\sin(\alpha^3\Delta s)(FB + a_3 b_2 FA)] = 0 , \qquad (A.1b)$$

If A and B are given functions of $\xi$ at s = 0, then by using equation (A.1a and b), $A(s,\xi)$ and $B(s,\xi)$ can be evaluated at any later time level.

A feature of leap-frog time differencing is the possibility of separation of the solution between successive time levels. If this should occur there is no way for the leap-frog scheme to detect if every second time level has a constant value added to it. To overcome this problem it has been suggested by Fornberg and Whitham (1978) that after calculating the solution to the time levels $s - \Delta s$, s and $s + \Delta s$, to then introduce the levels $s - \frac{1}{2}\Delta s$ and $s + \frac{1}{2}\Delta s$ as averages of the adjacent levels, and to restart the integration from these new levels. In the numerical experiments presented in chapter 3 this process was repeated every forty time steps, with the result that no separation between time levels was observed in any numerical integration.

In any numerical technique using discrete Fourier transforms, the functions being transformed are assumed to be periodic. Then if waves leave the computational domain through one boundary, they will re-enter through the opposite boundary. To filter out any radiation entering the computational domain from the adjacent domain the Von Hann window (or Hanning function) (see Blackman and Tukey (1958)) was employed at the right-hand computational boundary. Note that the computational reference frame moves to the right at a speed equal to the linear wave speed $c_n$, so radiation with phase speed less than $c_n$ will leave the computational domain through the left-hand boundary. Note also that because two phase speeds exist namely $c_n$ and $c_m$, if $c_m > c_n$ then there is the possibility that



Reproduced with permission of the copyright owner. Further reproduction prohibited without permission.

radiation can move to the right (see Figures 3.3a,b, 3.4a,b, 3.5a,b). The Von Hann window can be described by the function

$$W(\xi) = \begin{cases} 1 , & \text{for } 0 \leq \xi \leq L - m - 2\beta , \\ \cos\{\pi(\xi - L + m + 2\beta)/2\beta\} , & \text{for } L - m - 2\beta \leq \xi \leq L - \beta - m , \\ 0 , & \text{for } L - m - \beta \leq \xi \leq L - \beta , \\ \cos\{\pi(L - \xi)/2\beta\} , & \text{for } L - \beta \leq \xi \leq L . \end{cases} \tag{A.2}$$

The values chosen for $\beta$ and $m$ are dependent upon the size of the computational domain. At each time level in the numerical experiments presented in chapter 3, the functions $A(s,\xi)$ and $B(s,\xi)$ were multiplied by $W(\xi)$.

It has been shown by Fornberg and Whitham (1978) that the stability criterion for the proposed numerical technique is of the form $\Delta s/\Delta\xi^2 <$ constant. For the Korteweg-de Vries equation this constant is $3/2\pi^2$. When a stability analysis is done for the present system the stability condition becomes

$$\frac{\Delta s}{\Delta \xi^3} < \text{MIN}\left\{ \frac{1}{2\pi^2(1 + a_3)} , \frac{1}{2\pi^2(1 + a_3 b_3)} \right\} . \tag{A.3}$$

In the numerical experiments presented in chapter 3 the quantity $\Delta s/\Delta\xi^3$ was kept at or below 0.01.

The details of the technical data for each numerical experiment presented in chapter 3 are given in Tables 3.1 and 3.2. Note



Reproduced with permission of the copyright owner. Further reproduction prohibited without permission.

that the numerical calculations presented here were carried out in single precision on a DEC VAX 11/782 at the University of Melbourne.



Reproduced with permission of the copyright owner. Further reproduction prohibited without permission.

## APPENDIX B: THREE LAYER FLUID

Consider the case of two neighboring pycnoclines of constant Brunt-Väisälä frequency $N_1^2$ and $N_2^2$, separated by a region of constant density. For simplicity it is assumed that the fluid is bounded above by a rigid lid, the velocity $u_0(z)$ is identically zero everywhere and that each pycnocline has the same depth equal to one third of the total depth (Figure B.1). The Boussinesq approximation ($\sigma \to 0$), shall be taken so that $\rho_0$ in (3.1.1a) and similar subsequent equations is regarded as a constant. It then follows readily from (3.1.1a,b and c) that

$$\phi_s(z) = \begin{cases} \sin\{3\gamma_s(z + h)/h\} , & \text{for } -h \leq z \leq -2h/3 , \\ \gamma_s h^{-1}(3z + 2h)\cos\gamma_s + \sin\gamma_s , & \text{for } -2h/3 \leq z \leq -h/3 , \\ \cos\gamma_s \sin(3\alpha\gamma_s z/h)/(\alpha\cos(\alpha\gamma_s)) , & \text{for } -h/3 \leq z \leq 0 , \end{cases} \quad \text{(B.1a)}$$

where
$$c_s = N_1 h/3\gamma_s , \quad \text{(B.1b)}$$

$$\alpha = N_2/N_1 \quad \text{(B.1c)}$$

and
$$\frac{1}{\alpha}\tan(\alpha\gamma_s) + \tan\gamma_s + \gamma_s = 0 , \quad s = 1,2,--- . \quad \text{(B.1d)}$$

The speeds $c_s$ are determined by (B.1d). For each mode number s there are two solutions for $c_s$ representing waves travelling to the right and left respectively. The solution of (B.1d) for modes s = 1,---,5 are shown in Figure B.2 as a function of $\alpha$. There are a number of near -resonances, one of which is marked by an asterisk. For $\alpha$ = 0.42 there is a strong interaction between modes n = 2 and m = 3 where the values of $c_n$ and $c_m$ are



Reproduced with permission of the copyright owner. Further reproduction prohibited without permission.

$$\frac{c_n}{N_1 h} = 0.0751747 \quad , \quad \frac{c_n}{N_1 h} = 0.0640023 \quad . \qquad \text{(B.2)}$$

This is the case for which the numerical results of Figures 3.1 and 3.2 were obtained. The values of $a_1$, $a_2$, $a_3$, $b_1$ and $b_2$ are found from (3.5.2c,d) using (B.1a), and are listed in Table 3.1.

Figure B.1: The three-layer profile of $N^2$ discussed in Appendix B.

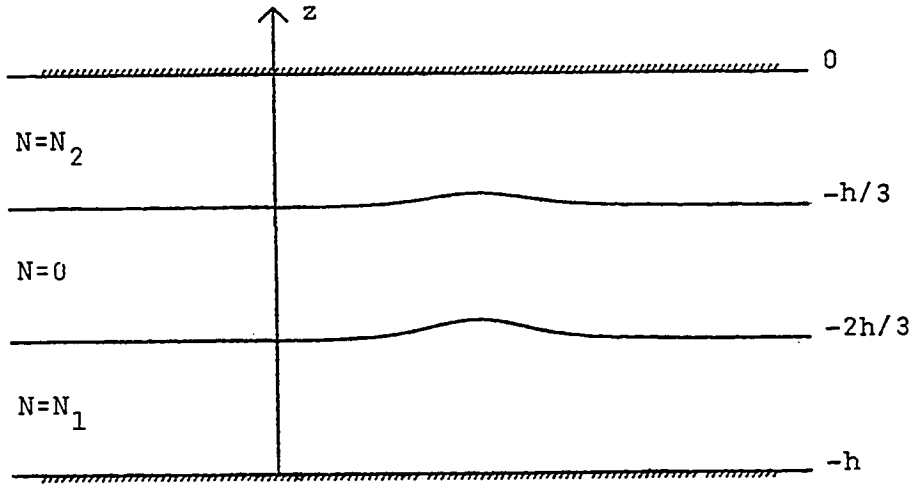




Reproduced with permission of the copyright owner. Further reproduction prohibited without permission.

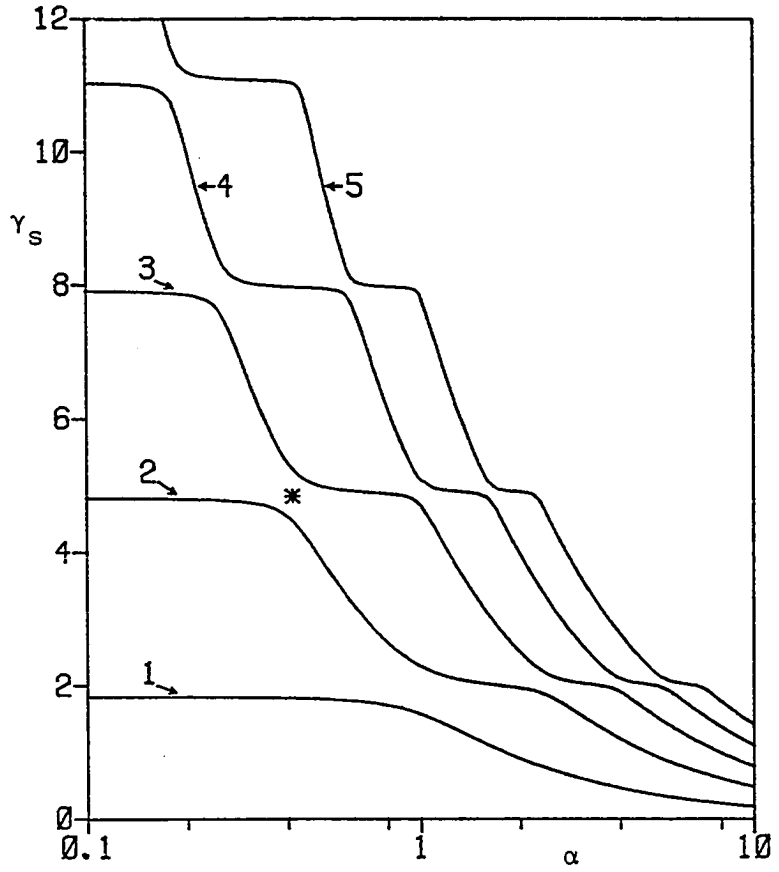


Figure B.2: A plot of $\gamma_s = N_1 h(3c_s)^{-1}$ against $\alpha = N_2 N_1^{-1}$ for the profile of Figure B.1, for modes s = 1,---,5. An example of a near-resonance between modes 2 and 3 is indicated by an asterisk.



Reproduced with permission of the copyright owner. Further reproduction prohibited without permission.

PLEASE NOTE:

Copyrighted materials in this document have not been filmed at the request of the author. They are available for consultation, however, in the author's university library.

These consist of pages:

148-163, Appendix C: A Second-order Theory For Solitary Waves In Shallow Fluids.

University Microfilms International
300 N Zeeb Rd., Ann Arbor, MI 48106 (313) 761-4700

Reproduced with permission of the copyright owner. Further reproduction prohibited without permission.

## BIBLIOGRAPHY


Ablowitz M.J., Kaup D.J., Newell A.C. and Segur H., 1973: "Nonlinear evolution equations of physical significance", Phys. Rev. Lett., 31, 125-127.

Ablowitz M.J., Kaup D.J., Newell A.C. and Segur H., 1974: "The inverse scattering transform-Fourier analysis for nonlinear problems", Stud. Appl. Math., 53, 249-315.

Ablowitz M.J., Ramani A. and Segur H., 1978: "Nonlinear evolution equations and ordinary differential equations of Painlevé type", Lett. Al Nuovo Cimento, 23, 333-338.

Ablowitz M.J., Ramani A. and Segur H., 1980a: "A connection between nonlinear evolution equations and ordinary differential equations of P-type. I", J. Math Phys., 21, 715-721.

Ablowitz M.J., Ramani A. and Segur H., 1980b: "A connection between nonlinear evolution equations and ordinary differential equations of P-type. II", J. Math. Phys., 21, 1006-1015.

Ablowitz M.J. and Segur H., 1981: "Solitons and the inverse scattering transform", SIAM, Philadelphia.

Abramowitz M. and Stegan I.A. 1965: "Handbook of mathematical functions", Dover, New York.

Akylas T.R. and Benney D.J. 1980: "Direct resonance in nonlinear wave systems", Studies in Applied Math., 63, 209-226.

Akylas T.R. and Benney D.J. 1982: "The evolution of waves near direct-resonance conditions", Studies in Applied Math., 67, 107-123.




Reproduced with permission of the copyright owner. Further reproduction prohibited without permission.

Banks W.H.H., Drazin P.G. and Zaturska M.B. 1976: "On the normal modes of parallel flow of inviscid stratified fluid", J. Fluid Mech., 75, 149-171.

Bell T.H. 1974: "Effects of shear on the properties of internal gravity wave modes", Duetsche Hydrographische Zeitschrift, 27, 57-62.

Benjamin T.B., 1966: "Internal waves of finite amplitude and permanent form", J. Fluid Mech., 25, 97-116.

Benjamin T.B., 1967: "Internal waves of permanent form in fluids of great depth", J. Fluid Mech. 29, 559-592.

Benney D.J., 1966: "Long nonlinear waves in fluid flows", J. Math. & Phys., 45, 52-63.

Benney D.J. and Ko D.R.S., 1978: "The propagation of long large amplitude internal waves", Studies in Applied Math., 59, 187-199.

Blackman R.B. and Tukey J.W., 1958: "The measurement of power spectra; from the point of view of communications engineering", Dover, New York.

Boussinesq J., 1871: "Theorie de l'intumescence liquid appelée onde solitaire ou de translation, se propagente dans un canal rectangulaire", Compte Rendus Acad. Sci. Paris, 72, 755-759.

Boussinesq J., 1872: "Theorie des ondes et de remous qui se propagent...", J.Math. Pures Appl., Ser. 2, 17, 55-108.

Davis R.E. and Acrivos A., 1967: "Solitary internal waves in deep water", J. Fluid Mech., 29, 593-607.

Drazin P.G., 1958: "The stability of a shear layer in an unbounded heterogeneous inviscid fluid", J. Fluid Mech., 4, 214-224.

Drazin P.G. and Howard L.N., 1966: "Hydrodynamic stability of parallel flow of inviscid fluid", Adv. Appl. Mech., 9, 54-89.

Eckart C., 1961: "Internal waves in the ocean", Phys. Fluids, 4, 791-799.



Reproduced with permission of the copyright owner. Further reproduction prohibited without permission.

Eliassen A., Hoilland E. and Riis E., 1953: "Two-dimensional perturbation of a flow with constant shear of a stratified fluid", Institute for Weather and Climate Research, Norwegian Academy of Sciences and Letters, Publ. no. 1.

Fenton J., 1972: "A ninth order solution for the solitary wave", J. Fluid Mech., 53, 257-271.

Fornberg R.B. and Whitham G.B., 1978: "A numerical and theoretical study of certain nonlinear wave phenomena", Phil. Trans. R. Soc. London Ser. A, 289, 373-404.

Gardner C.S., Greene J.M., Kruskal M.D. and Miura R.M., 1967: "Method for solving the Korteweg-de Vries equation", Phys. Rev. Lett., 19, 1095-1097.

Gardner C.S., Greene J.M., Kruskal M.D. and Miura R.M., 1974 "Korteweg-de Vries equation and generalizations. VI. Methods for exact solution", Comm. Pure Appl. Math., 27, 97-133.

Gear J.A. and Grimshaw R., 1984: "Weak and strong interactions between internal solitary waves", Studies in Applied Math. To appear.

Goldstein S., 1931: "On the stability of superposed streams of fluids of different densities", Proc. Roy. Soc. A, 132, 524-548.

Golubev V.V., 1953: "Lectures on integrals of equations of motion", State Publ. House, Moscow.

Grimshaw R., 1980/81: "Solitary waves in a compressible fluid", Pageoph., 119, 780-797.

Grimshaw R., 1981a: "A second order theory for solitary waves in deep fluids", Phys. Fluids, 24, 1611-1618.

Grimshaw R., 1981b: "Evolution equations for long, nonlinear internal waves in stratified shear flows", Studies in Applied Mathematics, 65, 159-188.



Reproduced with permission of the copyright owner. Further reproduction prohibited without permission.

Holmboe J., 1957: "Investigation of mountain lee waves and the air flow over the Sierra Nevada", Chap. 12, University of California, Los Angeles.

Howard L.N. 1961: "Note on a paper of John W. Miles", J. Fluid Mech., 10, 509-512.

Howard L.N. and Maslowe S.A., 1973: "Stability of stratified shear flows", Boundary-layer Met., 4, 511-523.

Ince E.L., 1956: "Ordinary Differential Equations", Dover, New York.

Joseph R.I. 1977: "Solitary waves in a finite depth fluid", J. Phys. A: Math. Gen. 10, L225-227.

Kakutani T. and Yamasaki N., 1978: "Solitary waves on a two-layer fluid", J. Phys. Soc. Japan, 45, 674-679.

Keulegan G.H., 1953: "Characteristics of internal solitary waves", J. Res. Nat. Bur. Stand., 51, 133-140.

Koop C.G. and Butler G., 1982: "An investigation of internal solitary waves in a two-fluid system", J. Fluid Mech., 112, 225-251.

Kubota T., Ko D.R.S. and Dobbs L.D., 1978: "Weakly-nonlinear, long internal waves in stratified fluids of finite depth", AIAA J. of Hydronautics, 12, 157-165.

Kuo S.S., 1972: "Computer applications of numerical methods", Addison-Wesley, Reading, Massachusetts.

Lamb H., 1932: "Hydrodynamics", Dover publications, New York.

Leibovich S. 1979: "Waves in parallel or swirling stratified shear flows", J. Fluid Mech., 93, 401-412.

Leonov A.I. and Miropol'skiy Y.Z., 1975: "Toward a theory of stationary nonlinear internal gravity waves", Akad. Nauk. SSSR. Izv., Atmospheric and Oceanic Physics, 11, 298-304.



Reproduced with permission of the copyright owner. Further reproduction prohibited without permission.

Liu A.K. and Benney D.J., 1981: "The evolution of nonlinear wave trains in stratified shear flows", Studies in Applied Maths., 64, 247-269.

Liu A.K., Kubota T. and Ko D.R.S., 1980: "Resonant transfer of energy between nonlinear waves in neighboring pycnoclines", Studies in Applied Mathematics, 63, 25-45.

Liu A.K., Pereira N.R. and Ko D.R.S. 1982: "Weakly interacting internal solitary waves in neighboring pycnoclines", J. Fluid Mech., 122, 187-194.

Long R.R., 1953: "Some aspects of the flow of stratified fluids I. A theoretical investigation", Tellus, 5, 42-58.

Long R.R., 1956: "Solitary waves in one- and two-fluid systems", Tellus, 8, 460.

Long R.R., 1965: "On the Boussinesq approximation and its role in the theory of internal waves", Tellus, 17, 46-52.

Maslowe S.A. and Redekopp L.G., 1980: "Long nonlinear waves in stratified shear flows", J. Fluid Mech., 101, 321-348.

Menkes J., 1959: "On the stability of a shear layer", J. Fluid Mech., 6, 518-522.

Menkes J., 1961: "On the stability of heterogeneous shear layer to a body force", J. Fluid Mech., 11, 284-290.

M$^{c}$Leod J.B. and Olver P.J., 1983: "The connection between partial differential equations soluble by inverse scattering and ordinary differential equations of Painlevé type", SIAM. J. Math. Anal., 14, 488-506.

Miles J.W., 1961: "On the stability of heterogeneous shear flows", J. Fluid Mech., 10, 496-508.

Miles J.W., 1963: "On the stability of heterogeneous shear flows, Part 2", J. Fluid Mech., 16, 209-227.



Reproduced with permission of the copyright owner. Further reproduction prohibited without permission.

Miles J.W., 1977a: "Obliquely interacting solitary waves", J. Fluid Mech., 79, 157-169.

Miles J.W., 1977b: "Resonantly interacting solitary waves", J. Fluid Mech., 79, 170-179.

Miles J.W., 1979: "On internal solitary waves", Tellus, 31, 456-462.

Miles J.W., 1980: "Solitary waves", Ann. Rev. Fluid Mech., 12, 11-43.

Oikawa M. and Yajima N., 1973: "Interactions of solitary waves-A perturbation approach to nonlinear systems", J. Phys. Soc. Japan, 34, 1093-1099.

Olver F.W.J. 1974: "Asymptotics and special functions", Academic Press, New York.

Ono H., 1975: "Algebraic solitary waves in stratified fluids", J. Phys. Soc. Japan, 39, 1082-1091.

Peters A.S. and Stoker J.J., 1960: "Solitary waves in liquids having non-constant density", Comm. Pure Appl. Math., 13, 115-164.

Rayleigh Lord, 1876: "On waves", Philos. Mag., Ser. 5, 1, 257-279.

Russell J.S., 1838: "Report of the committee on waves", Rep. Meet. Brit. Assoc. Sci., 7th, Liverpool, 1837, pp. 417-496, John Murray, London

Russell J.S., 1845: "Report on waves", Rep. Meet. Brit. Assoc. Sci., 14th, York, 1844, pp. 311-390, John Murray, London

Segur H. and Hammack J.L., 1982: "Soliton models of long internal waves", J. Fluid Mech., 118, 285-309.

Su C.H. and Mirie R.M., 1980: " On head-on collisions between two solitary waves", J. Fluid Mech., 98, 509-525.

Swanson C.A. 1968: "Comparison and oscillation theory of linear differential equations", Academic Press, New York.

Synge J.L., 1933: "The stability of heterogeneous liguids", Trans. Roy. Soc. Can. (3), 27, 1-18.



Reproduced with permission of the copyright owner. Further reproduction prohibited without permission.

Taylor G.I., 1931: "Effect of variation in density on the stability of superposed streams of fluid", Proc. Roy. Soc. A, 132, 499-523.

Ter-Krikoriv A.M., 1963: "Theorie exacte des ondes longues stationnaires dans un liquide heterogene", J. Mecanique, 2, 351-376.

Thorpe S.A. 1969: "Neutral eigensolutions of the stability equations for stratified shear flow", J. Fluid Mech., 36, 673-683.

Thorpe S.A. 1978: "On the shape and breaking of finite amplitude internal gravity waves in a shear flow", J. Fluid Mech., 85, 7-31.

Tung K.-K., Chan T.F. and Kubota T., 1982: "Large amplitude internal waves of 'permanent form'", Studies in Applied Math., 66, 1-44.

Tung K.-K., Ko D.R.S. and Chang J.J., 1981: "Weakly nonlinear internal waves in shear", Studies in Applied Math., 65, 189-221.

Turner J.S., 1973: "Buoyancy effects in fluids", Cambridge University Press.

Weidman P.D., 1978: "Internal solitary waves in a linearly stratified fluid", Tellus, 30, 177-184.

Weidman P.D. and Johnson M., 1982: "Experiments on leapfrogging internal solitary waves", J. Fluid Mech., 122, 195-213.

Weiss J., 1983: "The Painlevé property for partial differential equations II: Backlund transformation, Lax pairs, and the Schwarzian derivative", J. Math. Phys., 24, 1405-1413.

Weiss J., Tabor M. and Carnevale G., 1983: "The Painlevé property for partial differential equations", J. Math. Phys., 24, 522-526.

Whitham G.B., 1974: "Linear and nonlinear waves", Wiley-Interscience, New York.

Yih C., 1969: "Fluid Mechanics", M$^{c}$Graw-Hill, New York.

Yih C., 1980: "Stratified flows", Academic Press, New York.



Reproduced with permission of the copyright owner. Further reproduction prohibited without permission.

Zabusky N.J. and Kruskal M.D., 1965: "Interaction of "solitons" in a collisionless plasma and the recurrence of initial states", Phys. Rev. Lett., 15, 240-243.

Zakharov V.E. and Shabat P.B., 1972: "Exact theory of two-dimensional self-focusing and one-dimensional self-modulation of waves in nonlinear media", Sov. Phys. JETP, 34, 62-69.



Reproduced with permission of the copyright owner. Further reproduction prohibited without permission.